North Atlantic Climate Reconstruction during a Warm Event from the Last Glacial Revealed through Geochemical Analysis of a Scottish Flowstone.

EGLETON, RACHEL

North Atlantic Climate Reconstruction during a Warm Event from the Last Glacial Revealed through Geochemical Analysis of a Scottish Flowstone.

THESIS
submitted in fulfilment
of the requirements for the degree of
Master of Science
by Research

by

Rachel Egleton

Department of Earth Sciences
Durham University
2025

Abstract

North Atlantic Climate Reconstruction during a Warm Event from the Last Glacial Revealed through Geochemical Analysis of a Scottish Flowstone.

Rachel Egleton

Dansgaard-Oeschger (DO) warm events were interstadial intervals during the last glacial period characterised by abrupt increases in Northern Hemisphere temperature above background glacial conditions, followed by a gradual return to a stadial state. The mechanisms driving these rapid warming events, their spatial extent, and their influence on global climate cycles remain a focus of current research. Developing a clearer understanding of the triggers and controls of past climate states is critical for improving interpretations of contemporary forcing mechanisms and their cascading impacts on climate variability. This research presents new evidence for DO-12 warming at higher latitudes than previously recognised, based on a new flowstone chronology from Scotland. This chronology aligns well with SIOC19, supporting its adoption as the dominant chronology for the last glacial period. A novel method for reconstructing palaeotemperature and hydrological variability is introduced, derived from the temperature dependency of D_{Mg} and the degree of Prior Calcite Precipitation (PCP) occurring within the flowstone analogue. The reconstructed temperature range is notably large, with one possible explanation being the presence of an alternative subarctic climate regime in Scotland during DO-12. Spectral analysis of NAO-band cycles identifies a potential dampened meridional temperature gradient and stronger subtropical forcing during DO-12, attributed to northwards shifts in key Atlantic climate mechanisms. Overall, the results of this study contribute to a refined understanding of DO-12, its timing and spatial influence, the behaviour of the NAO under abrupt warming, and the resultant impacts on European climate. More broadly, this research enhances knowledge of climate cycle dynamics and the thresholds and cascade effects associated with rapid forcing changes, providing new insight into how these processes manifested during the last glacial period.

Table of Contents

Table of Figures

List of Abbreviations

DO	Dansgaard-Oeschger
DO-12	Dansgaard-Oeschger event 12
MIS3	Marine Isotope Stage 3
PCP	Prior Calcite Precipitation
AMOC	Atlantic Meridional Overturning Circulation
IRD	Ice Rafted Debris
ITCZ	Inter-Tropical Convergence Zone
DSOW	Denmark Straight Overflow Water
ISOW	Iceland-Scotland Overflow Water
NAC	North Atlantic Current
DWBC	Deep Western Boundary Current
AMO	Atlantic Meridional Oscillation
NAO	North Atlantic Oscillation
AABW	Antarctic Bottom Water
ICD	Incongruent Calcite Dissolution
COPRA	COnstructing Proxy Records from Age models
LA-ICP-MS	Laser Ablation Inductively Coupled Plasma Mass Spectrometry
PCA	Principal Component Analysis
PC1 & PC2	Principal Component 1 & 2
DTW	Dynamic Time Warping

Declaration

This thesis presented for a Master of Science by Research is my own work, except where acknowledgements are made within the text.

Rachel Egleton
Durham University
September 2025

Acknowledgements

I would like to sincerely thank my supervisor James Baldini for his guidance and invaluable advice throughout this project. His patience as I developed my understanding of the field was fundamental and this work would not have been possible without his supervision. I would also like to give thanks to Sebastain Breitenbach for his work on the caving project from which my speleothem sample was taken, his generous help with stable isotope analysis at Northumbria University and the use of COPRA. Lastly, I would like to thank the friends I made during my master's at Durham for their continuous support and encouragement, and for providing both motivation and welcome distractions over the past year.

1. Introduction

Researching palaeoclimate clarifies the variability, boundaries, and interconnectivity of our current climate system, offering valuable context for predicting its evolution based on current and future climate forcings. Numerous methods exist for reconstructing past climate, including the analysis of ice core geochemistry, foraminifera analysis from marine sediment cores, pollen spore analysis from terrestrial sediment cores, and geochemical analysis of speleothems (Landais *et al.,* 2003; Barker *et al.,* 2005; Lee *et al.,* 2024; Proctor *et al.,* 2002). The availability of more diverse spatial and temporal proxy data enables a better understanding of global palaeoclimate and enhances our understanding of climate system dynamics and subsequent variability.

Speleothems are a crucial archive for reconstructing past climate, offering several key advantages that make them indispensable over other archives. Due to their precise chronologies, global distribution, and capacity to yield high-resolution proxy data, speleothems have become central for understanding climate variability (Wong & Breecker, 2015). One of the primary strengths of speleothem is their ability to offer high-resolution temporal records (Baldini *et al.,* 2021; Breitenbach *et al.,* 2024). However, to fully understand regional climate dynamics, increasing the spatial extent of sampling is essential. The study of regional climate dynamics is critical for understanding past and present global climatic teleconnections (Wong & Breecker, 2015). These teleconnections will be discussed in more detail further on within this thesis.

Before the 1990s, speleothem research primarily used the $\delta^{18}O$ ratio for climate reconstruction, with variation largely interpreted as a temperature proxy (Duplessy *et al.,* 1970; Hendy & Wilson, 1968; Gascoyne *et al.,* 1980). Since the 1990s speleothem research has evolved significantly, now using $\delta^{18}O$ to investigate general changes in regional and global hydroclimate. Including the analysis of precipitation amount, shifts in moisture sources, and identification of climate cycles (Bar-Matthews *et al*., 1997, McDermott *et al.,* 1999, Bar-Matthews *et al.,* 1999). However, the controls on $\delta^{18}O$ in speleothems are highly complex, and values between speleothem in the same region can exhibit considerable variation (Lachniet, 2009). In parallel with developments in $\delta^{18}O$ analysis, $\delta^{13}C$ ratios are

now increasingly used to clarify past soil and vegetation dynamics (Baker *et al.,* 1997; Genty *et al.,* 2003).

In the 1980s Gascoyne (1983) suggested magnesium concentrations in speleothems as a temperature proxy. However, not all studies confirmed this relationship, for example Goede (1994), highlighting the need for careful interpretation of proxies between each speleothem. Since the 1990s, research now integrates more trace elements into speleothem climate reconstructions. For example, Mg/Ca ratios are now often used to reflect palaeohydrology, along with Sr/Ca and Ba/Ca ratios (Goede & Vogel, 1991; Roberts *et al*., 1998; Fairchild & Treble, 2009). The analysis of trace elements has extended the range of proxies that can be identified using speleothems. However, it is important to note that all these proxies are regionally variable and influenced by a variety of factors including local drip-water chemistry and the overlying soil composition. As such, whilst these proxies provide valuable information about past climate, their interpretation must consider the specific regional context in which the speleothem was formed.

Current research uses speleothems to create absolute chronologies for discrete events (such as the onset and termination of glacial periods) and for identifying regionally specific climate during these transitions (Past Interglacials Working Group of PAGES, 2015). Subsequent interpretation of this chronological information alongside other proxy datasets clarifies how the climate signal was spatiotemporally propagated (Wendt *et al.,* 2021; Scholz *et al.,* 2014). Given the high temporal resolution and absolutely dated records achievable, speleothems offer critical insights into the Earth's climate system, including past abrupt climate changes. By studying these archives, we can enhance our understanding of climate system responses to past perturbations and better understand the dynamics of climate cycles, their global teleconnections, and feedback mechanisms, which in turn will assist in predicting possible future perturbations (Corrick *et al.,* 2022; Boers *et al.,* 2018).

1.1 Aims

This thesis aims to address several gaps in the understanding of regional climate dynamics during the last glacial period, particularly in relation to Dansgaard-Oeschger (DO) event 12 (DO-12), occurring ~46 ka BP (Breitenbach *et al.,* 2024). A notable gap in current literature is the lack of speleothem data from higher latitudinal regions, north of Bleßberg cave (Germany) and Crag Cave (Ireland), an area previously thought too cold to allow for

speleothem growth during this period (Klose *et al.,* 2024; Breitenbach *et al.,* 2024; Frankhauser *et al.,* 2016; Weber *et al.,* 2018). By introducing new speleothem data from Uamh Mhor, Scotland, this research aims to challenge this assumption and contribute to a revised understanding of the latitudinal extent of speleothem growth during the last glacial, as well as offering new insights into regional climate during DO-12.

Research has previously struggled to constrain the timing of DO events in Europe due to a lack of independently dated proxy records, and the limited discovery of speleothems from this period. A lack of independently dated records leaves room for event timeline uncertainty (Fleitmann *et al.,* 2009; Buizert *et al.,* 2014; Liang *et al.,* 2019; Dong *et al*., 2018). This thesis aims to help fill this gap by presenting an independently dated speleothem record from Marine Isotope Stage 3 (MIS3), offering the potential for cross-comparison with the dominant existing chronologies.

There are few climate archives away from the highest latitude regions which are able to be used as palaeotemperature proxies during the last glacial period (Drysdale *et al*., 2020). This thesis aims to contribute a new data analysis technique to facilitate temperature reconstruction and an index for approximate dryness reconstruction from speleothems. This new analysis technique is based on using Mg/Sr concentrations from speleothems in the context of temperature dependency of the Mg partition co-efficient within certain speleothem growth conditions to reflect different regional temperature scenarios. A dryness index is quantified based off the strength of control of Prior Calcite Precipitation (PCP) on Mg/Sr concentrations, with stronger PCP occurrence indicating dryer climate conditions (Fairchild & Treble, 2009; Tolzmann, 2013; Karmann *et al.,* 2007). This aims to facilitate the introduction of a new method to constrain palaeotemperature reconstructions, which may be further utilised in regions previously unable to constrain palaeotemperature and precipitation.

Furthermore, the sample location of this research in Northern Scotland is an ideal location to improve our understanding of the timing and duration of North Atlantic climate cycles during DO warming events in Europe. By cross-correlating new speleothem data with existing records from different regions, this research aims to validate and expand on current knowledge of climate cycles within the North Atlantic (Baldini *et al.,* 2015b; Dong *et al.,* 2018; Nagashima *et al.,* 2011; Ramirez *et al.*, 2023). Therefore, contributing to a more comprehensive understanding of how North Atlantic climate and climate cycles may have

differed between contemporary dynamics and the last glacial period in the context of DO warming events.

This will be accomplished through examining a flowstone (SMFMB20230528-1) from Uamh Mhor cave, Scotland. Utilising trace element data backed with stable isotope data, uranium-thorium dating, principal component analysis, dynamic time warping, spectral analysis, sea spray and PCP control analysis, the creation of a temperature and dryness index and comparison to contemporary climate cycles within the North Atlantic. Overall, this study aims to use this analysis to address current research gaps by providing new high-latitude and high-resolution speleothem data, independent speleothem dating allowing for cross-correlation against current chronologies, a new method to reconstruct palaeotemperature and precipitation patterns from speleothem and increased knowledge of dominant North Atlantic climate cycles during DO warming events and their regional connections. This ultimately contributes to a more nuanced analysis of North Atlantic climate from the last glacial period.

1.2 Structure

Chapter [2] of this thesis presents a review of current literature that is split into seven parts. Part one is a review of current research on the last glacial period, specifically MIS3. Part two focuses on climate events and climate cycles within the North Atlantic region. Part three is an overview of speleothem use for climate reconstruction, their formation and dating techniques. Part four illustrates the use of trace elements as proxies and how they can be interpreted. Part five introduces the use of stable isotopes as proxies and how they can be used alongside trace elements. Part six introduces the process of prior calcite precipitation and its climate reconstruction potential. Part seven discusses regional climate in Europe from secondary datasets during the last glacial period.

Chapter [3] presents the location of the flowstone sample SFMB20230528-1, the study area Uamh Mhor, its geology and landscape. Additionally, there is an introduction to other palaeo-datasets and their global context as well as modern datasets used within this thesis.

Chapter [4] is an overview of the methods used for preparation and analysis applied to the sample used within this thesis.

Chapter [5] is a synthesis of results and the main discussion section, further subdivided into a discussion of trace element data and period of growth, sample comparison to other palaeoclimate records from DO-12, identification of palaeoclimate proxies and their controls, climate reconstruction through reconstructed temperature and dryness index, comparison of Uamh Mhor to existing chronologies, an analysis of climate variability through DO-12, and the comparison of climate reconstruction from DO-12 to modern North Atlantic climate. This section concludes with limitations recommendations for future research.

Chapter [6] is the conclusion of this thesis.

2. Background

2.1 Period of Study

2.1.1 Last Glacial Period and DO Events

The last glacial period lasted from ~120-15 ka BP and was characterised by abrupt millennial-scale oscillations consisting of colder stadials and warmer interstadials, known as Dansgaard-Oeschger (DO) events (Fohlmeister *et al*., 2023; Modeley *et al*., 2014; Corrick *et al.*, 2020; Dansgaard *et al.,* 1993; Ampel *et al.,* 2010; Dokken *et al.,* 2013; Genty *et al.,* 2003; Zhang *et al.*, 2017). The first discovery of DO events during this period was within the Camp Century ice core from Greenland (Dansgaard *et al.,* 1984). Research now finds DO signals within palaeoclimate proxies in both hemispheres (Dansgaard *et al.,* 1993; Johnsen *et al.,* 1992; Clement and Peterson, 2008). During the last glacial, Marine Isotope Stage 3 (MIS3) was a warmer interstadial period lasting from ~57-27 ka BP. Within MIS3, there are 11 identified DO events ranging from DO-5 to DO-15 (Rasmussen *et al.,* 2014; Weber *et al.,* 2018; Pedro *et al.,* 2022).

Research has identified 24 DO events in the GRIP and GISP2 ice cores from Greenland during the last glacial period (GRIP Members, 1993; Grootes *et al.,* 1993). More recently, research identifies 25 DO events from the NGRIP ice core, also currently used for the GICC05 chronological framework (Kindler *et al*., 2014). The creation of chronologies allows for an agreed synchronisation of palaeoclimate events. Rasmussen *et al*. (2014) and Seierstad *et al*. (2014) constructed a chronology for the past ~104 ka BP called GICC05, mainly based off NGRIP data, with the additional incorporation of GRIP, and GISP2 ice core data. Studies

note that like previous chronologies GICC05 allows for the creation of age offsets due to uncertainties in lamination, which increases further back within the chronology (Fleitmann *et al*., 2009; Buizert *et al*., 2015). However, the chronology is still widely supported within literature encompassing MIS3. For example, it was recently utilised with data from Wulu and Dragon Cave to interpret $\delta^{18}O$ signals from DO11-12 (Liang *et al*., 2019; Dong *et al.,* 2018).

Each DO event features an abrupt change to warmer conditions within the Northern Hemisphere. These abrupt climate changes can occur in a matter of decades, reflecting temperatures generally around 10-15 °C but with changes of up to 16 ±3 °C during DO-11 noted by Kindler *et al.* (2014) (Huber *et al.,* 2006; Boers *et al.,* 2018; Erhardt *et al.,* 2019; Pedro *et al.,* 2022). These elevated temperature interstadial periods continue for ~200-400 years then a gradual transition back to colder stadial conditions occurs over ~50-200 years (Dokken *et al.,* 2013; Boers *et al.,* 2018). Most DO interstadial events vary in magnitude and length, despite featuring similar abrupt climate changes. It was suggested there may be a quasi-periodicity for the onset of DO events ~1,470 years (Schulz, 2002; Braun *et al*., 2005). However, current research suggests this observation was likely noise induced (Ditlevsen *et al.,* 2007; Harrison & Goñi, 2010; Boers *et al.,* 2018).

The main forcing mechanism for DO events remains uncertain and a matter of debate (Baldini *et al.,* 2015a; Vettoretti *et al.,* 2022; Fohlmeister *et al.,* 2023; Menviel *et al.,* 2020). Most theories explaining DO event forcing look specifically at shifting Atlantic Meridional Overturning Circulation (AMOC) dynamics (Henry *et al.,* 2016). One of the leading theories, first proposed by Broecker *et al.* (1985), suggests DO event forcing is linked to sudden shifts in AMOC from freshwater budget fluctuations in the North Atlantic and controlled by Arctic sea ice extent (Genty *et al.,* 2003; Ampel *et al.,* 2010; Landais *et al.,* 2021, p.178; Dokken *et al.,* 2013; Menviel *et al.,* 2014; Zhang *et al.,* 2017; Boers *et al.,* 2018). However, some recent papers have explored the role of explosive volcanism within the Southern Hemisphere as a forcing mechanism for the onset of interstadials (Baldini *et al*., 2015b; Lohmann *et al.,* 2024). Despite the continued uncertainty of DO forcing, an amplification mechanism is noted when Heinrich events precede a DO interstadial transition (Mann *et al.,* 2021). For example, if a Heinrich event occurs within the preceding stadial, there is a subsequent observed increase in strength of the DO warm event (Pedro *et al*., 2022), an example of this is noted in the next section.

2.1.2 Heinrich Events and Stadial Periods

Heinrich events are defined as intervals of time featuring large amounts of Ice Rafted Debris (IRD) within deep ocean sediment cores in the Northern Hemisphere. The significant presence of IRD is suggested to derive from ice loss from the Laurentide Ice Sheet due to a binge-purge mechanism, leading to a period of climate cooling (Peral *et al.,* 2024; Weber *et al.,* 2018). Research suggests Heinrich stadials are the result of Heinrich events as freshwater ice input can further slow the AMOC and induce a period of global cooling (Böhm *et al*., 2015; Heinrich, 1988; Menviel *et al*., 2020). Furthermore, Heinrich events and Greenland interstadials are potentially linked; for example, Heinrich Stadial 5 (~49.2-47.6 ka BP), one of coldest stadials, occurred immediately before DO-12, the warmest observed DO event during MIS3 (Weber *et al.,* 2018; Pedro *et al.,* 2022; Menviel *et al*., 2020). As a result, research now interprets Heinrich events as a potential amplification mechanism for DO interstadial transitions (Pedro *et al.,* 2022).

2.2 Global Climate Connections

2.2.1 Atlantic Meridional Overturning Circulation (AMOC)

During MIS3, research associates DO interstadial events with the strengthening of the AMOC, and a tight coupling to North Atlantic sea-ice (Menviel *et al*., 2020; Genty *et al*., 2003). The AMOC consists of warm northward surface flow and cold southward deep flow in the Atlantic (Landais *et al*., 2021, p.177) (Fig. 1). It operates actively during Greenland interstadials but slows or pauses during stadials. Changes in AMOC are controlled by perturbations in atmospheric CO_2, meltwater input, and ice-sheet extent (Menviel *et al.,* 2020). The AMOC is strongly regulated by vertical stratification, alternatively known as the vertical density gradient, which is primarily controlled by salinity and ocean temperature (Zhang *et al*., 2017).

Research shows that AMOC strength varies between stadial and interstadial conditions (Baker *et al.,* 2015; Liu *et al.,* 2023; Baldini *et al.,* 2015a; Landais *et al.,* 2021; Dhungana *et al.,* 2010). With AMOC collapse or weakening occurring during North Atlantic stadials, causing a southward Inter-Tropical Convergence Zone (ITCZ) shift, meaning less heat transport to the North Atlantic. Instead, this heat pools in the Southern Ocean, leading to more warming around Antarctica with a lag time of ~200 ±100 yrs (Corrick *et al.,* 2020).

Although, Southward movement of the ITCZ can cause a salinity increase in the subtropical Northern Atlantic during colder stadial periods. Which can work as a precondition for NADW formation and a return to interstadial conditions when there is a strong AMOC mode (Zhang *et al.,* 2017).

AMOC variability strongly affects European climate, albeit with an approximate 200-year lag noted between AMOC strengthening and European warming (Woillez *et al.,* 2013; Landais *et al.,* 2021, pp.177-8). During North Atlantic DO warm phases, a stronger AMOC phase moves heat from the tropics and Southern Hemisphere to the high latitudes in the North Atlantic. This causes a thermal asymmetry between the Southern and Northern Atlantic and leads to a northward ITCZ shift and cooling around Antarctica and within the Southern Hemisphere creating a bipolar seesaw effect (Corrick *et al.,* 2020). This effect will be discussed further in the next section.

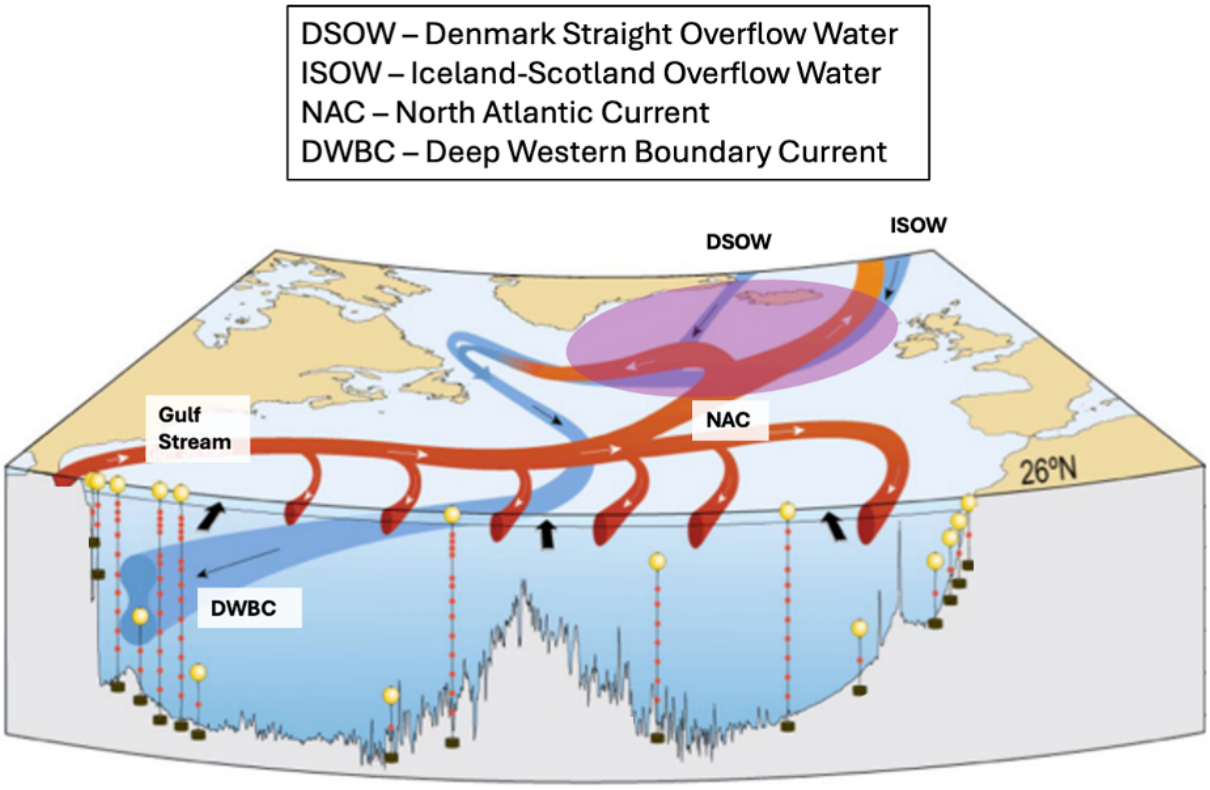

Figure 1. AMOC circulation within the North Atlantic region. Purple area notes zone of downwelling. Adapted from McCarthy *et al*. (2017).

2.2.2 Atlantic Meridional Oscillation (AMO)

The AMO is defined as a quasi-periodic alternation between warmer and colder sea surface temperature in the North Atlantic (Börget *et al.,* 2020). A positive AMO mode indicates a warmer and wetter period in Northern Europe whereas a negative mode indicates a colder and dryer period in Northern Europe (Drinkwater *et al*., 2014). The periodicity of the AMO has been noted to fluctuate ~50-90 years over the last 8 ka BP (Knudsen *et al.,* 2011). However, recent research notes AMO to change in frequency through time, for example, ~90-180 years from 1200-1500 BP and ~30-90 years in the last 100 years (Börget *et al.,* 2020). The control of these changes in mode is still debated, the main control is believed to be variations in AMOC (Delworth *et al.,* 2017; Drinkwater *et al.,* 2014). Alternatively, Clement *et al.* (2015) suggests AMO is controlled by stochastic forcing from mid-latitude atmospheric circulation and Börget *et al.* (2020) notes changes in AMO may be related to volcanic eruptions shown through the AMO's quasi-periodicity.

AMO has a global influence on climate through large-scale climate controls and teleconnections. For example, AMO is believed to control rainfall patterns in the Sahel and Brazil through interhemispheric heat distribution (Knudsen *et al.,* 2011). Furthermore, Wang *et al*. (2009) notes warm modes of AMO link to warmer winters in China and stronger East Asian summer monsoons, due to positive AMO causing a northwards shift in the ITCZ. This is due to the AMO positive phase causing stronger winds over the North Atlantic leading to heat loss in the Labrador Sea, enhancing deep water formation and strengthening the AMOC (Börget *et al.,* 2020; Sun *et al.,* 2015). The strengthening of wind influencing AMOC, also results in an observed relationship between AMO and North Atlantic Oscillation (NAO). The NAO will be discussed further in the next section. As a result of the positive AMO mode strengthening the westerlies across the North Atlantic, the East-West position of the Icelandic low and the Azores High is moved NW - SE respectively (Börget *et al.,* 2020). The opposite is seen to occur during negative AMO phases. This reinforces the idea that AMO has a global as well as a European climate influence through continental climate links and relationships with other climate cycles.

2.2.3 North Atlantic Oscillation (NAO)

NAO dominates climate variability in the North Atlantic, characterised by sea level pressure differences between the subpolar (Icelandic) low and subtropical (Azores) high. This change

in pressure gradient causes a mid-latitude westerly flow of wind known as the westerlies (Wang *et al.,* 2012). A Positive NAO phase results in the strengthening and northwards movement of the westerlies over the Atlantic bringing warmer and more moist air to Northern Europe (Wang *et al*., 2012; Olsen *et al.,* 2012) (Fig. 2). Alternatively, a negative NAO phase causes colder and dryer conditions in Northern Europe, due to a weakening and southwards movement of the westerlies (Olsen *et al.,* 2012). The periodicity of NAO is noted to have large variations within research due to the nature of raw NAO data being highly noisy (Seip *et al*., 2019). However, the general accepted range of NAO periodicity is ~2-10 years (Rossi *et al.,* 2011; Luterbacher *et al.,* 2001; Olafsdorrir *et al.,* 2013). Börget *et al.* (2020) notes AMO as a control of spatial variation of NAO periodicity based on model simulations. This is due to the influence of the AMO on the strength of the westerlies controlling the location of the pressure nodes over the North Atlantic. This further strengthens the relationship between NAO and AMO.

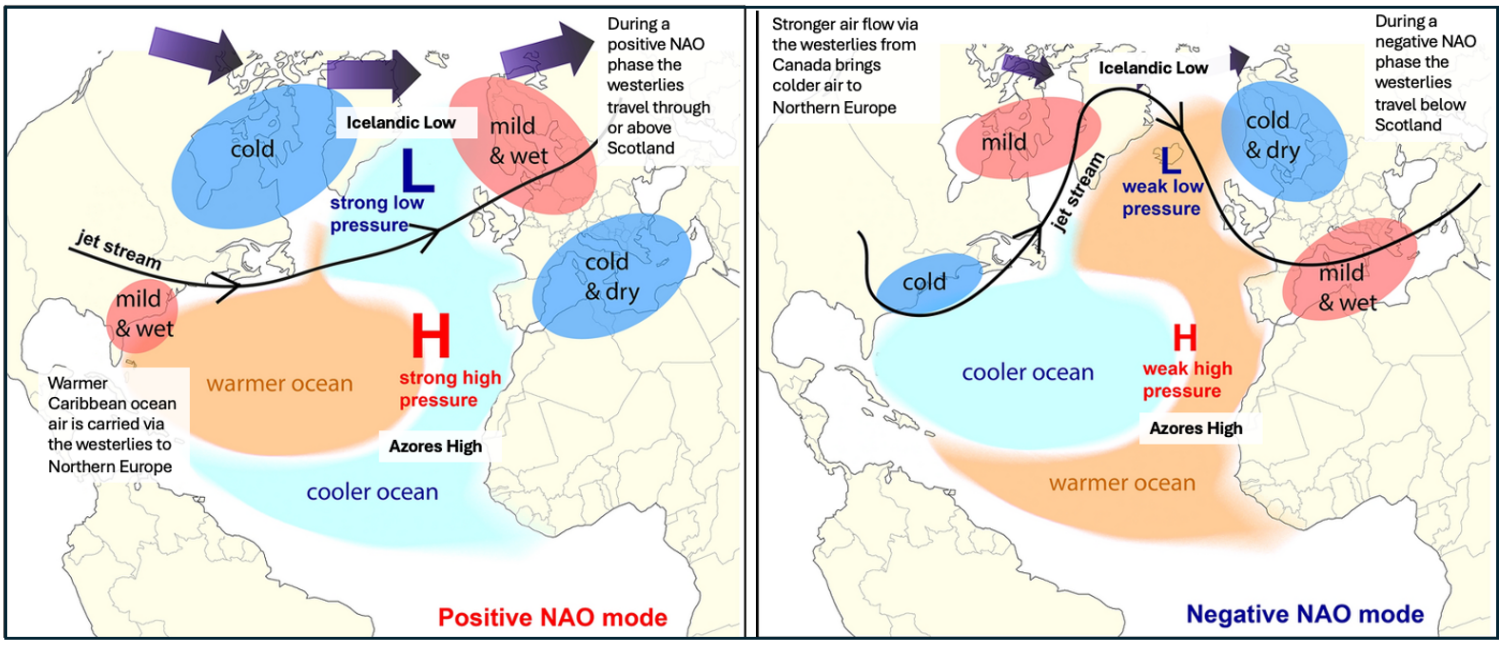

Figure 2. Positive and negative NAO phases in the North Atlantic region including westerlies/jet stream movement and changes in pressure gradients. Adapted from Baez *et al.* (2021).

2.3 Speleothems

2.3.1 Speleothems as Climate Archives

Speleothems are mineral deposits found in caves due to deposition from percolating dripwater, primarily composed of calcium carbonate in the form of calcite or aragonite (Demeny *et al.,* 2016). Speleothem deposits commonly include stalactites, stalagmites, and flowstones among other deposits. Research more commonly utilises stalagmites and flowstones due to their stability, uniformity, and continuous growth, as opposed to stalactites (Birks *et al.,* 2014, pp.242-6). Speleothems although commonly subaerial can also grow subaqueously, this is a relatively common deposition condition overlooked in current literature (Wroblewski *et al.,* 2017). First noted in Birmingham Crawlway Cave, USA by White (1956), with the term "subaqueous flowstone" coined by Hill (1992). Both subaerial and subaqueous speleothem deposits are valuable as they provide high-resolution temporal data on regional climate variability and climate cycles, derived from stable isotope and trace element records within their laminae (Oster *et al.,* 2020; Mattey *et al.,* 2010; Held *et al.,* 2024; Klose *et al.,* 2024). The study of palaeoclimate through critical archives such as speleothems, enhances our understanding of the Earth's climate system, particularly in relation to abrupt climate changes. These insights are vital for predicting how the climate system may respond to future forcing (Corrick *et al.,* 2022).

Speleothems offer high precision records, due to their long-term incremental, theoretically closed system records of stable isotope ratios, trace elements, and capacity for precise U-Th dating. Therefore, speleothems are an ideal archive for identifying the timing, patterns, and spatial extent of DO events (Held *et al.,* 2024; Baldini *et al*., 2021; Wong & Breecker, 2015; Fairchild & Treble, 2009). Additionally, speleothems remain well-preserved and generally undisturbed as geochronometers, with dating ranging from a few thousand years to approximately 650 ka BP (Wendt *et al.,* 2021; Baker *et al.,* 2011). Through U-Th disequilibrium dating, both stalagmites and flowstones can be precisely dated within this timeframe (Sanchez-Moreno *et al.,* 2022; Pawlak *et al.,* 2019; Scholz *et al.,* 2014). U-Th dating will be explored further later within this chapter.

Speleothem deposits are widely distributed across the globe, offering regional proxy information. In some instances, speleothems are correlated with other palaeoclimate archives, such as ice cores or marine sediment cores, increasing their utility in the reconstruction of

past climate (Cheng *et al.,* 2016; Buizert *et al.,* 2015; Wendt *et al.,* 2021; Wong & Breecker, 2015). However, high-latitude reconstructions of past climate conditions using speleothems covering the last glacial period remain rare (Held *et al.,* 2024). Speleothems provide insight into past climate conditions during periods such as the last glacial through various proxies, including stable isotopes of oxygen ($\delta^{18}O$), carbon ($\delta^{13}C$), trace elements, and growth rates (Proctor *et al*., 2000; Oster *et al.,* 2020). However, interpretations of each proxy can vary widely between different regions globally (Wong & Breecker, 2015; Mattey *et al.,* 2010).

2.3.2 Speleothem Formation

The formation of speleothems begins when rainwater, rich in H_2CO_3, infiltrates the overlying soil. Upon contact, the water dissolves the stored CO_2 within the soil, increasing the concentration of H_2CO_3. When this water reaches the karst layer, the carbonic acid dissolves carbonate rocks such as limestone or dolomite. This process results in dripwater saturated in calcite. When the dripwater reaches the cave, the lower concentration of CO_2 in the cave air causes degassing of CO_2 from the dripwater. This leads to the supersaturation of calcite, resulting in $CaCO_3$ precipitation and speleothem formation (Eq. 1) (Scholz *et al.,* 2014; Fairchild *et al.,* 2006; McDermott, 2004; Constantin, 2015).

The chemical equation summarising the process is:

$$CO_{2\,(g)} + H_2O_{\,(aq)} + CaCO_{3\,(s)} \leftrightarrow Ca^{2+}_{(aq)} + 2HCO_{3\,(aq)}$$

Equation 1. Speleothem calcite deposition.

The formation process requires specific conditions for growth, including lower cave CO_2 concentrations than within the karst layer, carbonate geology, surface temperatures typically above 0 °C and wet climate conditions (Isola *et al.,* 2019; Tolzmann, 2013). Additionally, soil depth and vegetation play an essential role in developing the soil CO_2 store, allowing percolating water to become more acidic and dissolve available carbonate rocks. However, any change in these conditions during formation may cause interruptions in growth, these breaks are called hiatuses (Pawlak *et al.,* 2019). Research finds more hiatuses occurring at higher latitudes because speleothem-forming conditions occur less frequently at higher latitudes, where alpine or forested biomes dominate (Constantin, 2015; Birks *et al.,* 2014, p.244).

It is important to note that changes in water geochemistry can also halt or corrode speleothem growth. For example, if a fissure in the cave roof becomes too large and water percolation increases too rapidly, acidic water may begin to dissolve the $CaCO_3$ of the speleothem. Similarly, higher CO_2 concentrations within the cave can reduce carbonate precipitation. This occurs due to higher CO_2 concentrations suppressing the amount of CO_2 degassing from dripwater, preventing calcite deposition (Constantin, 2015). Furthermore, speleothems rarely grow at a constant rate, their growth is often discontinuous or can halt completely during a hiatus. For example, in colder climate conditions, permafrost can prevent water from percolating underground, halting the processes of speleothem formation. In contrast, during more arid periods, a lack of rainfall can similarly prevent dissolution of carbonate rocks necessary for speleothem growth (Constantin, 2015; Birks *et al.*, 2014, p.246). This is relevant during the last glacial period as climate shifts frequently disrupted speleothem growth in higher latitude regions (Klose *et al.,* 2024). For example, Klose *et al*. (2024) notes there are multiple flowstone hiatuses from Bleßberg Cave, Germany during MIS3. These are interpreted as a response to colder stadial conditions causing a lack of liquid water, lack of vegetation above the cave system, and re-routing of drip water (Klose *et al.,* 2024).

2.3.3 U-Th Dating

U-Th dating ($^{230}Th/^{234}U$) has become one of the most accurate and widely applied dating techniques for speleothems in recent decades (Ulusoy *et al.,* 2014; Tolzmann, 2013). U-Th dating was first applied to speleothems in the 1970s (Thompson *et al.,* 1975; Spötl & Boch, 2019, p.1096). The age of formation of speleothem can be determined by measuring the ratio of $^{230}Th/^{234}U$ (Eq. 2) (Tolzmann, 2013; Wendt *et al.,* 2021; Scholz & Hoffmann, 2008; Spötl & Boch., 2019; Ulusoy *et al.,* 2014). Recent advances in U-Th dating allow for an even more precise age determination for the last ~500-650 ka BP (Pawlak *et al.,* 2019; Wendt *et al.,* 2021; Baker *et al*., 2011; Spötl & Boch, 2019). This is a significant advantage over other climate archives, which are often dependent on ^{14}C dating (Sanchez-Moreno *et al.,* 2022).

$$\left[\frac{230\mathrm{Th}}{238\mathrm{U}}\right]\mathrm{A} = 1 - \mathrm{e}^{-\lambda_{230}\mathrm{t}} + \left(\frac{\delta 234\mathrm{U_m}}{1000}\right)\frac{\lambda_{230}}{\lambda_{230} - \lambda_{234}}\left(1 - \mathrm{e}^{-(\lambda_{230} - \lambda_{234})\mathrm{t}}\right)$$

Equation 2. U-Th dating equation (Wendt *et al.,* 2021).

The U-Th dating method relies on the disequilibrium between uranium and thorium isotopes, where in a closed system, the parent and daughter nuclides eventually reach a state of secular equilibrium (Wendt *et al.,* 2021). Over time, the amount of ^{230}Th increases due to the decay of the parent isotope ^{234}U (Fig. 3). This method is effective because uranium is highly soluble in water whereas thorium is not. As a result, clean dripwater contains small amounts of uranium but no appreciable concentration of thorium. Upon the formation of calcite crystals, ^{238}U and ^{234}U will start to decay into a series of intermediary isotopes, eventually decaying into ^{230}Th.

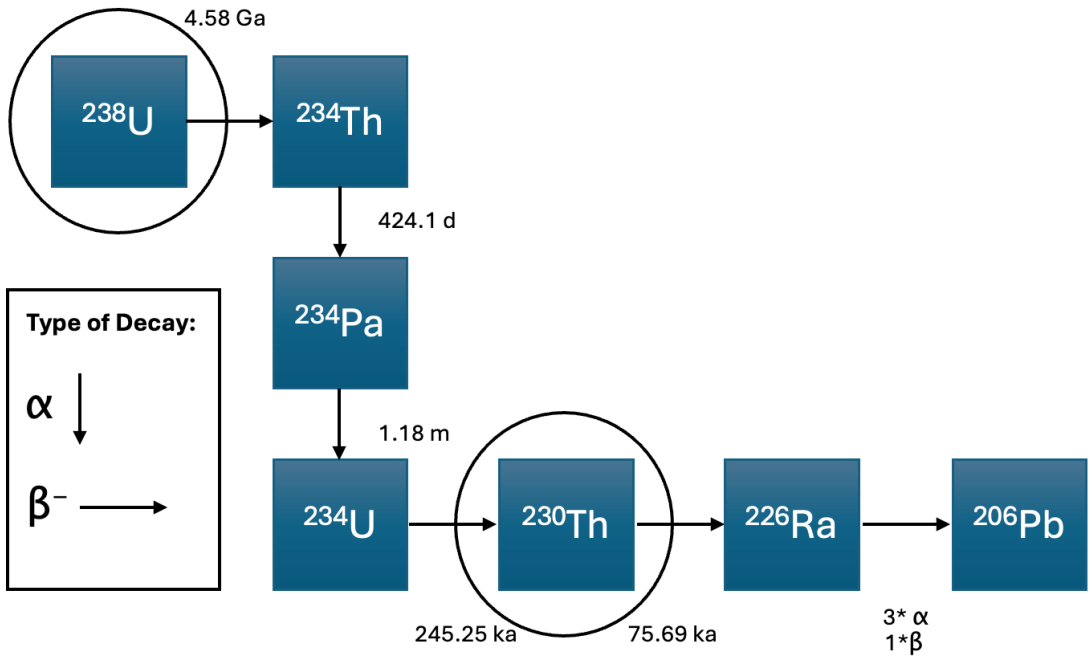

Figure 3. ^{238}U Radioactive decay chain, adapted from Tolzmann (2013).

U-Th dating still involves several uncertainties. For example, if dripwater is contaminated with thorium, initial ^{230}Th content can cause the sample to appear older than the real age (Tolzmann, 2013). One solution to this issue is additionally measuring ^{232}Th concentrations. ^{232}Th and ^{230}Th are both contaminants within dripwater but unlike ^{230}Th, ^{232}Th is not part of the ^{238}U decay chain. Therefore, its presence is used to assess the degree of detrital contamination within the speleothem. Detrital contamination makes U-Th dating more challenging due to higher age uncertainties (Sanchez-Moreno *et al.,* 2022). Despite present research generally suggesting contamination of speleothems by hydrogenous thorium in

dripwater negligible, contamination still makes U-Th dating more challenging due to higher age uncertainties (Wendt *et al.,* 2021; Spötl & Boch, 2019, pp.1096).

Another complication arises if speleothem formation does not occur under a closed system. This is because mixing of uranium and thorium or contamination from surrounding material may create an open radiometric system. This is one reason why research typically avoids the use of stalactites for U-Th dating, as uranium continuously enters stalactites through the central canal or seepage, inhibiting a closed system. Stalagmite contamination occurring during a hiatus can also inhibit a closed system. This is because the system becomes more susceptible to contamination from detrital thorium and dust deposition (Constantin, 2015). Any post-depositional addition or loss of uranium during any point of formation can change the $^{230}Th/\ ^{234}U$ ratio, leading to either artificially younger or older age estimates (Scholz *et al.*, 2014).

2.4 Trace Elements

Variations in trace elements within speleothems provide insights into hydrological processes and partitioning at the water-calcite interface (Roberts *et al.,* 1998). However, interpreting trace element data is complex and site-specific, and consequently palaeoclimate studies use trace elements less often than oxygen and carbon isotope ratios (Fairchild & Treble, 2009; Stoll *et al*., 2012). Research often compliments trace element analysis with stable isotope data ($\delta^{18}O$ and $\delta^{13}C$), providing valuable information on rainfall and water availability through Mg, Ba, and Sr concentrations (Fairchild *et al.,* 2001; Peral *et al.,* 2024).

The incorporation of trace elements in speleothems occurs through three main processes: (Tolzmann, 2013)

1. **Cation Exchange:** During formation, Ca can be exchanged with other elements because Ca^{2+} is a divalent cation within solution. Meaning during formation Ca^{2+} can be exchanged with other divalent cations (e.g., Ba^{2+}, Mg^{2+}, Sr^{2+}), allowing them to integrate into the $CaCO_3$ lattice.
2. **Filling of Crystal Defects:** Elements such as P, F, and Na can be incorporated into the calcite lattice through the infilling of defect points within the crystal lattice structure.

3. **Aqueous Inclusions:** Elements such as Na and Cl can become incorporated within the speleothem within solution through aqueous inclusions.

The trace elements most used within current literature can be arranged into two groups:

- **Group 1:** Includes Mg, Ba, and Sr, typically used as a proxy for precipitation (Riechelmann *et al.,* 2020; Peral *et al.,* 2024; Weber *et al.,* 2018). They substitute for Ca in the carbonate lattice and can also reflect water availability and climate shifts (Fairchild & Treble, 2009).
- **Group 2:** Includes elements such as P, Al, Th, U, Cu, and Pb, which primarily reflect detrital contamination (Riechelmann *et al.,* 2020). However, P and Y can also serve as proxies for soil and vegetation changes, and U can serve as a proxy for soil redox conditions and hydrology when accompanied by Sr (Fairchild & Treble, 2009; Tolzmann, 2013).

2.4.1 Group 1: Mg, Ba, Sr

Present research interprets Mg as a signal of precipitation and PCP. Past studies have widely interpreted Mg as a proxy for precipitation when accompanied by a covariation of $\delta^{13}C$ and $\delta^{18}O$ (Peral *et al.,* 2024; Weber *et al.,* 2018). Alternatively, a positive relationship between Mg and $\delta^{13}C$ can infer PCP as a significant control (Fairchild & Treble, 2009). This is because large elevations in the Mg/Ca ratio indicate there is more Ca being precipitated and CO_2 degassing before speleothem formation, causing the preferential fractionation of ^{12}C out of the dripwater, causing an enrichment in ^{13}C (Dabkowski *et al*., 2016; Fairchild & Treble, 2009).

Current research finds Sr and Ba as more complex and harder to interpret than Mg but grouped analysis of trace element correlation can work to mitigate this. Dabkowski *et al.* (2016) found Sr to mainly depend on rainfall availability and intensity, consistent with Weber *et al*. (2018), who interpreted Sr and Mg in terms of rainfall intensity. However, Weber *et al*. (2018) also interpreted Sr invoking soil pCO_2 shifts, consistent with previous interpretations (Stoll *et al.,* 2012). Overall, the grouped correlation of Mg, Ba, and Sr with $\delta^{13}C$ and $\delta^{18}O$ can strongly reflect water availability (Huang *et al.,* 2001; McDermott, 2004; Karmann *et al*.,

2007; Van Beynen *et al.,* 2008; Fairchild & Treble, 2009). Research typically infers water availability from increases in Mg, Ba, and Sr coupled with increases in $\delta^{18}O$ and $\delta^{13}C$, suggesting drier climate conditions and lower pCO_2 (Peral *et al.,* 2024). Equivalently, decreases in Mg, Ba, Sr, $\delta^{18}O$, and $\delta^{13}C$ indicate wetter climate conditions and higher pCO_2. Furthermore, Vansteenberge *et al.,* (2020) and Peral *et al.,* (2024) also note, antiphase relationships between Mg, Ba, and Sr to indicate drier climate conditions.

2.4.2 Group 2: P, Al, Th, U, Cu, Pb

Elevated levels of P alongside Mg suggest periods of higher moisture availability; alternatively, decreases in P indicate drier periods (Oster *et al.,* 2020; Baldini *et al.,* 2002). Higher P concentrations additionally suggest increased soil activity, with lower values indicating vegetation degradation. U concentrations can be an indicator of contamination, yet Tolzmann (2013) notes U concentrations can also be interpreted as changes in soil redox conditions as the mobility of U depends heavily on oxidation state, controlled by redox conditions in the overlying soil and epikarst. With more oxidising conditions causing increased U mobility and reducing conditions inhibiting U mobility (Jamieson *et al*., 2016; Zhou *et al.,* 2005). Furthermore, if accompanied by Sr, U can also be used as a proxy for hydrological conditions (Tolzmann, 2013). In comparison, Al, Th, Cu, and Pb are predominant indicators of detrital contamination, as they are not naturally present in the calcite lattice within a closed system (Riechelmann *et al.,* 2020). The interpretation of trace elements varies widely across different speleothems, due to the influence of controls such as overlying vegetation, soil type, and water sources. This means the interpretation of trace elements between speleothem can have large variability and different proxy information due to unique influences during formation.

2.5 Stable Isotopes

2.5.1 Oxygen Isotope Ratios

The controls on speleothem $\delta^{18}O$ are highly complex, and variations in $\delta^{18}O$ values can be substantial, even within the same region (Lachniet, 2009). As such, few studies have been able to reconstruct a clear universal climate signal from $\delta^{18}O$, as site-specific factors influence each speleothem's isotopic composition (Birks *et al.,* 2014, p.263). Current research predominantly interprets $\delta^{18}O$ as a proxy for precipitation at the time of formation

(δ^{18}Ow) (Couchoud *et al*., 2009; Dabowski *et al.,* 2016; Dhungana, 2010; Peral *et al.,* 2024). Isotopically heavier or more positive δ^{18}O values typically reflect drier conditions, whereas more negative and lighter δ^{18}O values correspond with wetter periods due to less ^{16}O being locked up within glaciers. This is particularly apparent during the last glacial period due to the numerous transitions between stadial and interstadial periods (Fuller *et al.,* 2008; Oster *et al.,* 2020; Lora *et al.,* 2017; Tolzmann, 2013). Furthermore, when correlated with elements such as Mg, Ba and Sr, δ^{18}O can also reflect water availability (Huang *et al.,* 2001; McDermott, 2004; Vansteenberg *et al.,* 2020; Peral *et al.,* 2024). Increases in Ba, Mg, and Sr concentrations, coupled with decreases in δ^{18}O and δ^{13}C values, suggest warmer and drier conditions. However, if these trace elements exhibit antiphase relationships with each other, the interpretation can be more complex, and indicate alternate controls are occurring (Vansteenberge *et al*., 2020).

δ^{18}O values within speleothem typically reflect the isotopic composition of precipitation, which various environmental factors influence, including the ice volume effect (global ice volume extent controlling ocean water δ^{18}O), altitude effect (isotopic depletion of δ^{18}O with increasing altitude), latitude effect (isotopic depletion of δ^{18}O with increasing distance from the equator), continental effect (isotopic depletion of δ^{18}O due to rainout over landmasses – Rayleigh fractionation), amount effect (isotopic depletion of δ^{18}O due to heavier rainfall), and the temperature effect (lighter isotopes evaporating more readily than heavier isotopes) (Tolzmann, 2013; McDermott, 2004). Therefore, research must consider these fractionation processes when interpreting δ^{18}O, as large regional variations in isotopic signature can occur due to the extent of these effects occurring (Mook, 2000; Fuller *et al.,* 2008). In Villars Cave, France, δ^{18}O values range from -5.67‰ to -4.76‰ ±0.09‰ (Dabkowski *et al.,* 2016), with similar values expected in the UK (Fuller *et al*., 2008). However, location factors such as latitude effect, continental effect, amount effect, and the temperature effect, will all vary at a different higher latitude location (Williams & Fowler, 2002; Baldini *et al.,* 2005).

2.5.2 Carbon Isotope Ratios

Present research recognises δ^{13}C as a proxy for precipitation, primary productivity, and vegetation shifts (Peral *et al.,* 2024; Dabkowski *et al.,* 2016; Dhungana, 2010; Fleitmann *et al.*, 2004; Weber *et al.,* 2018; Tremaine *et al.,* 2011). Denser vegetation and higher soil activity correspond with lower δ^{13}C values. Conversely, higher values of δ^{13}C indicate

vegetation degradation or increased flushing (Allen *et al.,* 2018; Hartland *et al*., 2012). When $\delta^{13}C$ values increase (becoming isotopically heavier) alongside Mg concentrations, they indicate colder and drier conditions. Whereas more negative (lighter) $\delta^{13}C$ and lower Mg concentrations are associated with warmer and wetter periods marked by denser vegetation and thicker soil layers (Oster *et al*., 2020; Weber *et al.,* 2018; Baker *et al.,* 2011; Baldini *et al.,* 2005). This is because cold and dry climates reduce vegetation density and microbial activity, leading to lower CO_2 production and higher $\delta^{13}C$ values (Held *et al.,* 2024; Baldini *et al*., 2005; Gascoyne, 1992; Genty *et al.,* 2006). Overall, during warmer and wetter periods, such as DO interstadials, increased vegetation development results in more biogenic CO_2, resulting in a lowering of $\delta^{13}C$ values (Baldini *et al.,* 2005; Dabkowski *et al.,* 2016; Arienzo *et al*., 2017; Tolzmann, 2013).

Regionally specific conditions such as soil CO_2, drip rate, dissolved bedrock, and rate of PCP also influence $\delta^{13}C$ values (Dulinski & Rozanski, 1990; Birks *et al.,* 2014, p.258). In the British Isles, an area dominated by C3 vegetation, $\delta^{13}C$ values typically range from -12‰ to -6‰, though studies have shown higher values of $\delta^{13}C$ in 75% of flowstone samples and 57% of stalagmites from British caves in comparison to other regions globally (Baker *et al.,* 1997). Baker *et al*. (1997) interprets the main control of their $\delta^{13}C$ data from sites all around the UK as PCP. This is because fractionation likely occurred before speleothem formation, due to above average values of $\delta^{13}C$ than those expected for C3 dominant regions. Within the context of DO-12, $\delta^{13}C$ data from Bunker Cave, Germany, displays a slow decrease to ~-9‰ (Weber *et al.,* 2018), rather than an abrupt transition into the DO event seen within other records, e.g., NGRIP $\delta^{18}O$ data (Kindler *et al.,* 2014). This may be due to a buffering effect of the soil, with soil recovery and vegetation formation taking longer after the termination of Heinrich stadial 5 before DO-12. Whereas, at the end of DO-12, Weber *et al.* (2018) interpret a significant increase in $\delta^{13}C$ ~43.3 ka BP, indicating a fast deterioration of soil back into a stadial period.

Future research needs an improved understanding of $\delta^{13}C$ fluctuations, particularly in temperate regions dominated by C3 vegetation for more accurate palaeoclimate reconstructions (Baldini *et al.,* 2005). The use of trace elements alongside stable isotopes can also provide critical insights into $\delta^{13}C$ variability. For example, Hellstrom & McCulloch (2000) found that variation in Ba concentrations ruled out PCP as a major influence on $\delta^{13}C$

increases. This demonstrates the importance of multi-proxy approaches to reduce uncertainty within stable isotope interpretation and climate reconstructions (McDermott, 2004).

2.6 Prior Calcite Precipitation (PCP) and Climate Reconstruction

2.6.1 PCP

In karstic environments, PCP occurs when dripwater either on the roof of the cave or within a karst cavity, comes into contact with air at lower CO_2 concentrations. This causes degassing of CO_2 and prior supersaturation of drip water, leading to calcite precipitation before final precipitation within a speleothem. Degassing enriches elements such as Mg, Sr and Ba, relative to Ca concentrations, and leads to isotopically heavier $\delta^{13}C$ within the speleothem (Tolzmann, 2013; Fairchild *et al.,* 2000; Fairchild & Treble, 2009). PCP strongly influences Mg, with elevated Mg/Ca ratios often indicating PCP occurrence (Fairchild, 2006). However, Mg should be cross correlated with proxies such as Sr, Ba, and $\delta^{13}C$ and $\delta^{18}O$, because Mg data can also be a proxy for rainfall (Weber *et al.,* 2018; Fairchild, 2006; Dabkowski *et al*., 2016). Although PCP commonly controls Mg concentrations and $\delta^{13}C$ within speleothems, research does not consider this control problematic for the identification of other proxies unless there is a statistically significant regression between In(Mg/Ca) and In(Sr/Ca) using the Sinclair test (Sinclair *et al.,* 2012).

2.6.2 Controls on PCP and Climate Reconstruction Potential

Tolzmann (2013) suggests that PCP is more prominent during drier climate periods, this is partly due to the temperature dependence of the Mg partition coefficient, which has the capacity to control the rate of PCP occurrence. There are two main controls on the rate of PCP, the Mg partition coefficient (D_{Mg}) and the Sr partition coefficient (D_{Sr}). Partition coefficients are the relationship between the trace element to calcium ratio of the carbonate compared to the parent solution (Drysdale et al., 2019). D_{Mg} is well documented to have a temperature dependence, in turn impacting the rate of PCP (Gascoyne, 1983; Huang & Fairchild, 2001; Day & Henderson, 2013; Wassenburg *et al.,* 2020). However, some speleothem studies have noted a stronger relation of Mg variations to hydrological changes than to temperature (Cruz *et al*., 2007; Weber *et al.,* 2018; Tremaine & Froelich, 2013).

The main dependence on D_{Sr} is suggested to be based on growth rate (Huang and Fairchild, 2001; Treble *et al.,* 2003; Belli *et al.,* 2017). However, there have also been studies which do not find this same growth rate dependency (Tremaine & Froelich, 2013; Day & Henderson, 2013). It has been suggested by Drysdale *et al.* (2019) based on the previous study by Huang & Fairchild (2001), that D_{Sr} may also be controlled by Na/Sr from the parent water, where higher Na concentrations can outcompete Sr from incorporation into the calcite lattice of the speleothem. This has been studied by Drysdale *et al.* (2019) through the analysis of seawater-analogues based on their higher Na concentrations in comparison to cave-analogues, but this control has not yet been concluded.

2.7 Mainland European Climate during MIS3

Studies have highlighted the sensitivity of speleothems in Europe to both regional and global climatic changes, with variation $\delta^{18}O$, $\delta^{13}C$, and trace elements allowing for detailed interpretations of climate fluctuations during the last glacial (Genty *et al.,* 2003; McDermott, 2004). For example, speleothem records from France, such as in Villars Cave, provide insights into temperature and precipitation changes during MIS3, with $\delta^{18}O$ and $\delta^{13}C$ indicating shifts in climate related to North Atlantic precipitation variations (Genty *et al.,* 2003; Guiot *et al.,* 1993). Similarly, speleothems from Bunker Cave, Germany, reveal a complex relationship between vegetation changes and $\delta^{13}C$ during transitions from stadial to interstadial periods (Weber *et al.,* 2018).

- **Villars Cave:** During DO-12 (~45.3 ka BP), the lowest values of $\delta^{13}C$ were recorded. Low $\delta^{13}C$ values correlate with higher $\delta^{18}O$ in ice cores, signifying warmer conditions and higher precipitation rates. This large shift in $\delta^{13}C$ also suggests a shift in vegetation dynamics during DO-12. DO events are less clearly seen within the $\delta^{18}O$ data, although $\delta^{18}O$ does correlate with regional pollen records, suggesting a temperature rise of ~8 °C during the period (Genty *et al.,* 2003; Guiot *et al.,* 1993).
- **Bunker Cave:** Research found that speleothem growth phases in Bunker cave correlate closely with periods of strong AMOC, reduction in influence of AABW, reduced sea ice, and low IRD within ice cores (Weber *et al*., 2018).
- **Han-sur-Lesse Cave:** Research observed $\delta^{18}O$ values varying between -3.8‰ to -5.8‰ and $\delta^{13}C$ between -1.5‰ to -5‰. A clear delay appears in the onset of climate amelioration and vegetation proxies for DO-12, attributed to delayed increases in

temperature and water availability for the right conditions to incept vegetation development. A slow climate deterioration is noted at the end of DO-12, with increases in $\delta^{13}C$, Mg, and Sr (Peral *et al.,* 2024).

- **Füramoos Cave:** Research describes DO-12 as one of the warmest interstadials of MIS3 and suggests this related to a maximum in obliquity (Sanchez Goñi *et al.,* 2008). It is further suggested this may indicate why vegetation growth was amplified to northern latitudes >40° during this specific DO event, allowing for speleothem formation at higher latitudes during DO-12 compared to other DO events during MIS3 (Sanchez Goñi *et al*., 2008; Kern *et al*., 2022).

3. Site Overview and Regional Geological Setting

3.1 Location in Context – Uamh Mhor, Knockan Basin

The Uamh Mhor cave within the Knockan basin is located within the region of Assynt, Northwest Scotland (Fig. 4). The Assynt region is located 15 km NE of Ullapool and 50 km SW of Durness. Uamh Mhor is overlain by an outcrop of 34 km^2 of dolomitic limestone of the Durness Group, alongside various clastic deposits believed to originate from local glacial deposits (Breitenbach *et al.,* 2024; Lawson, 1993; 1983; 1981; Atkinson & Lawson, 1995, p.61). The main source of cave water for the Uamh Mhor system is Loch Claonaite, which drains through all of the cave systems of the Allt nan Uamh region, controlling cave water levels (Lawson, 1981). In the late Pleistocene, the area of Assynt was dominated by imbricated stacks of dolomite which formed the foundation of a karst landscape. A low water table was present as a result of valley deepening, which likely enabled the formation of large cave systems such as Uamh an Tartair (knockan) and Uamh an Claonaite long before this period started (Atkinson & Lawson, 1995, p.61; Bradwell & Ballantyne, 2021, p.233). In the present day, the area of Assynt is dominated by a heather moorland landscape and blanket peatland (Breitenbach *et al.,* 2023).

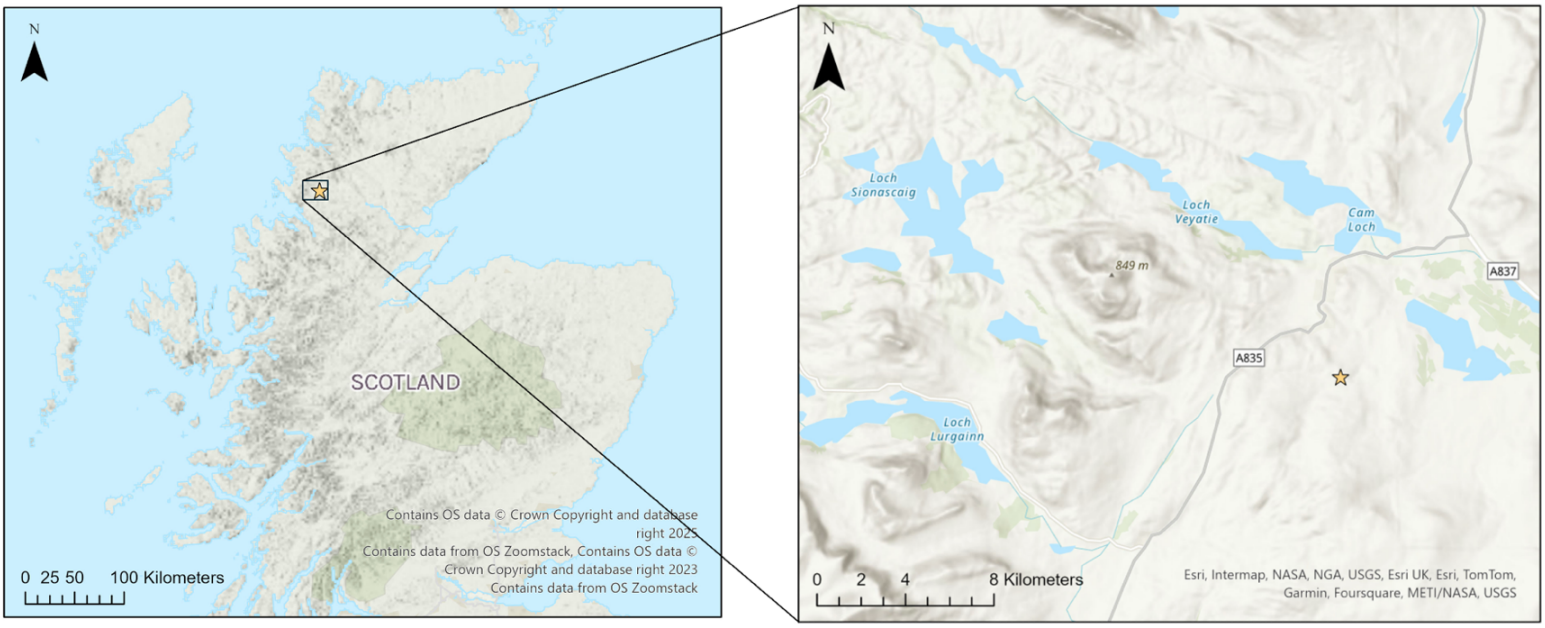

Figure 4. Location of Uamh Mhor, Knockan (star) within the region of Assynt.

3.2 Scottish Climate during MIS3

Northwest Scotland has a strong relationship between precipitation, NAO, and AMOC via the North Atlantic Drift. Within the region of Northwest Scotland, a positive NAO index is associated with intensified westerly winds and increased rainfall (Proctor *et al.,* 2000). Isotopically lighter or lower $\delta^{18}O$ values are also linked to wetter and warmer conditions, potentially providing a proxy of NAO patterns (Fuller *et al.,* 2008). Speleothem growth rates in the region are found to relate to NAO states, with lower growth rates corresponding to more negative NAO phases, whereas warmer, wetter conditions and a positive NAO phase accompany higher growth rates (Baker *et al*., 2015). The NAO exerts a significant influence on the climate of Scotland, with stronger westerlies leading to higher precipitation during positive NAO winters (Proctor *et al.,* 2000). This suggests that during interstadial periods, the climate in Northwest Scotland was primarily shaped by seasonal circulation patterns, with the NAO state playing a pivotal role, especially in response to large climate shifts.

3.3 Secondary Datasets and their Global Context

Speleothem stable isotope and trace element data from various regions, across Europe, Asia and South America, have been vital in extending the analysis of DO events beyond Greenland and identifying global teleconnections. Notable studies include Bleßberg Cave in Germany, the highest northern latitude speleothem identified from central Europe to date,

Hulu Cave in China and Marota Cave in Brazil all featuring DO event signals (Klose *et al.,* 2024; Liang *et al.,* 2019; Strikis *et al.,* 2018). These speleothem records provide crucial insights into the regional manifestations of DO events, offering a broader perspective on how abrupt climate shifts may influence or be influenced by different parts of the climate system. A better understanding of MIS3 and its associated DO events is crucial for reconstructing the climate dynamics and rapid climate shifts dominating the last glacial period.

4. Methodology

4.1 Flowstone Sampling

The flowstone sample SFMB20230528-1 (Fig. 5) was taken from Uamh Mhor, Knockan (58.3700° -4.9740° W) (Fig. 4), 213 m above sea level, as part of the Scottish Speleothem Dating Project 2024 (Breitenbach *et al.,* 2024). Uamh Mhor is an unroofed cave, with geomorphic evidence suggesting unroofing during the last glaciation (Breitenbach *et al.,* 2024). The flowstone samples were taken from a solutional hollow within the cave. They were deposited after an initial flowstone deposit on top of a layer of silty mud of ~1-2 mm. Followed by erosion of the top layer by smooth solutional fretting over their faces and overlain by an indurated gravel layer. SFMB20230528-1 and its sister sample UEA810527-2, are both white crystalline calcite flowstones. The dense calcite structure of the flowstones suggest they formed within an interior cave rather than exposed to open air which results in more granular calcite structures (Breitenbach *et al.,* 2024). Before any analysis was undertaken, the flowstones were analysed for evidence of recrystallization or inclusions and cleaned by ultrasonication in distilled water for 2–3 minutes. The flowstone SFMB20230528-1 was selected for its clean internal structure with no signs of hiatuses, clear visible layering (Fig. 5) and unique chronological setting within DO-12.

Figure 5. (A) Initial scan of flowstone SMFMB20230528-1 from the Scottish Speleothem Dating Project. (B) Photo of flowstone after sampling.

4.2 Uranium-Thorium (U-Th) Dating

4.2.1 U-Th Date Sampling

Uranium-Thorium ($^{234}U/^{230}Th$) dating was conducted to determine the age of the flowstone sample, as speleothem are considered closed systems, despite the potential contamination due to growth hiatuses, this method ensures accurate dating (Wu *et al.,* 2024; Hoffman *et al.*, 2009; Drysdale *et al.,* 2012; Constantin, 2015). Dating was performed by analysing ^{234}U and ^{230}Th isotopes from 150 mg of carbonate dust sampled at three equidistant points along the growth axis (Fig. 6). The first U-Th date (45,855 ±153 yrs BP) and the base of the sister sample UEA810527-2 (46,397 ±225 yrs BP) previously underwent dating as a part of the Scottish Speleothem Dating Project, the initial micro-milling was carried out by using a Sherline Micromill at Northumbria University (Breitenbach *et al*., 2024). The two additional dates were sampled for with a NewWave Research Micromill at Durham University. All

samples were radiometrically dated at the University of Oxford's radiometric dating laboratory using a Multi-Collector Inductively Coupled Plasma Mass Spectrometer (MC-ICP-MS), following the established method by Vaks *et al*. (2013).

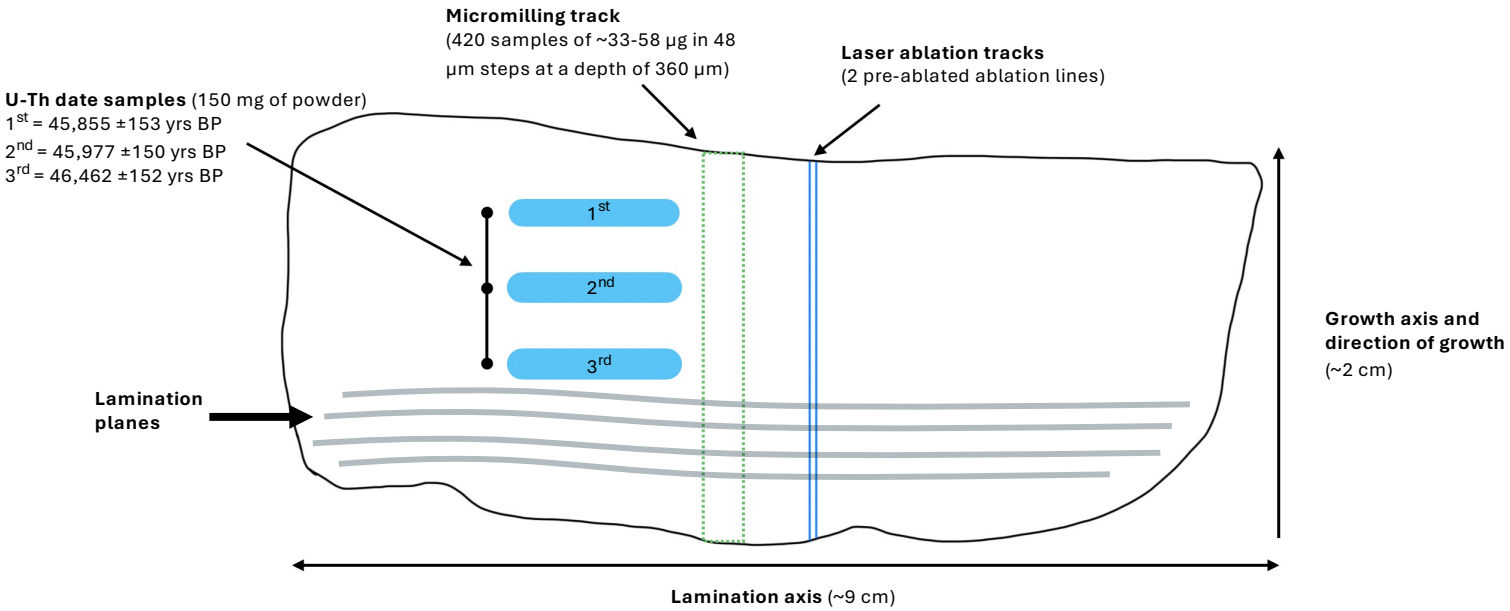

Figure 6. Schematic of the sampling procedure undertaken on flowstone SMFMB20230528-1 from Uamh Mhor.

4.2.2 Uamh Mhor (SMFMB20230528-1) Chronology

The three U-Th dates undertaken for Uamh Mhor range from 45,855 ±153 yrs BP, 45,977 ±150 yrs BP and 46,462 ±152 yrs BP (Fig. 6). An age-depth model was conducted through COnstructing Proxy Records from Age models (COPRA) software, based on these three U-Th dates (Fig. 7). Within COPRA a non-linear, piecewise cubic Hermite interpolation age-depth model was utilised, built from a Monte-Carlo ensemble of age uncertainties. The U-Th dates demonstrate a slower growth rate between the two initial U-Th dates between 46,462-45,978 BP at ~40.98 µm/year, during initial growth stages. The growth rate is seen to increase from the initial rate to ~15.88 µm/year between 45,977-45,855 BP, the height of the DO event. The U-Th date for the base of the sister sample UEA810527-2 (46,397 ±225 yrs BP), notes a younger age of the flowstone base than observed in the 3rd U-Th date from SMFMB20230528-1. Although there is a larger uncertainty produced from the U-Th dating of the sister sample, this still presents chronological uncertainty within the initial growth of the flowstone. This discrepancy may reflect dating uncertainty, layer position changes

between SMFMB20230528-1 and UEA810527-2 or contamination from detrital material. However, the growth period between the three U-Th dates for SMFMB20230528-1 remains chronologically consistent, with a faster growth rate between the 2nd and 1st U-Th dates during the height of the DO event. Further boundary dating would improve model precision, but this is outside the scope of the current project.

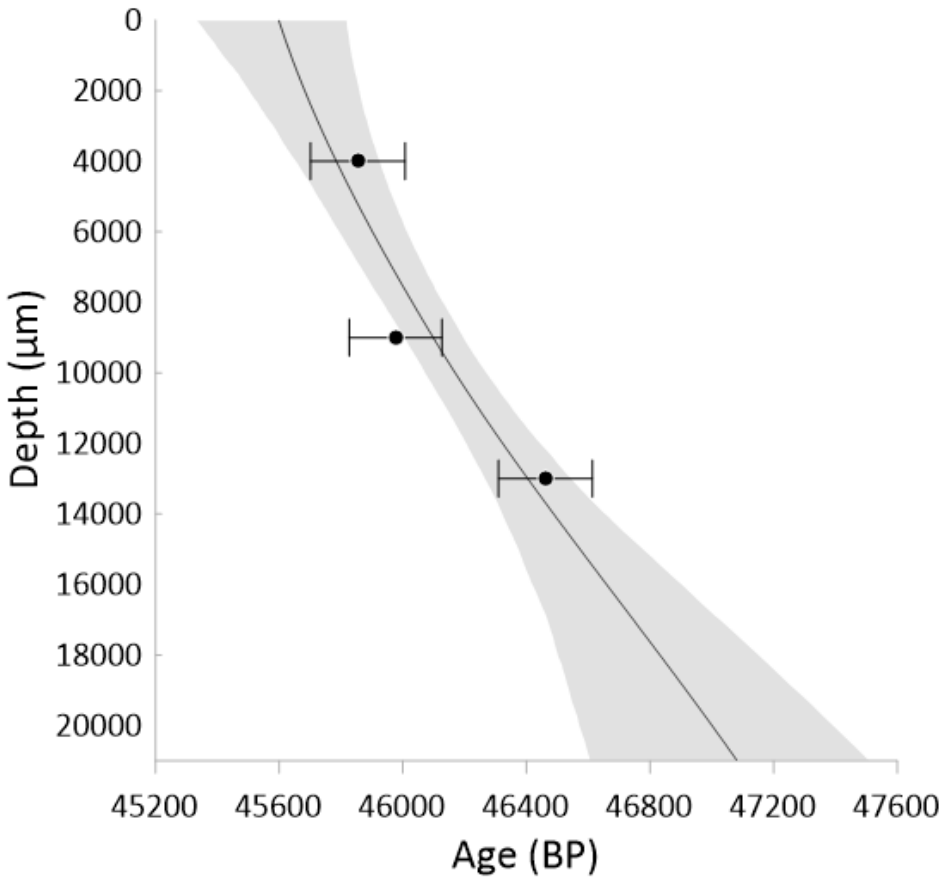

Figure 7. SFMB20230528-1 Chronology. A piecewise cubic Hermite interpolation age-depth model created within COPRA. Black line signifies the modelled age-depth and the grey shaded area signifies the 2.5 %-quantile and 97.5 %-quantile confidence interval of the U-Th chronology produced by COPRA. Black points indicate U-Th ages at individual depths within the sample and their associated age uncertainty of 2σ.

4.3 Stable Isotope Analysis

4.3.1 Micro-milling Sample Preparation

To produce a high-resolution stable isotope record, micro-milling was selected as the preferred method. In comparison, other methods such as laser ablation offer a higher processing speeds, but consequently this can result in lower precision data (Hoffman et al., 2009; Spötl & Mattey, 2006; Mattey *et al.,* 2010; Frappier *et al.,* 2002; Mangini *et al.,* 2005).

Micro-milling was conducted using a NewWave Research Micromill with a 4 mm steel drill bit. The sample was securely fixed to the micro-mill stage to prevent movement, and the equipment was calibrated according to the sample's size, shape and plane angles (Riechelmann *et al.,* 2020; Drysdale *et al.,* 2012). Incisions were made at 48 μm steps along the lamination planes, parallel to the growth axis starting from the oldest end of the sample (Fig. 6). Sampling intervals of 100-250 μm are typical for high resolution speleothem sampling (Hoffman *et al.,* 2009; Mattey *et al*., 2008; Spötl & Mattey 2006; Dhungana, 2010). However, due to the slow growth rate initially calculated for the flowstone based on the first U-Th date and a U-Th date taken from a sister sample (~24 μm/year), 48 μm was used to enhance the possible detection of annual patterns within the data whilst ensuring sampling duration was suitable for the extent of time for this thesis.

A milling depth of 360 μm was used to ensure sufficient powder (~33-58 μg) was collected for stable isotope analysis. Given the estimated sample growth of ~24 μm/year, this depth still provides high-resolution data whilst accounting for lamination trajectory uncertainties (Baldini *et al.,* 2021; Drysdale *et al*., 2012). To prevent contamination, the drill and sample surface were cleaned with ethanol between milling each sample (Spötl & Mattey, 2006; Drysdale *et al.,* 2012). The carbonate powder produced was transferred into 4.5 ml vials for stable isotope analysis.

4.3.2 $\delta^{18}O$ and $\delta^{13}C$ Isotope Analysis

Stable isotope analysis ($\delta^{18}O$ and $\delta^{13}C$) was conducted using a ThermoScientific MAT 253 Stable Isotope Gas-Source Mass Spectrometer at Northumbria University. International standards IAEA-603 and NBS-18 were used alongside in-house standards Pol-2 and Plessen. A total of 420 vials of ~33-58 μg of carbonate powder were produced for analysis in batches of 61. Batch analysis was conducted to prevent cyclical signal contamination during analysis

and allow for faster processing of samples due to analysis backlog. Samples were additionally analysed in a randomised order between batches to further prevent contamination from laboratory conditions (Baldini *et al*., 2021). Due to analysis backlog within the laboratory, stable isotope analysis could not be conducted on all samples before the completion of this thesis. However, due to the sampling strategy and the range of randomised samples able to be processed, the $\delta^{18}O$ and $\delta^{13}C$ samples which were processed were robust enough to enable corroboration with the results of trace element analysis.

4.4 Trace Element Analysis

4.4.1 Analysed Elements

Specific trace elements were selected for analysis based on their potential climate proxy signals:

- **Sr, Mg and Ba** – Potential indicators of precipitation levels, local vegetation changes and soil weathering (Riechelmann *et al*., 2020; Mattey *et al.,* 2010; Warken *et al.,* 2018)
- **Al, Th and P** – Potential indicators of detrital material, soil composition and vegetation dynamics (Riechelmann *et al.,* 2020).
- **Pb and Cu** – Potential indicators of detrital contamination or groundwater chemistry shifts due to high precipitation and metal transport changes (Borsato *et al*., 2007).
- **Si** – Potential indicator of soil weathering, rainfall and calcite precipitation. High Si/Ca ratios observed to correlate with low rainfall (Hu *et al.,* 2005).
- **U** – Potential indicator of soil redox reactions, as U is more soluble in oxidizing conditions, with increased rainfall facilitating greater U incorporation into speleothem carbonate (Hellstrom & McCulloch, 2000).

4.4.2 Laser Ablation Inductively Coupled Plasma Mass Spectrometry (LA-ICP-MS)

Although LA-ICP-MS has a lower precision than micro-milling (Spötl & Mattey, 2006), this technique was undertaken due to its rapid analytical capability. Despite this lower precision,

laser ablation remains a robust method for identifying elemental concentrations in speleothem records (Fairchild *et al.,* 2006; Ridley *et al.,* 2015; Baldini *et al.,* 2021).

LA-ICP-MS was conducted at Durham University using a New Wave UP-193 laser system coupled with a ThermoScientific iCAP TQe ICP-MS. A rectangular spot size of 10 x 140 µm, an advance rate of 10 µm/s, and a laser repetition rate of 15 Hz were utilised. Pre-ablation lines were run before official track runs to ensure a clean sample surface and to reduce levels of contamination. Two ablation lines were conducted on the sample to enable cross comparison of results to reduce uncertainty within data analysis (Fig. 6). For standardisation purposes elements were calibrated to the standards NIST 610, NIST 612 and BHVO2 repeatedly during analysis, with instrument drift monitored through deviations in ^{43}Ca concentrations expected within speleothem to be approximately 40% of total calcium content.

4.5 Secondary Data

4.5.1 Palaeodata

Secondary data from Europe and the Caribbean will be utilised for this thesis, alongside ice-core data from Greenland (Fig. 8). This palaeodata is being used for a cross-comparison of potential proxies identified from Uamh Mhor and assess the extent of correlation with the current highest resolution datasets from the same period. Furthermore, allowing for a comparison between age dating and growth onsets and terminations. It is important to note there is a strong lack of trace element data globally during DO-12, highlighting the unique contribution of trace element data during DO-12 from Uamh Mhor.

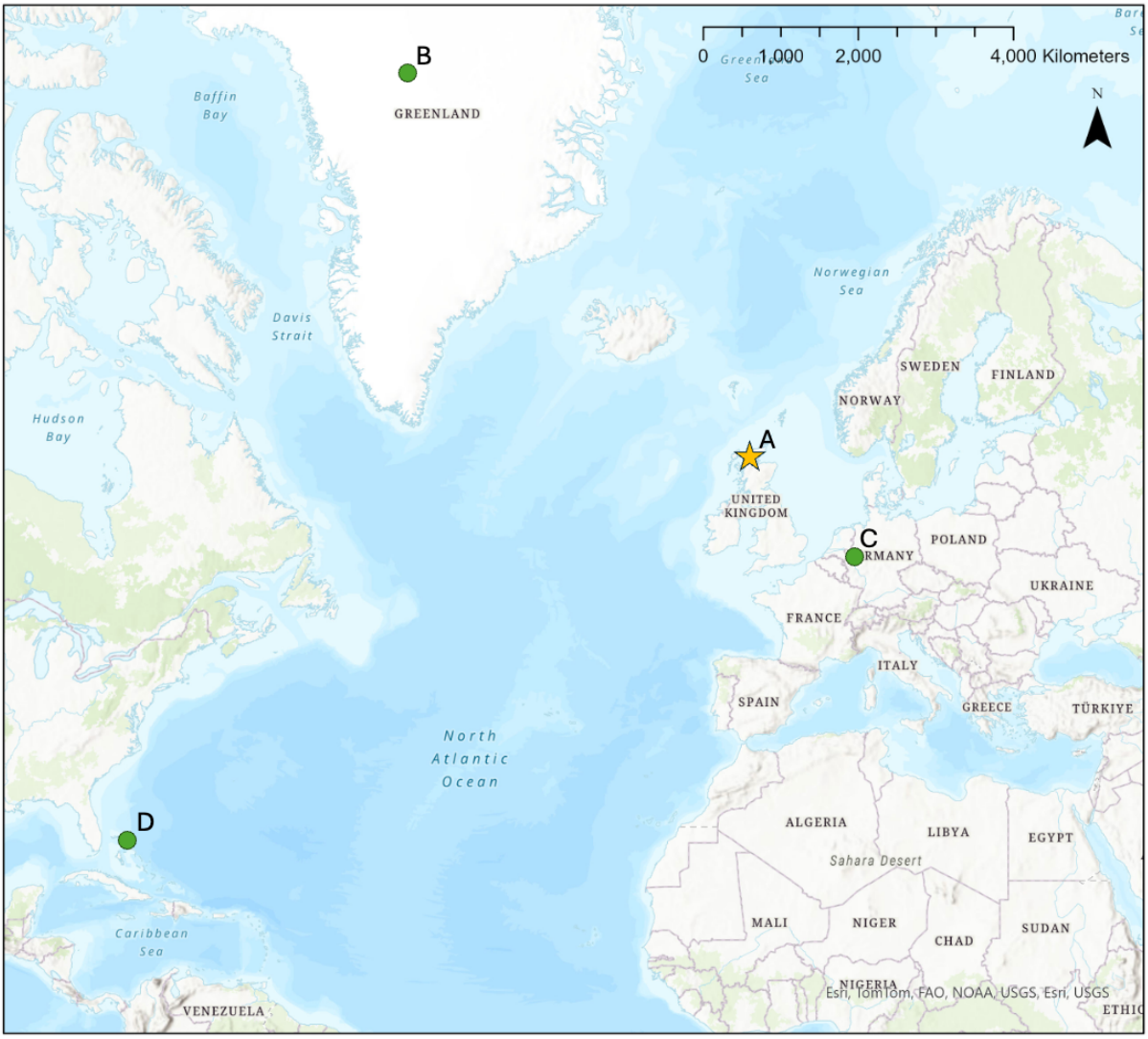

Figure 8. Location of Uamh Mhor (A) and other palaeo datasets (B – Ngrip (Svensson *et al.,* 2008), C – Bunker cave (Weber *et al.,* 2018), D – Abaco cave (Arienzo *et al.,* 2017)) within a North Atlantic regional context.

4.5.2 Contemporary Data

Modern precipitation data from the past century has been utilised from four sites closely located to the North Atlantic, Bordeaux (France), Aberporth (Wales), Kinlochewe (Scotland) and Wick (Scotland) (Menne *et al.,* 2012). These records were chosen based not only on relative coastal location but due to the length of their continuous records to be able to identify significant NAO-like cycles within spectral analysis. This has limited the number of modern records able to be utilised. This data is used to identify any differences in the palaeo-NAO signal from DO-12 and the present NAO signal across the North Atlantic region over the past century.

4.6 Data Analysis Methods

4.6.1 Principal Component Analysis (PCA)

PCA was conducted within MATLAB to identify correlations between trace elements within the sample through time and highlight the strength of correlations to explained variance within the data. A timeseries plot, a loading plot and a biplot were produced for Principal Components (PC1 and PC2) identified within analysis.

4.6.2 Dynamic Time Warping (DTW)

DTW was conducted within MATLAB to assess the level of synchronicity between this study and secondary palaeo datasets from Bunker Cave, Germany and Abaco Cave, Bahamas, the two closest resolution datasets available over the period of DO-12. DTW works through analysing the best fit of one interpolated dataset to another through shifting values (warping/wiggle) over a designated time interval to assess for a maximum correlation to the second dataset. Due to Uamh Mhor having the largest number of U-Th dates with the lowest uncertainty for the period, Uamh Mhor was used as the most reliable chronology, with Bunker and Abaco being warped to the new SFMB20230528-1 chronology.

4.6.3 Spectral Analysis (REDFIT - Morlet)

REDFIT Spectral analysis was conducted through PAST software on Mg from Uamh Mhor and additional Mg datasets from Bunker Cave, Germany (Weber et al., 2018) and Abaco Cave, Bahamas (Arienzo *et al.,* 2017). Each dataset analysed was interpolated and de-trended before analysis. This was conducted to identify significant cycle lengths between regions surrounding the North Atlantic over the period 45,720-46,500 BP, this period was constrained due to hiatuses within the other datasets. Spectral analysis was also conducted on modern precipitation datasets from Bordeaux, Aberporth, Kinlochewe and Wick (Menne *et al.,* 2012) to analyse for the length of contemporary climate cycles around the North Atlantic region. This was then compared to the palaeoclimate cycle lengths identified in the North Atlantic region during DO-12.

4.6.4 Sinclair Test

The Sinclair test, introduced in 2012 by Sinclair *et al*., was utilised to assess the potential level of PCP occurring within the sample and its potential control on stable isotope and trace element concentrations. This was conducted through the analysis of the slope of regression between In(Mg/Ca) against In(Sr/Ca).

4.6.5 Sea Spray and PCP Vector Calculations

Sea spray and PCP vectors were calculated for the specific regional conditions for Uamh Mhor. An analysis of Mg/Sr precipitation control was conducted due to Mg concentrations potentially being a proxy for sea spray as well as PCP. Higher sea spray contributions within precipitation result in higher Mg concentrations within dripwater, and consequently higher deposition of Mg within speleothems. The vector more closely aligned with the Mg/Sr data from the speleothem indicates the strongest control on Mg and Sr concentrations.

A model for calculating sea spray and PCP vectors was utilised, and input conditions adjusted, from Forman *et al*., (2025) for dolomitic limestone bedrock (Drysdale *et al.,* 2019; BGS, 1979; BGS, 1956; Jakic *et al.,* 2016). Different PCP vectors based on temperature controlled distribution coefficient for magnesium (D_{Mg}) values were calculated under various temperature scenarios based on previous research from a variety of cave and dripwater environments (Gascoyne, 1983; Huang *et al.,* 2001; Huang & Fairchild, 2001; Fairchild *et al.,* 2010; Day & Henderson, 2013; Tremaine & Froelich, 2013; Howson *et al.,* 1987; Hartley & Mucci, 1996; Oomori *et al.,* 1987; Mucci, 1987; Burton & Walter, 1991; Mucci & Morse, 1983; Drysdale *et al.,* 2019). The D_{Mg} equation from previous literature which best fit the Mg/Sr data from Uamh Mhor is from Drysdale *et al.* (2019; 2020). This is notably the only paper whose D_{Mg} equation, when used to calculate a PCP vector, showed to fit within the bounds of our data due to abnormally high Mg/Sr values.

4.6.6 Temperature Reconstruction and Dryness Index Creation

An estimated temperature value for each individual Mg/Sr datapoint was calculated based on the slope of the temperature dependent PCP vector each individual Mg/Sr datapoint fits onto, input into the equation for the relationship between slope of PCP vectors in relation to temperature. This was calculated based on temperature scenarios of 1, 10 and 25 ^{o}C fitted to the Drysdale *et al.* (2019; 2020) D_{Mg} equation.

Dryness was reconstructed through each individual Mg/Sr datapoint being assigned into a dryness Index. The values are based on the distance of each datapoint along its respective PCP vector. Distance along the PCP vector was calculated for each Mg/Sr datapoint through Pythagoras' theorem (Fig 9). Based on its respective temperature value this was applied within the equation for the linear relationship between temperature values and Mg vector origin, minus the minimum length, divided by the maximum length and multiplied by 100. This creates an index between 0-100 for each datapoint based on the distance along the respective PCP vector. The index values imply driest conditions closest to 100 and highest moisture conditions closest to 0.

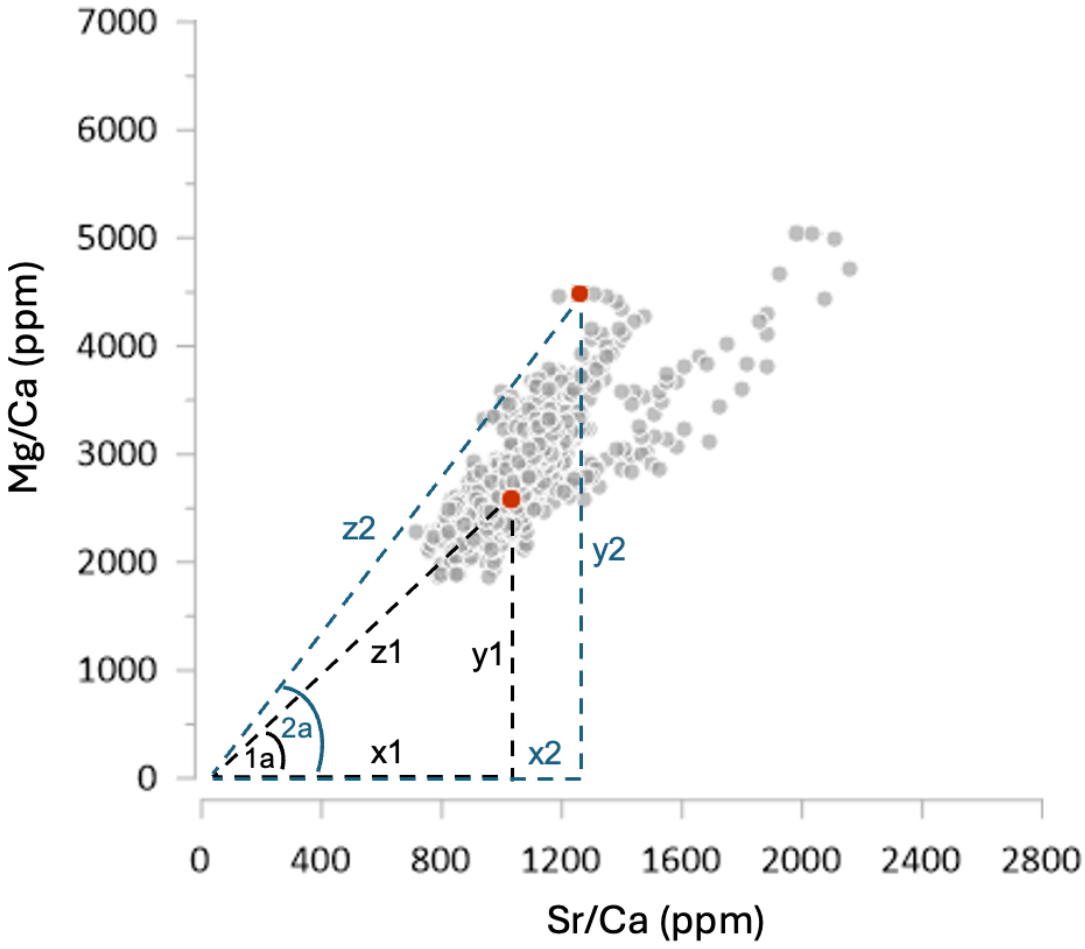

Figure 9. Method for calculating Temperature and Dryness Index for each Mg/Sr datapoint, (example of two data points (black (1) and blue (2) lines) using PCP vector angles (1a and 2a) and Pythagorean theorem to assess distance of points along their respective PCP vector (z1 and z2).

Temperature and dryness reconstructions are further interpreted alongside stable isotope data ($\delta^{18}O$ and $\delta^{13}C$). It is important to note not all stable isotope samples could be fully analysed due to an analytical error with the laboratory and time constraints for this research. However, enough stable isotope data points exist to be able to reasonably compare the pattern of data with the results from temperature and dryness reconstructions.

5. Results and Discussion

5.1 Trace Elements

Trace element concentrations in the Uamh Mhor flowstone were analysed to assess their variability during the DO-12 interval and to identify potential climatic and hydrological drivers. Focus was placed on Mg and Sr, given their established roles as proxies for PCP processes and hydroclimate variability in speleothem records. The analysis also considers the potential contribution of other trace elements to the overall geochemical signal.

5.1.1 Timing of Growth Onset and Termination

Speleothem growth at Uamh Mhor terminates around 45.6 ka BP ±153 yrs, which is notably earlier than other European speleothem records for the same period, such as Bunker Cave at 42.8 ka BP ±720 yrs (Weber *et al*., 2018) and Villars Cave at 42.3 ka BP ±508 yrs (Genty *et al*., 2003). The absence of geochemical evidence for hiatuses or significant contamination supports the reliability of this chronology. This earlier cessation, likely influenced by the cave's high latitude location, provides rare insight into hydroclimatic conditions in a region previously thought too cold for sustained speleothem growth during this interstadial.

5.1.2 Trends in Cu, P, Th, Al, Pb, Si, U and Ba

Cu (Fig. 10) and P (Fig. 11) remain at consistently low concentrations throughout the record, with running averages not exceeding 1.6 ppm. This stability, supported by similarly low concentrations of Th and Al (Fig. 11), suggests the absence of significant detrital contamination or growth hiatuses. A single Pb anomaly (~31 ppm at ~46,414 BP) is not mirrored in other detrital indicators (Cu, Al, Th, P), indicating an isolated event rather than obvious contamination. Al and P (Fig. 11) display similar low-amplitude variations that could reflect subtle changes in source water composition. A small number of elevated Al values

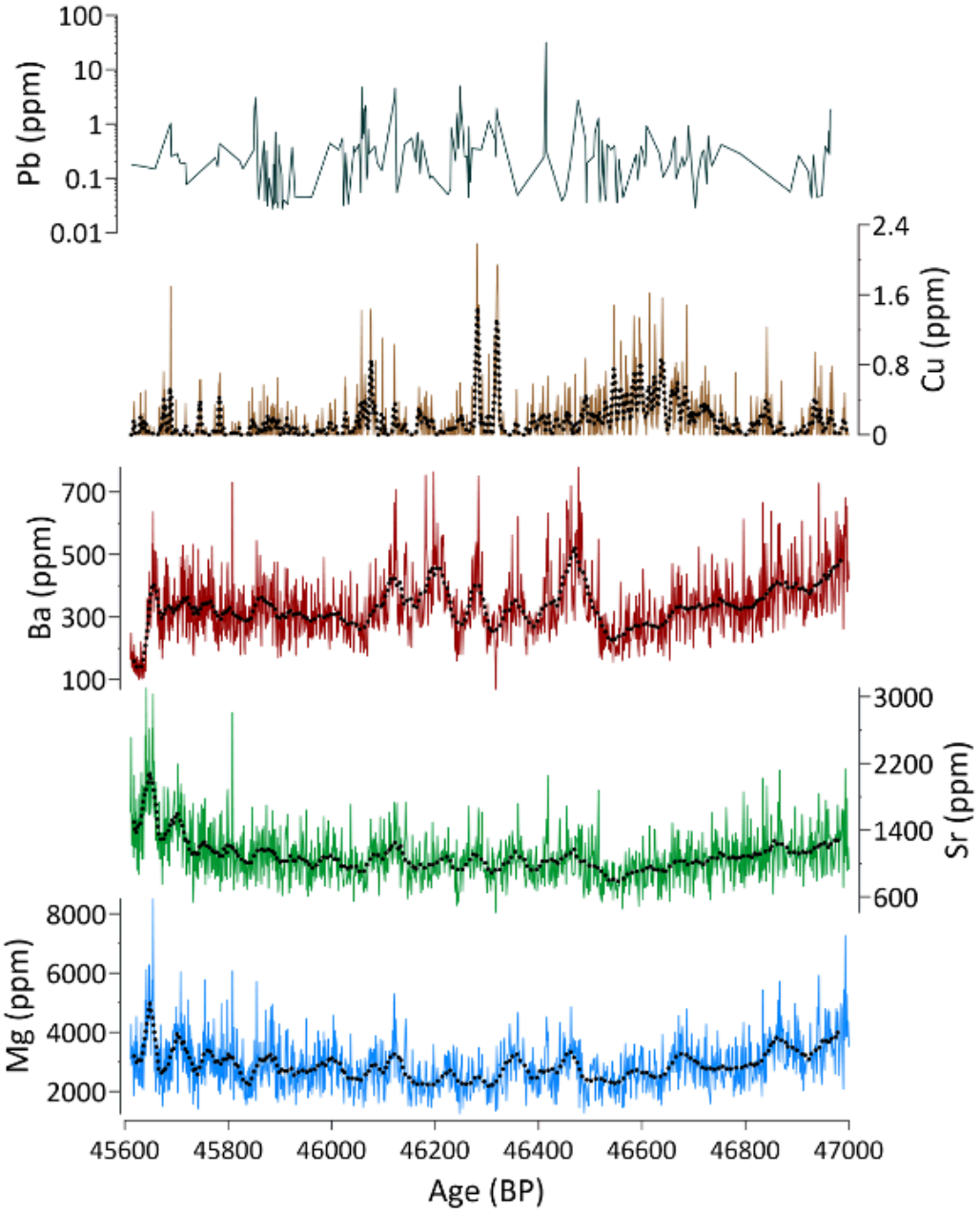

Figure 10. Divalent cations Mg (blue), Sr (green), Ba (red), Cu (brown), Pb (cyan) with 23-year running means denoted in black dotted lines. The data coverage extends for 1,090 years, from 45,610-46,700 BP.

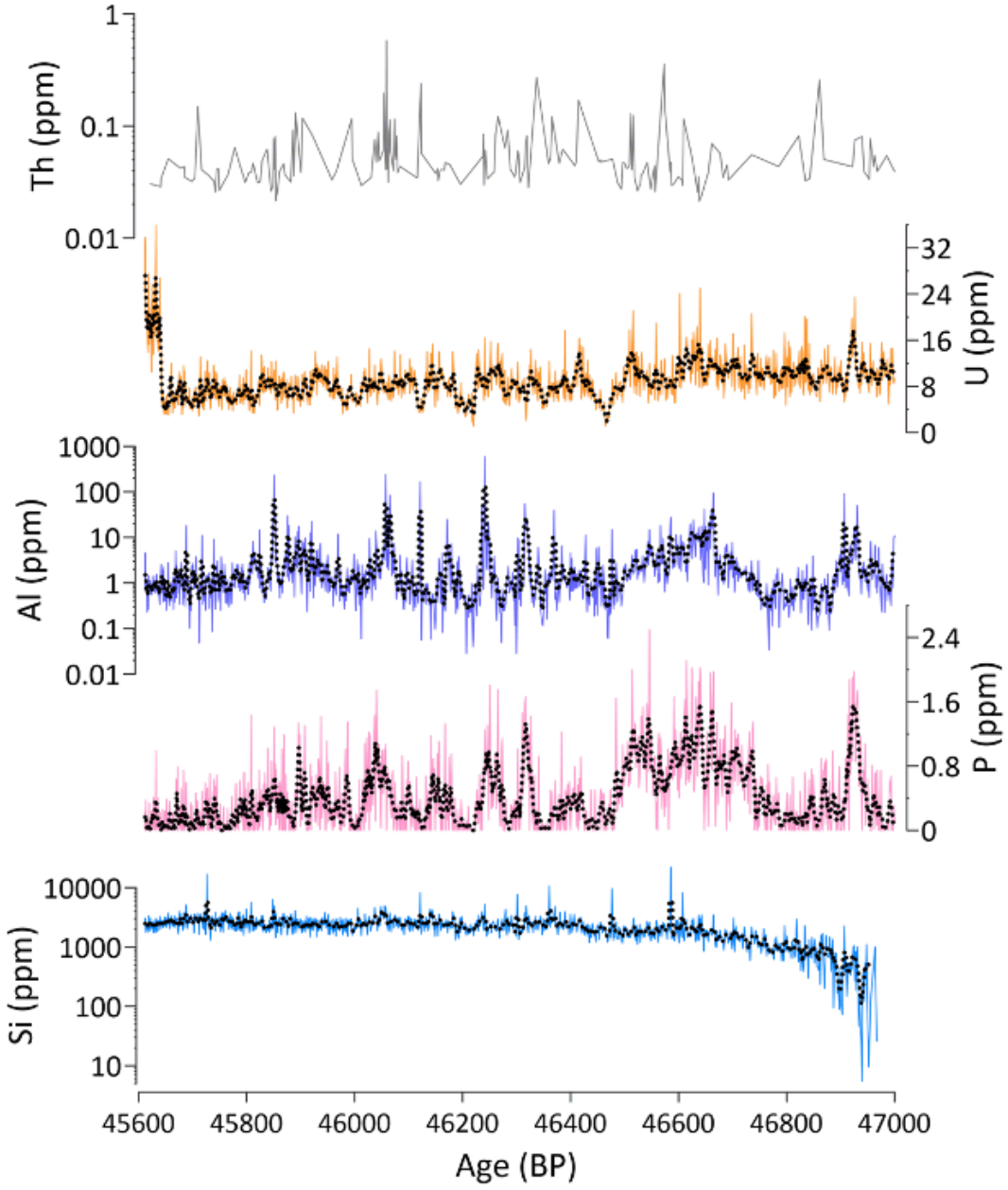

Figure 11. Multivalent nonmetals Si (blue), P (pink), Al (purple), U (yellow), Th (grey), with 23-year running means denoted in black dotted lines.

(e.g. 590 ppm at ~46,240 BP) may correspond to episodic soil disturbances or short-lived erosion events (Riechelmann *et al.*, 2020). Si (Fig. 11) demonstrates a pronounced logarithmic increase of ~3000 ppm coincident with the onset of DO-12, after which concentrations stabilise. This trend suggests intensified chemical weathering and increased surface erosion, possibly linked to warmer and wetter conditions. However, the lack of a

corresponding decrease in Si concentrations in the youngest part of the record raises questions about the persistence of these processes if glacial conditions had fully returned.

U and Ba (Fig. 11) display an inverse relationship at the youngest part of the record (~45,650 BP), with U concentrations increasing sharply by ~24 ppm whereas Ba decreases by ~350 ppm. This divergence may indicate changing redox conditions, with U being more mobile under oxidising conditions, and Ba under reducing conditions (Hercman *et al*., 2020). Alternatively, the observed trends may result from changes in hydrological pathways or enhanced groundwater concentration.

5.1.3 Mg and Sr Variability and Climate Proxy Potential

Divalent cations Mg and Sr (Fig. 10) show a gradual decline in concentration during the transition into DO-12, spanning approximately ~46,550-47,000 BP. At the onset of the record, Mg and Sr concentrations average ~2000 ppm and ~1000 ppm respectively. Towards the youngest part of the record (~45,650 BP) both exhibit a sharper increase in concentration, reaching ~4000 ppm (Mg) and ~1600 ppm (Sr), consistent with a return to glacial conditions. This pattern contrasts with the NGRIP $\delta^{18}O$ signal, which characteristically displays an abrupt onset to interstadial conditions (Kindler *et al*., 2014). The trace element signal at Uamh Mhor likely reflects the lag in supra-cave hydrological adjustment following abrupt warming, which prevents the initial abrupt warming signature seen within NGRIP $\delta^{18}O$ due to growth initiation at the height of this initial warming, whilst still displaying the more gradual re-establishment of stadial conditions. Kindler *et al.* (2014) also note that Heinrich events are often followed by extended warming phases, such as preceding DO-12, which may further explain the observed transition. It is also likely that speleothem growth at Uamh Mhor ceased before the full termination of DO-12 due to sudden environmental shifts, such as loss of a moisture source or extreme cooling. Although, given the cave's higher latitude setting, the termination of DO-12 would lead to an earlier cessation of growth at Uamh Mhor relative to lower latitude records, e.g. Bunker cave (Klose *et al.*, 2024b).

PCA (Fig. 12) clearly reveals PC1 dominated by high loadings of Mg and Sr, and to a lesser extent Ba. This is consistent with previous studies that associate Mg/Ca and Sr/Ca ratios with PCP processes (Fairchild, 2006; Dabkowski *et al.,* 2016). However, alternative potential controls must be tested before attributing these elements solely to PCP (Sinclair *et al*., 2012), these controls will be explored in subsequent sections. PC2 displays strong positive loadings

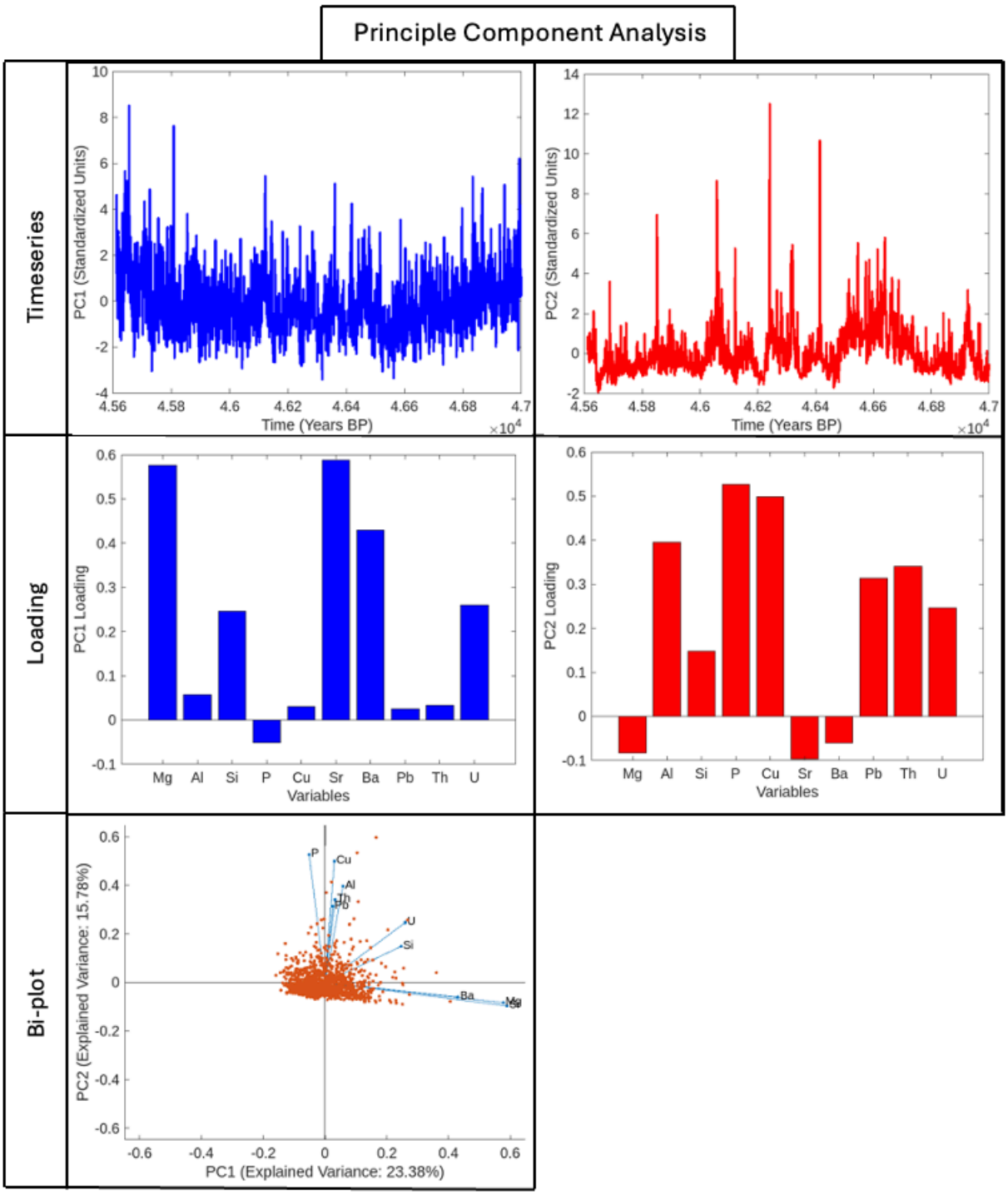

Figure 12. Principal Component Analysis (PCA) for all trace element data from 45,620-47,000 BP. PC1 is represented in blue and PC2 is represented in red, with the biplot showing the strength of the relationship of each element with PC1 and PC2.

for typical detrital elements, suggesting it represents a detrital signal. The negative loading of Mg, Sr and Ba in PC2, alongside the lower variance of these elements relative to others in the biplot, supports their distinction from the detrital signal. These PCA results highlight the strong geochemical coherence of Mg and Sr, with Ba as a potential secondary signal, supporting their use as the most robust potential climate proxies within this dataset. Their reliability is critical for facilitating climate reconstruction which will be elaborated upon in subsequent sections.

5.2 Comparison to other Palaeoclimate Records from DO-12

Having established the internal geochemical behaviour of the flowstone and the climatic significance of Mg and Sr variability, the next step is to assess how this pattern aligns with independent palaeoclimate records from across the North Atlantic region. Comparative analysis of Mg concentrations from Uamh Mhor with high-resolution speleothem records from Bunker Cave (Germany) and Abaco Cave (Bahamas) assesses the wider applicability of the Uamh Mhor data and their alignment with published speleothem records during DO-12. This cross-validation helps identify any potential anomalies within the Uamh Mhor record, which may indicate site-specific influences on Mg variability, regional climate differences, or asynchronous environmental responses. Furthermore, it provides insight into whether Mg exhibits a coherent signal across speleothem records from different latitudes, supporting its use as a climate proxy within the North Atlantic region.

5.2.1 Dynamic Time Warping (DTW) Correlation

A strong positive correlation is observed between Uamh Mhor and Bunker ($R^2 = 0.592$), and Abaco ($R^2 = 0.636$) (Fig. 13). At not point does warping reach the maximum allowable threshold of 100 years, suggesting that similar climatological processes influenced the datasets at broadly the same time. However, notable temporal shifts are required to maximise the correlation; for example, a large positive warping occurring between 46,500-46,100 BP is required, and a negative warping evident from 45,825-45,720 BP. This pattern suggests that either i) the onset of DO-12 occurs at different intervals across the different regions, ii) a combination of latitudinal differences and differential initiation of speleothem growth, iii) U-Th dating uncertainties, or iv) site-specific geochemical controls on Mg incorporation.

Comparison of U-Th age dating shows that Uamh Mhor is supported by three U-Th dates within the DO-12 interval, whereas Bunker and Abaco have only two each (Fig. 14). Uamh Mhor also displays lower analytical uncertainty, with a 2σ uncertainty of ±153 yrs, compared to much wider ranges in the secondary datasets, including a 2σ uncertainty of ±209 yrs from Abaco and ±720 yrs from Bunker. The lower uncertainty strengthens the reliability of the Uamh Mhor chronology and introduces new knowledge on the timing of climate development and speleothem growth at higher latitude regions in comparison to lower latitude regions within DO-12.

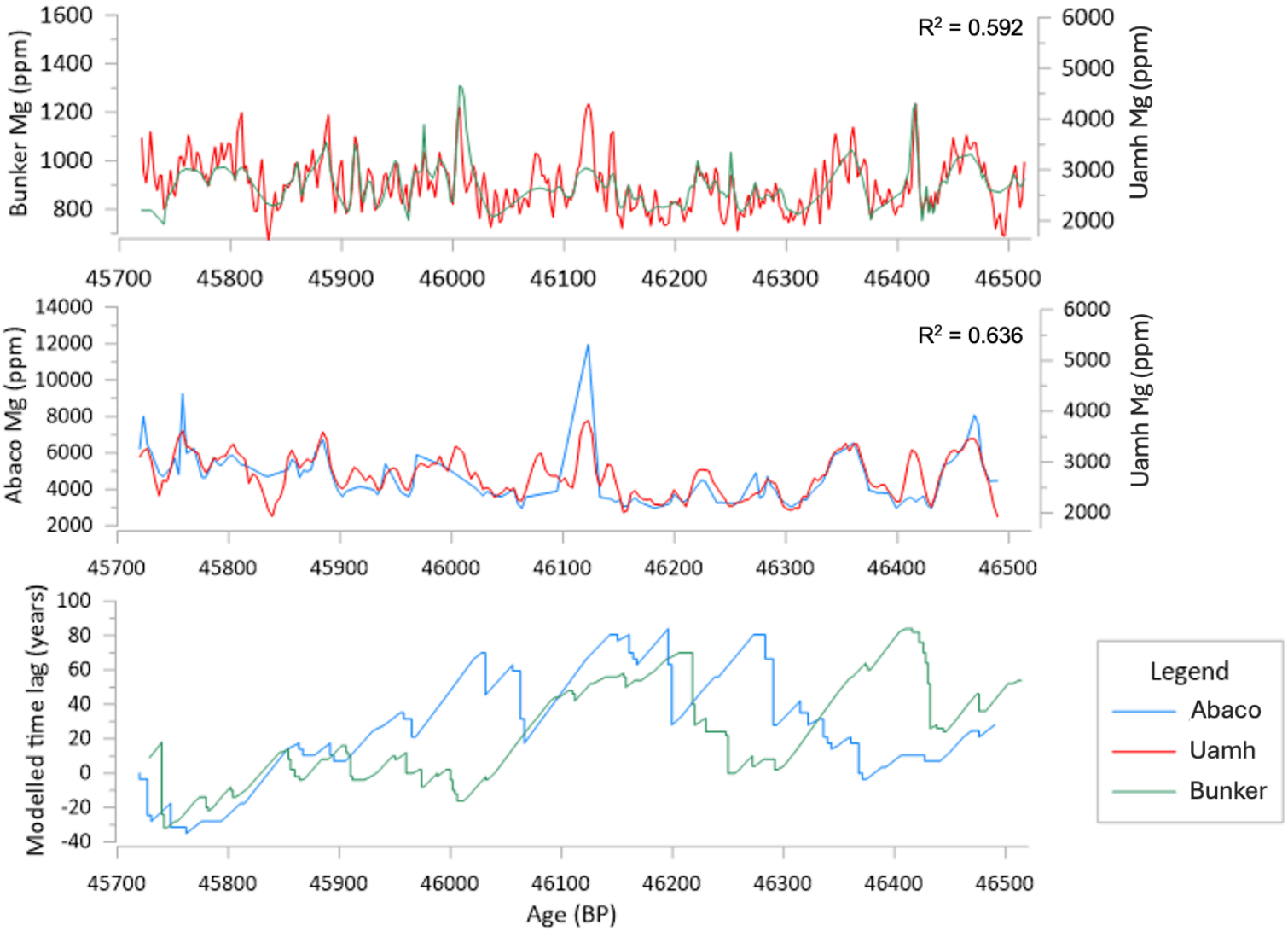

Figure 13. DTW of Abaco (blue) and Bunker (green) Mg concentrations against Uamh Mhor (red) Mg concentrations (ppm) from 45,720 to 46,500 BP. Savitzy-Golay 5 smoothening was applied to Uamh and Bunker datasets, with the exception of

Abaco due being at a lower resolution. A 100 year warp spacing was allowed for Abaco and Bunker Mg, displayed through modelled time lag.

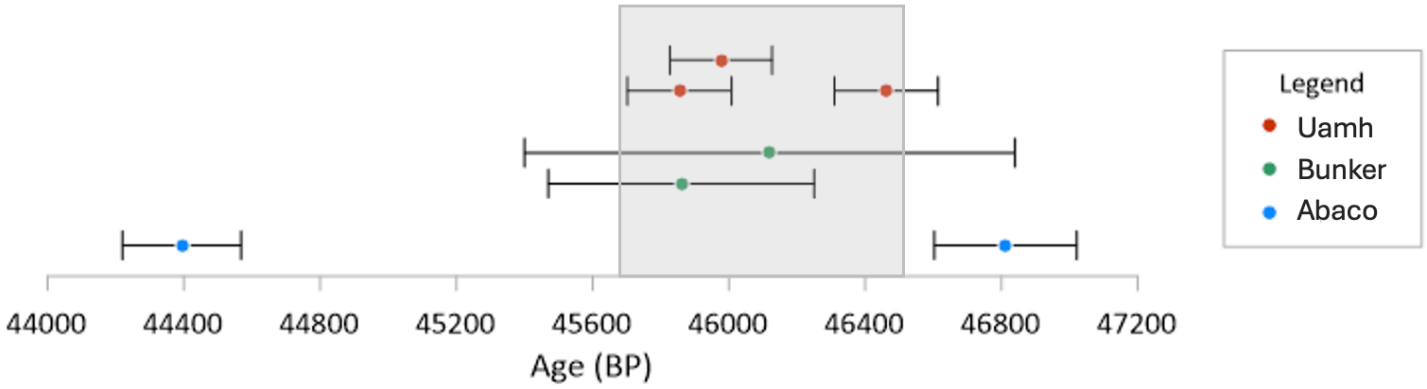

Figure 14. U-Th ages and uncertainties of Abaco (blue), Bunker (green) and Uamh Mhor (red) have been represented across the period of 44,000-47,200 BP. The period of study analysed within this thesis has been highlighted in grey.

5.2.2 Spectral Analysis and Climate Cyclicity

Spectral analysis was applied to Uamh Mhor Mg concentrations to investigate the potential for the sample to record cyclicity within the frequency ranges commonly associated with major climate modes (Fig. 15), such as the NAO (2-10 years) (Olafsdottir *et al.,* 2013; Seip *et al.,* 2019). Longer periodicities have been attributed to the AMO (30-90 years) and the AMOC (90-180 years) (Börget *et al.,* 2020).

Analysis of the Abaco and Bunker data (Fig. 15) reveals limited expression of high frequency NAO-related periodicities. Specifically, no consistent NAO-band (2-10 year) signals are observed, apart from one significant ~10-year cycle detected in the Abaco record at the 95% confidence interval. The relatively low resolution of existing datasets for this interval likely limits their ability to resolve short-term oscillations. In contrast, the higher temporal resolution of the Uamh Mhor record enables detection of previously unresolved high frequency variability in the North Atlantic climate during DO-12.

In the Uamh Mhor record, three statistically significant NAO-range cycles are identified at 7.7, 2.7 and 2.3 year periodicities (Fig. 16). The 7.7 year cycle aligns well with prior NAO Index identification (Seip *et al.,* 2019; Proctor *et al.,* 2000), whereas the shorter 2.7 and 2.3

year cycles may reflect the shortest dominant NAO frequencies. This appears to be the first record of NAO detected during DO-12, which is made possible by Uamh Mhor's bi-annual-scale resolution.

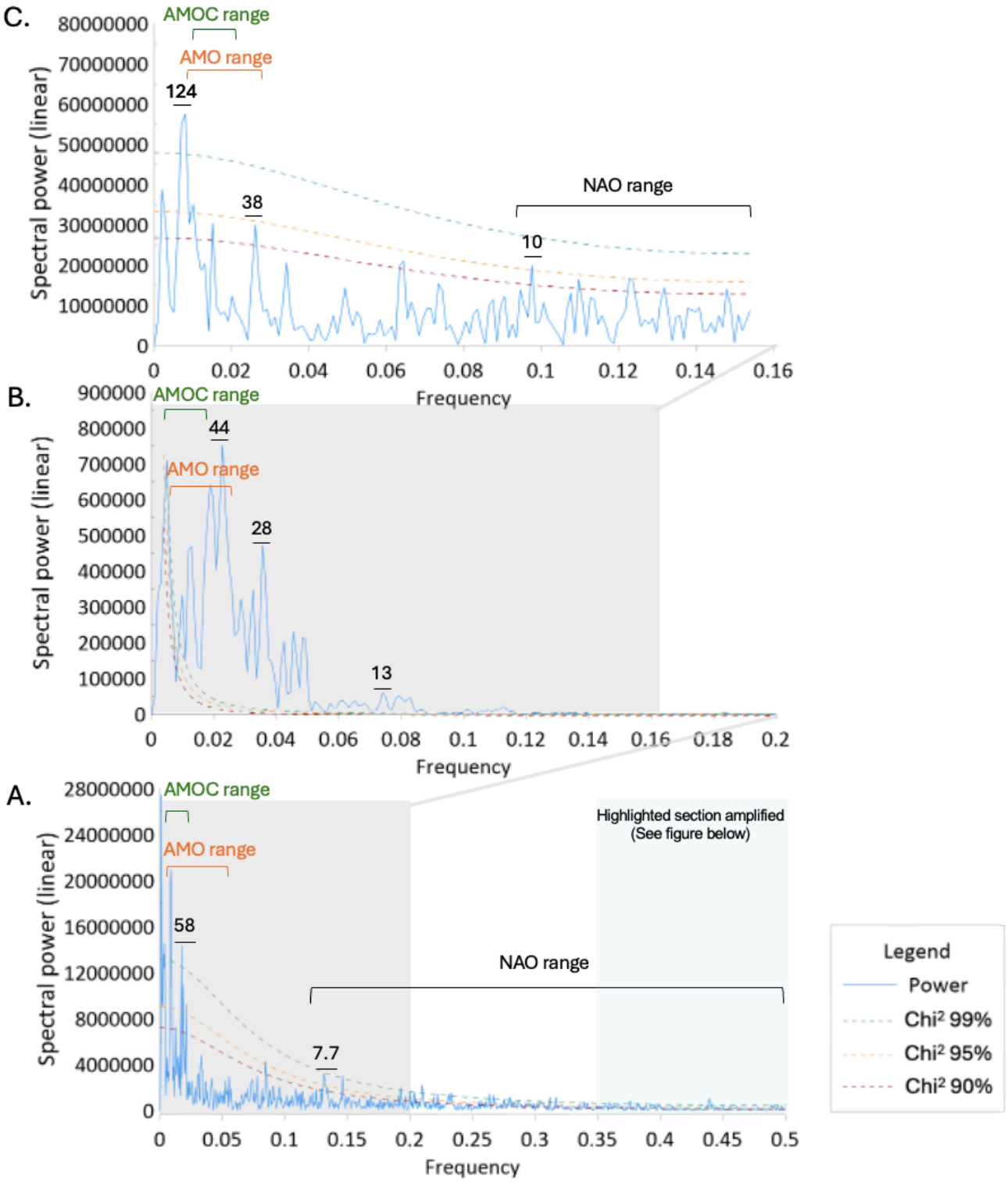

Figure 15. REDFIT – Morlet spectral analysis of Mg (ppm) data from Uamh Mhor (A), Bunker (B) and Abaco (C) (Weber *et al.,* 2018; Arienzo *et al.,* 2017). Mg data has been de-trended through polynomial fitting. Confidence limits of Chi^2 90%, 95% and 99% have been calculated. Dominant cycles are denoted above spectral power peaks. Grey boxes represent the difference in frequency axis between each graph. Cycle ranges of NAO, AMO and AMOC have been noted above impacted peaks. Amplified section of Uamh Mhor graph (blue box) is displayed in Fig. 16.

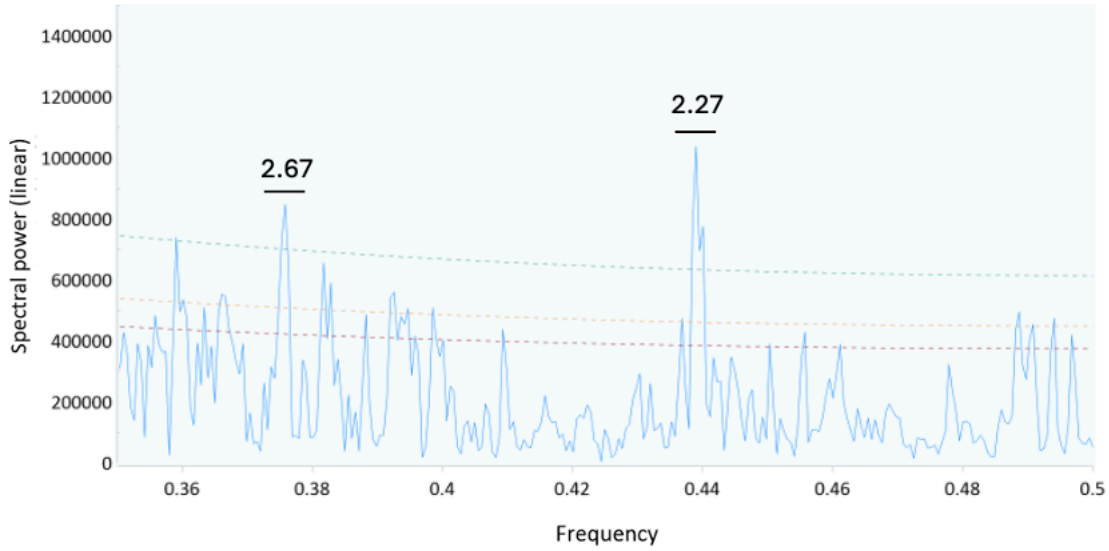

Figure 16. Amplified section of Uamh Mhor Mg (ppm) REDFIT – Morlet spectral analysis from 0.35-0.5 frequency. Mg data has been de-trended through polynomial fitting. Confidence limits of Chi^2 90%, 95% and 99% have been calculated. Dominant cycles are denoted above spectral power peaks.

5.2.3 Regional Mg Significance and Implications for PCP as a Dominant Mg Control

The coherence of Mg trends across all three records, seen through temporal warping through DTW analysis, highlights its significance as a climate proxy. Mg concentrations are widely used to reconstruct PCP amounts due to their sensitivity to hydrological variability, specifically their enrichment during drier conditions when PCP is enhanced (Fairchild & Treble, 2009; McDonald *et al.,* 2004; Fohlmeister *et al.,* 2012). In a European context, PCP rates are strongly modulated by regional hydroclimate variability, with the NAO acting as a

principal control on moisture availability (Baker *et al.,* 2015). Consequently, Mg concentrations in European speleothem may serve as indirect evidence for past NAO variability.

The detection of NAO-range cyclicity in spectral analysis of Mg from Uamh Mhor supports the interpretation that PCP is the dominant control on Mg incorporation in this flowstone. This is consistent with the shared hydrological drivers between PCP rate and NAO variability. Whilst alternative controls cannot be ruled out, the combination of DTW correlation, low dating uncertainty and NAO-band cycle identification from spectral analysis provide a strong foundation for using Mg as a robust proxy for North Atlantic climate reconstruction during DO-12. Further evaluation of competing controls on Mg will be addressed in the following sections.

5.3 Identification of Palaeoclimate Proxies and their Controls

While PCA and DTW analysis identifies the broader climatic relevance of Mg and Sr within the Uamh Mhor record (Fig. 12), understanding the specific mechanisms controlling their variability requires a more detailed evaluation of shared geochemical controls. One of the most widely accepted interpretations for the co-variation of Mg and Sr in speleothem is PCP, where Ca is preferentially removed from solution at higher rates than trace elements such as Mg and Sr, increasing the Mg/Ca and Sr/Ca ratios within dripwater (Fairchild *et al.,* 2000; Huang *et al.,* 2001; Cruz *et al.,* 2007; Mattey *et al.,* 2008; Fairchild & Treble, 2009). However, other potential controls including Incongruent Calcite Dissolution (ICD) and sea spray must also be considered to ensure a valid interpretation of the dominant control on Mg and Sr concentrations (Sinclair *et al.,* 2012).

5.3.1 PCP as a Dominant Control of Mg and Sr

Following the methodology of Sinclair *et al.* (2012), the slope of In(Mg/Ca) vs In(Sr/Ca) can help identify a dominant PCP control within speleothem. The slopes are created from the differential partitioning behaviour of Mg and Sr (D_{Mg} and D_{Sr}), based on equations from Banner (1995) and Huang & Fairchild (2001). Sinclair *et al.* (2012) report a slope range for PCP between 0.709 and 1.003, which is considered largely independent of regional influences such as rock composition. Wassenburg *et al.* (2020) suggest a broader slope range for PCP (0.71-1.45), based on site specific partition coefficients. At Uamh Mhor, the

calculated slope is 0.77, which falls within both diagnostic ranges for PCP dominance (Fig. 17), supporting PCP as the primary control on Mg and Sr variability.

The PCP slope is generally considered insensitive to temperature, although a drawback of this method is that growth rates may also affect D_{Sr} (Sinclair *et al.,* 2012). However, experimental work by Gabitov *et al*. (2014) indicates that substantial changes in D_{Sr} only occur at growth rates exceeding 316 μm/year. Because the estimated growth rates at Uamh Mhor are significantly lower, growth rates are unlikely to significantly alter the PCP slope in this case.

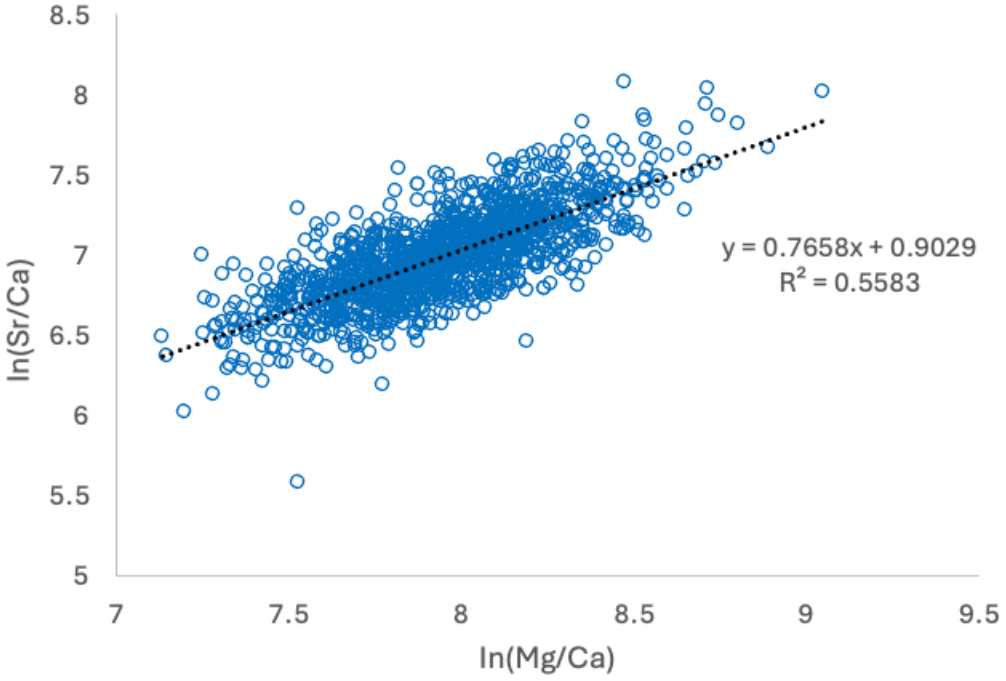

Figure 17. Sinclair test showing the relationship between In(Mg/Ca) and In(Sr/Ca) with a linear trendline fitted to show the slope of the relationship.

5.3.2 Incongruent Calcite Dissolution (ICD) and Sea Spray as Alternate Controls

ICD as described by Sinclair (2011) can also produce PCP-like slopes, typically within the range of 0.88-0.97. Uamh Mhor is at risk of potential ICD due to its dolomitic limestone/dolostone lithology, as dolomite tends to dissolve calcite more incongruently

(Putnis *et al.,* 2014). Given that the Uamh Mhor slope of 0.77 falls outside this range, ICD is not considered a significant control on Mg and Sr in this sample.

A third potential influence is sea spray, particularly relevant for speleothems located in or close to coastal environments (Forman *et al.,* 2025; Sinclair *et al.,* 2012). Due to Uamh Mhor's proximity to the North Atlantic, this mechanism requires consideration. To test this, site specific vectors representing sea spray and PCP influence were created and plotted against Mg and Sr concentrations. The data was then smoothed using a Savitzky-Golay filter to produce a bi-annual resolution (Fig. 18); this was conducted to improve coherence over the raw dataset, which features sampling intervals of approximately 0.6-1.4 years.

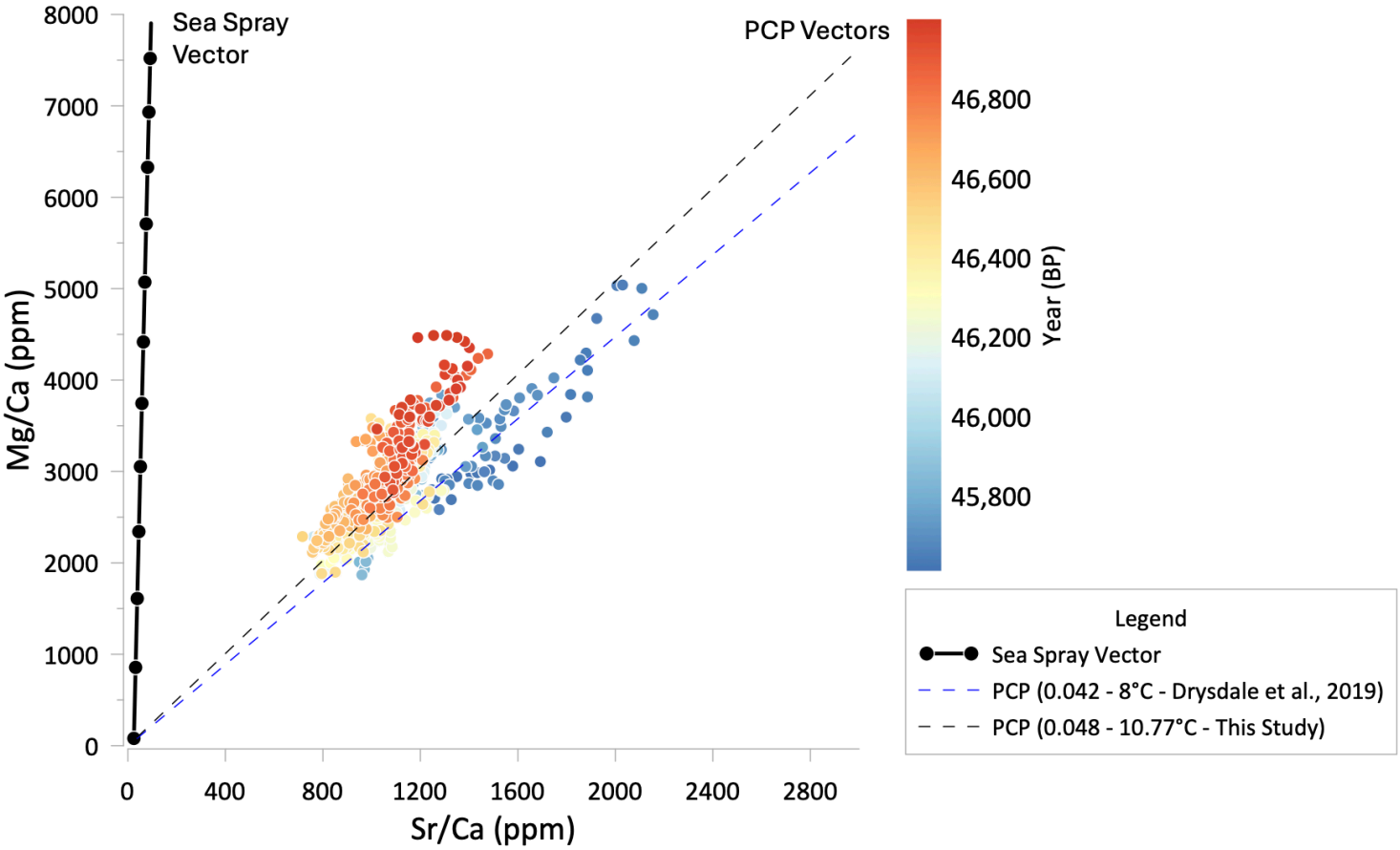

Figure 18. Control of Sea Spray in comparison to PCP upon Mg and Sr concentrations. Mg and Sr concentrations from LA-ICP-MS analysis for SMFMB20230528-1 have been interpolated to intervals of 2 years and been smoothened using a Savitzky-Golay filter (10). These concentrations are shown against sea spray (solid black line) and PCP (dashed lines) vectors. The sea spray

vector was modelled based on differing amounts of marine aerosol contribution (Forman *et al.*, 2025; Baldini *et al.,* 2015a). The PCP vector was modelled on bedrock concentrations and partition coefficients for dolomitic limestone (Drysdale *et al.,* 2019; BGS, 1979; BGS, 1956; Jakic *et al.,* 2016). PCP vectors have been calculated based on D_{Mg} values for an average temperature of 8 °C based on Drysdale *et al*. (2019) at 0.042, with a D_{Mg} for this study modelled based on best fit of the Drysdale equation within our data cloud.

A best fit PCP vector was calculated with a D_{Mg} value of 0.048, within the Drysdale *et al.* (2019) equation, corresponding to an average temperature of approximately 10.77 ºC. The alignment of the data cloud along the PCP vector and the agreement with the Sinclair test, gives robust evidence to interpret PCP as the dominant control on Mg and Sr concentrations at Uamh Mhor. Although a minor sea spray contribution cannot be excluded, it is not sufficiently influential to compromise the interpretation of PCP as the primary control.

The PCP vector exhibits a shift in gradient overtime, with steeper slopes indicating higher temperatures (based on the temperature dependence of the PCP vector slope due to changes in D_{Mg}), with steep slopes occurring at initial period of growth with a gradual decline towards cooler conditions beginning ~46 ka BP. This trend is consistent with temperature reconstructions from the NGRIP $\delta^{18}O$ record, which suggest a warming of approximately 12 ºC during DO events in MIS3, with a suggested maximum of ~16 ±3 ºC (Kindler *et al.,* 2014). Comparable estimates from speleothem analysis at Han-sur-Lesse cave in Belgium supports a mean temperature reconstruction for DO-12 of ~12 ºC (Peral *et al.,* 2024), further corroborating the initial temperature interpretation from Uamh Mhor.

5.3.3 Influence of D_{Mg} on PCP Interpretation

D_{Mg} equations from a wide variety of papers were tested for the creation of a PCP vector specific to Uamh Mhor (Fig. 19). These equations span a range of experimental and natural conditions, including analogues from cave environments, seawater analogues, laboratory settings and various speleothem deposits. Among the tested literature, the equation from Drysdale *et al.* (2019) was the only equation able to produce a vector matching the observed Mg/Sr data cloud from Uamh Mhor. Additionally, accompanied by a logical temperature estimate consistent with palaeoclimate conditions expected during DO-12.

The similarity between Drysdale's D_{Mg} equation and Uamh Mhor data is particularly striking, especially when contrasted against all tested D_{Mg} equations (Fig. 19). D_{Mg} values consistently show a positive correlation with temperature, and a noticeable distinction exists between D_{Mg} values from cave analogues and those from seawater analogues. However, within this framework, both the Drysdale paper and the Uamh Mhor data appear to have anomalously high D_{Mg} values in comparison with expected temperature (Fig. 19), suggesting a different set of environmental or depositional controls may be occurring. Drysdale *et al.* (2019) explored several possible explanations for elevated Mg and Sr concentrations in their study, ultimately ruling out factors such as source water pCO_2, growth rate variability and differences in saturation states. Instead, they proposed high Mg and Sr values could result from low-ionic strength and low-saturation waters, or elevated Na concentrations in dripwater; which may outcompete Sr for incorporation into the calcite lattice (Huang & Fairchild, 2001). An additional explanation discussed within this thesis is the factor of depositional setting.

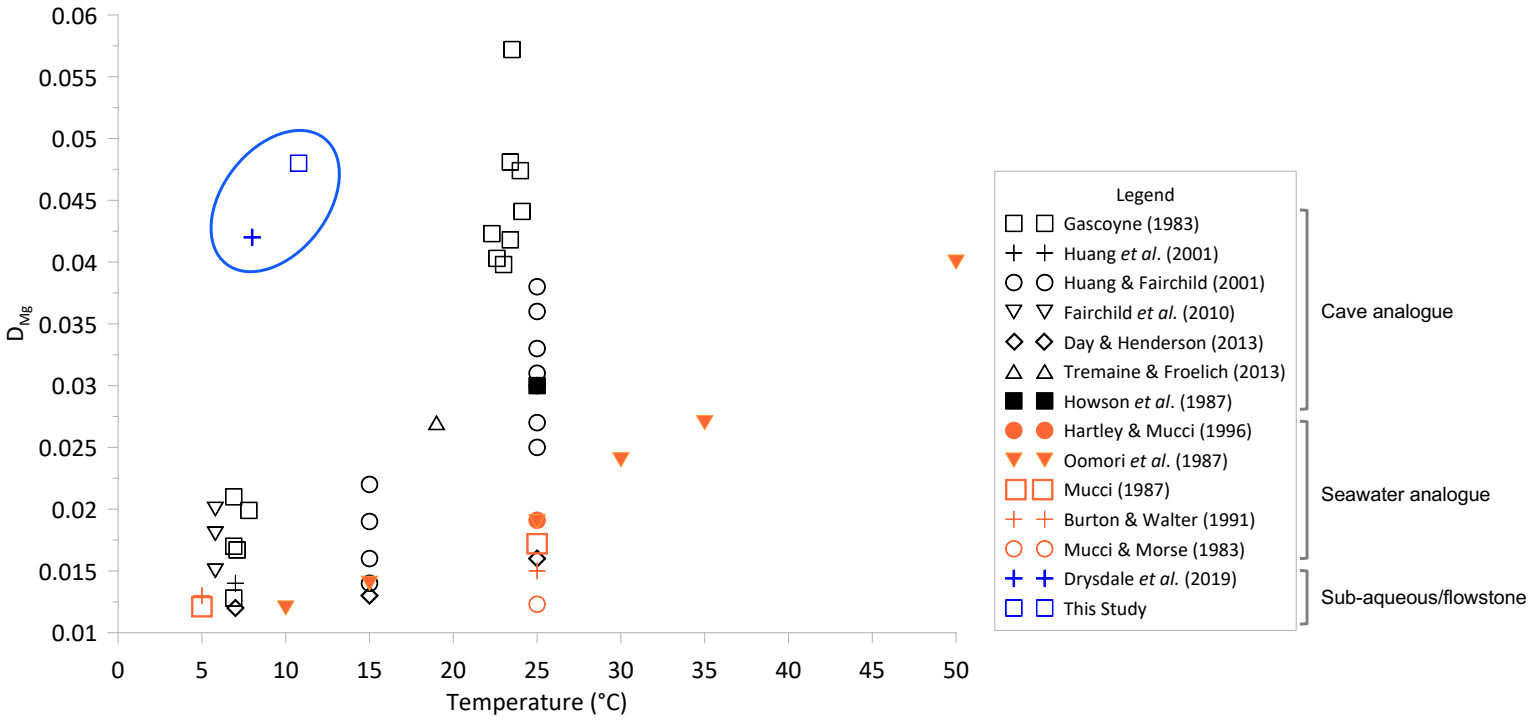

Figure 19. Adapted from Drysdale *et al.* (2019). D_{Mg} values based on temperature control compared from a range of field and laboratory experiments. A range of environments including cave analogues (black) and sea water conditions (orange) have been included for environmental deposition diversity. Subaqueous speleothems

and flowstones (blue) are shown separately from stalagmite analogues (cave analogues and seawater analogues).

The overwhelming majority of partition coefficient research to date has focused on stalagmites, stalactites, or experimental calcite grown under drip conditions. In contrast, Drysdale *et al.* (2019) utilises a subaqueous speleothem, which grow under fundamentally different hydrological conditions. These speleothem deposits, including subaqueous speleothem and flowstones under differing depositional conditions have been previously overlooked. This additionally raises the possibility that the flowstone from Uamh Mhor developed under subaqueous conditions or in a setting characterised by persistent water flow, such as from constant sheet flow or ponding behind rimstone/gour dams (Auler & Smart, 2001; Demeny *et al.,* 2024). Although no visual evidence of rimstone/gour structures were preserved at the sampling site, likely due to the significant cave erosion, meaning the potential for subaqueous or semi-aqueous deposition cannot be ruled out.

The depositional environment has important implications for partitioning behaviour. Stalagmites formed under drip conditions are typically subject to stronger hydrological controls. This hydrological control is likely due to calcite being deposited rapidly into drip-fed speleothem through a thin film of water that degasses CO_2 very efficiently, which can obscure temperature signals. Alternatively, a subaqueous or flowing depositional environment enables temperature to be the dominant control on Mg concentrations (Drysdale *et al.,* 2020; Demeny *et al.,* 2024). A subaqueous or flowing depositional environment also exhibits stronger temperature dependence through D_{Mg} values, due to minimal influence from kinetic fractionation and CO_2 degassing (Drysdale *et al.,* 2020; Demeny *et al.,* 2024). It is also believed that very low growth rates are also responsible for a stronger temperature dependency within D_{Mg} and reduced changes to D_{Sr} (Drysdale *et al.,* 2020; Gabitov *et al.,* 2014). Notably, the growth rates of the Uamh Mhor flowstone (~23.64 and ~10.76 μm/year) fall well below the theoretical threshold at which growth rate is suggested to significantly influence D_{Sr}. These low growth rates further support the interpretation that temperature, rather than hydrological variability, is the dominant control on Mg partitioning at Uamh Mhor under PCP conditions. Despite this, it is important to still note other possible controls which may be influencing both the Drysdale and Uamh Mhor data including the influence of low-ionic strength and low-saturation waters.

In summary, the application of the D_{Mg} equation from Drysdale *et al.* (2019) provides the best fit to the Uamh Mhor Mg/Sr data and yields realistic palaeotemperature estimates for DO-12. The unique depositional setting of the flowstone, potentially involving subaqueous or continuous flow conditions, may explain this similarity and highlights the importance of considering speleothem morphology when interpreting trace element proxies. These findings highlight the need for further research into the partitioning behaviour of Mg and Sr in non-drip-fed speleothem.

5.4 Climate Reconstruction from Temperature and Dryness Index

Having identified the dominant geochemical controls and confirmed the reliability of Mg/Sr as a climate proxy, this can now be applied to reconstruct palaeotemperature and hydrological variability during DO-12. Building on the early work of Gascoyne (1983), who proposed Mg/Ca ratios as a potential temperature proxy and Tremaine & Froelich (2013) who suggest that PCP could be used to infer dryness, this study combines the temperature dependence of Mg incorporation into calcite with PCP amount to develop a reconstruction of temperature and dryness for Northwest Scotland during DO-12. A similar approach was previously attempted by Roberts *et al.* (1998), involving the identification of seasonal temperature changes from interannual variations in Mg/Ca from a Scottish stalagmite during the Holocene. However, longer-term variations in Mg/Ca were unable to be explained by through this framework, more likely reflecting hydrological changes rather than temperature, preventing conclusive temperature estimates.

5.4.1 Stable Isotope Validation of the Dryness Index

The dryness index as outlined in 4.5.6 was assessed using $\delta^{13}C$, a well-established proxy for moisture, with lower $\delta^{13}C$ values generally associated with warmer and wetter conditions (Fig. 20) (Dabkowski *et al.,* 2016; Vansteenberge *et al.,* 2020; Peral *et al*., 2024). $\delta^{18}O$ often used as a temperature proxy, was also evaluated (Fig. 21). Although, its interpretation is typically complicated by multiple site-specific controls (McDermott, 2004; Genty *et al.,* 2003). Additionally, raw Mg and Sr concentrations have been displayed against the stable isotope data to evaluate and compare the statistical correlation between reconstructed temperature and the dryness index against the raw trace element data (Fig. 21).

Both $\delta^{13}C$ and $\delta^{18}O$ show strong correlations with the dryness index ($p = 1.04 \times 10^{-16}$ and $p = 1.20 \times 10^{-4}$ respectively), but neither is significantly correlated with reconstructed temperature (Fig. 21). This lack of correlation does not undermine the temperature reconstruction, instead it suggests that both $\delta^{13}C$ and $\delta^{18}O$ primarily reflect moisture/dryness variability. Although, $\delta^{13}C$ appears to be the more robust moisture proxy for European speleothems, as $\delta^{18}O$ variability is often small and strongly influenced by cave-specific processes (Couchoud *et al*., 2009).

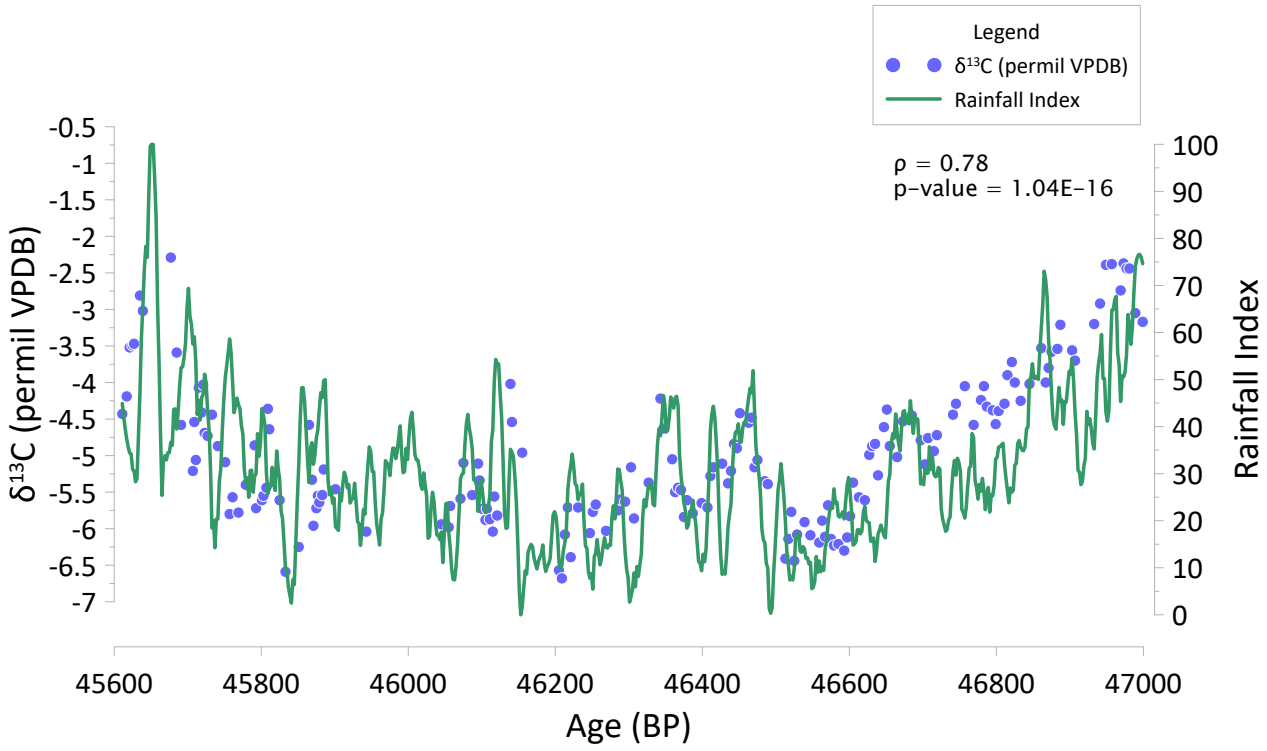

Figure 20. $\delta^{13}C$ (purple points) and Dryness Index (green line) are cross correlation with calculated statistical significance tests (Spearman's rho (ρ) and Pearson's Correlation (p-value)) across the timeframe of study of the Uamh Mhor sample 45,600-47,000 BP.

Interestingly both $\delta^{13}C$ and $\delta^{18}O$ have stronger monotonic relationships with Sr (Spearman's $\rho = 0.84$ and $\rho = 0.75$ respectively) than with Mg (Fig. 21). However, Pearson's correlations show both stable isotopes featuring more significant relationships with the dryness index, indicating that the combined use of Mg and Sr, rather than either element alone, provides a more stable and physically interpretable measure of hydrological and temperature changes, reducing the impact of potential Sr outliers whilst retaining temperature sensitivity through Mg partitioning.

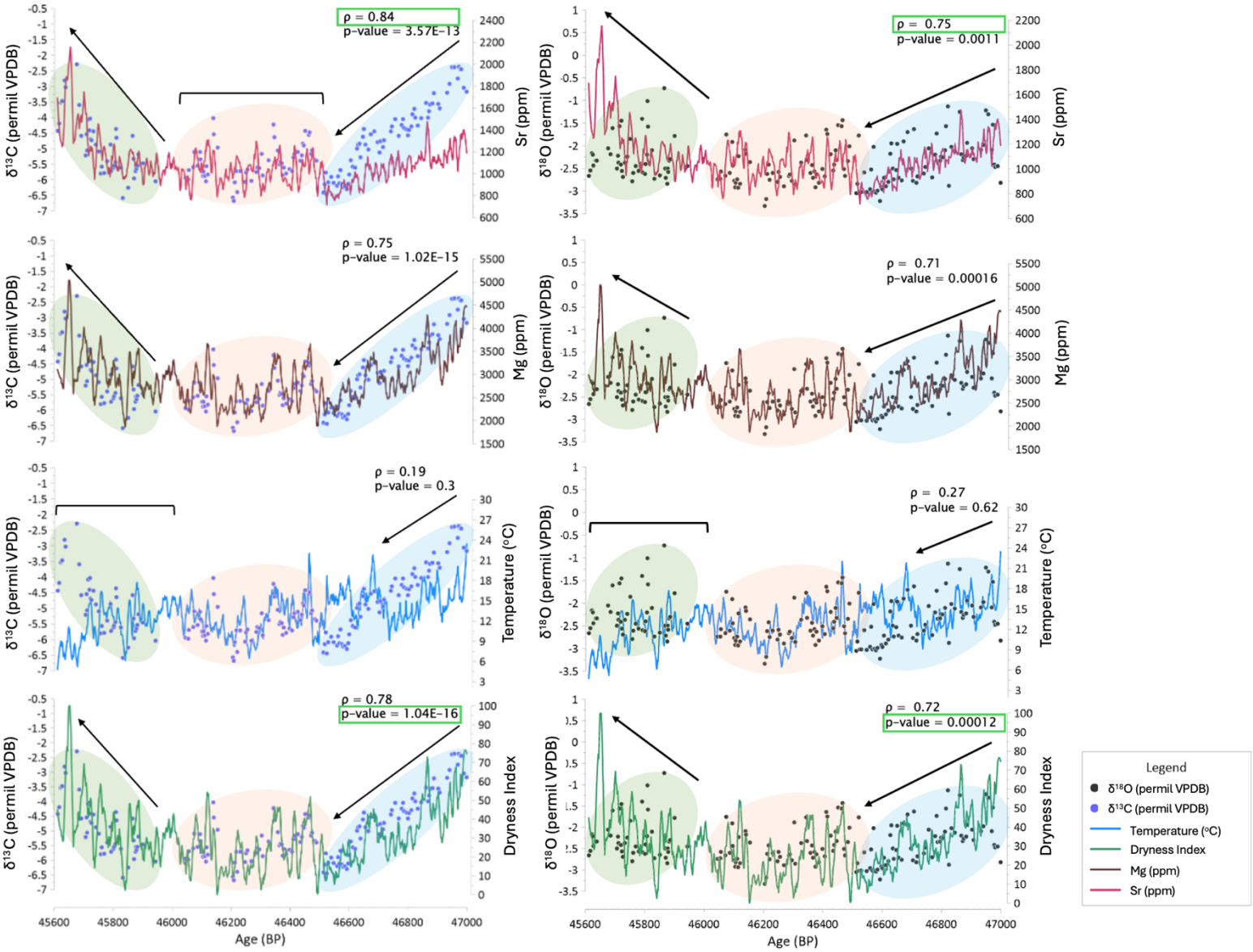

Figure 21. $\delta^{13}C$ (purple points) and $\delta^{18}O$ (black points) have undergone cross correlation and statistical significance tests against Dryness Index (green line), Temperature (°C) (blue line), Mg (ppm) (brown line) and Sr (ppm) (red line) across the timeframe of study 45,600-47,000 BP. Both Spearman's rho (ρ) and Pearson's Correlation (p-value) have been conducted and displayed alongside each dataset, this was conducted to assess potential linear and monotonic relationships respectively, with the highest (lowest) ρ (p-value) for both $\delta^{13}C$ and $\delta^{18}O$ highlighted.

5.4.2 Reconstructed Temperature during DO-12

Temperature estimates for Uamh Mhor range from ~4-23 °C, suggesting relatively warm conditions for an interstadial during the last glacial period. These high values could potentially reflect:

1. **Seasonal bias** - Calcite deposition may have occurred preferentially during warmer months when moisture was more readily available, producing summer weighted rather than annual temperature estimates (Baldini *et al.,* 2021; Baker *et al.,* 2021).
2. **Event strength** - DO-12 is suggested to have been an exceptionally strong interstadial reflected in-terms of $\delta^{13}C$ excursions, potentially amplified by the preceding Heinrich Stadial 5 (Weber *et al.,* 2018; Peral *et al.,* 2024).
3. **Different regional climate** - The reconstructed temperature range is consistent with present day seasonal temperature ranges in subarctic regions (Siberia, Alaska, Canada), consistent with the suggestion by Pederzani *et al*. (2021; 2024) that northern Europe during the last glacial resembled modern subarctic tundra.

5.4.3 Implications for Climate Proxy Development

Although $\delta^{13}C$ does not correlate significantly with reconstructed temperature, its strong relationship with the dryness index, derived from the same PCP vector-based framework, supports the theoretical validity of using PCP vectors to reconstruct both temperature and hydrological conditions. The absence of an isotope-temperature correlation reflects the fact that neither $\delta^{13}C$ nor $\delta^{18}O$ from Uamh Mhor are direct temperature proxies in this setting, rather than any flaw in the reconstruction approach. However, a comparison of chronologically adjusted NGRIP $\delta^{18}O$ data and Uamh Mhor reconstructed temperature (Fig. 22) shows a similar pattern of decline from the initiation of growth at Uamh Mhor until eventual termination. Overall, this study presents a more reliable framework for reconstructing environmental conditions using flowstones and integrating Mg temperature sensitivity with the Sr hydrological signal under a dominant PCP control. This dual-proxy approach enables a more nuanced and robust reconstruction of DO-12 climate conditions, and the stronger morphological temperature dependency of Mg, provide valuable contributions to further understand North Atlantic climate cycle dynamics during abrupt climate events.

5.5 Timing of DO-12

5.5.1 Comparison of the Uamh Mhor Chronology to Existing Chronologies

With reconstructed climate conditions for the Uamh Mhor record now established, the next logical step is to evaluate how the chronology aligns with existing chronologies covering DO-12. This allows assessment of the timing and duration of the event in a broader North Atlantic context.

A lag of approximately ~200 years is observed between the onset of DO-12 in the Uamh Mhor temperature and dryness records and the corresponding signal in the NGRIP $\delta^{18}O$ record (Fig. 22). Reconstructions indicate that by ~47,000 BP, Northern Scotland was already experiencing elevated temperatures and increased moisture availability, as reflected by the initiation of speleothem growth at Uamh Mhor. Given the large age uncertainties associated with NGRIP and the GICC05 chronology, it is highly probable that the GICC05 chronology is slightly too young during this period. Greenland Ice core chronologies are known to have larger uncertainties with increasing age, reaching ±2600 yrs at ~60,000 BP (Corrick *et al.,* 2020). In comparison, a new more precise chronology created by Corrick *et al.* (2020), SIOC19, suggests a new age of onset for DO-12 at ~47,071 ±145 yrs BP, in comparison to ~46,810 ±1912 yrs BP for the GICC05 chronology (Svensson *et al.,* 2008).

The newer SIOC19 chronology, constructed from 63 independently dated speleothem records across the last glacial period, aligns closely with the Uamh Mhor chronology. Placing the onset of DO-12 approximately ~70 years prior to initial speleothem growth. This would allow sufficient time for permafrost to thaw and supra-cave hydrological and thermal conditions favourable to speleothem growth to develop, particularly in a higher latitude region such as North Scotland. As previously mentioned, adjusting the NGRIP $\delta^{18}O$ chronology to the SIOC19 DO event onset timing (black dotted line, Fig. 22), there is a gradual decline in $\delta^{18}O$ consistent with the Uamh Mhor temperature trend, occurring from the warmest initial period of DO-12 (Fig. 23). There appears to be a small discrepancy between temperature and the adjusted NGRIP chronology, with the latter displaying peaks slightly older than within temperature reconstructions, within the factor of a few decades. This is likely a result of age-uncertainty or differences in dataset resolution, both of which fall within this range for the period. The gradual pattern of decline through DO-12 with matching peaks between the two

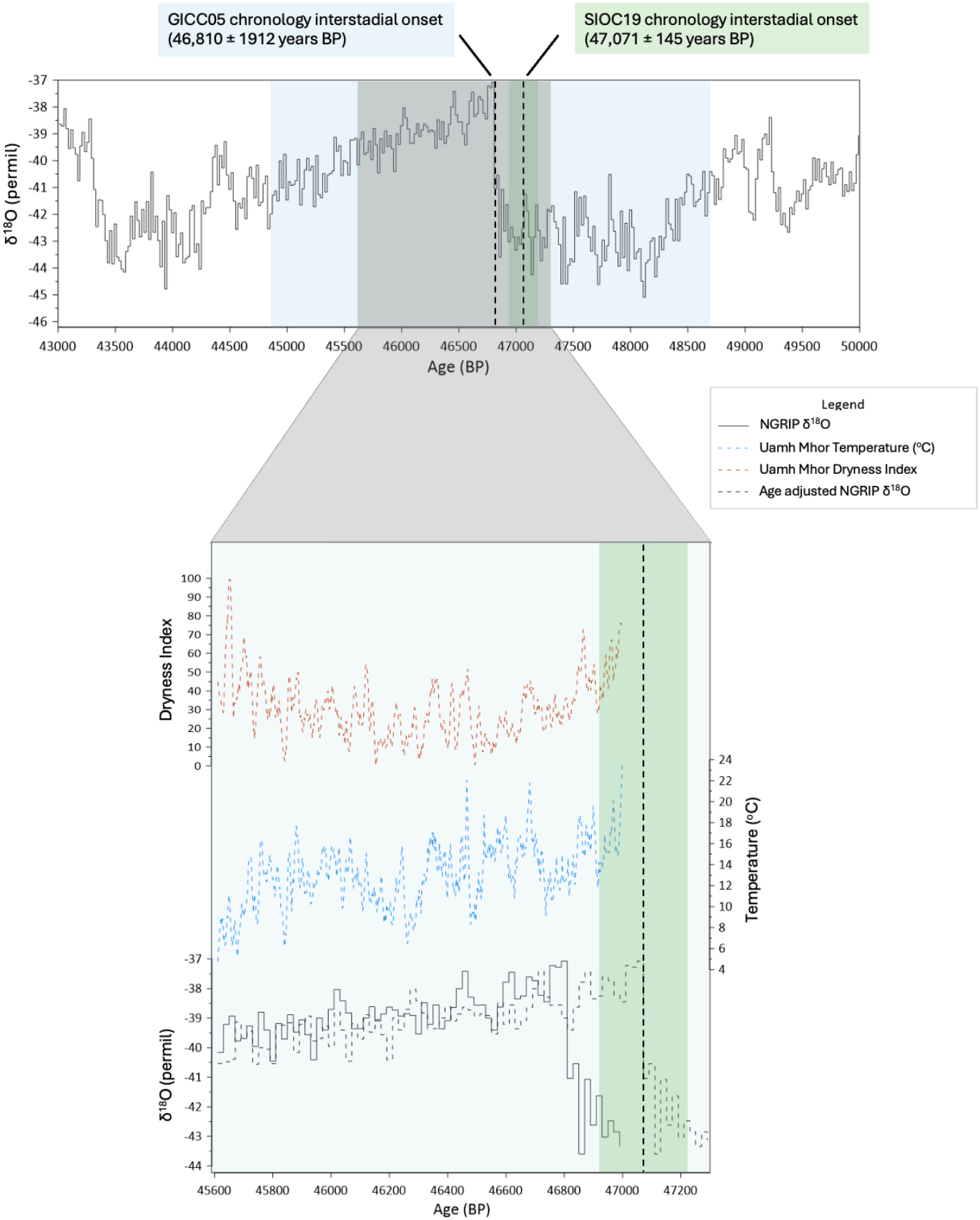

Figure 22. Temperature (°C) and dryness index reconstructions for DO-12 regional climate conditions around Scotland (47,000-45,600 BP) are compared to $\delta^{18}O$ from

the NGRIP ice core for the period of DO-12 (grey box) and its surrounding chronological context (43,000-50,000 BP). Dates for the onset of DO-12 have been compared for two chronologies, GICC05 (Svensson *et al.,* 2008) and SIOC19 (Corrick *et al.,* 2020), with the blue (GICC05) and green (SIOC19) boxes noting their respective age uncertainties across the period. NGRIP $\delta^{18}O$ has then been adjusted (from 46,810 ±1912 yrs BP) to the SIOC19 chronology DO-12 onset date (47,071 ±145 yrs BP) displayed through the overlapping black dotted line.

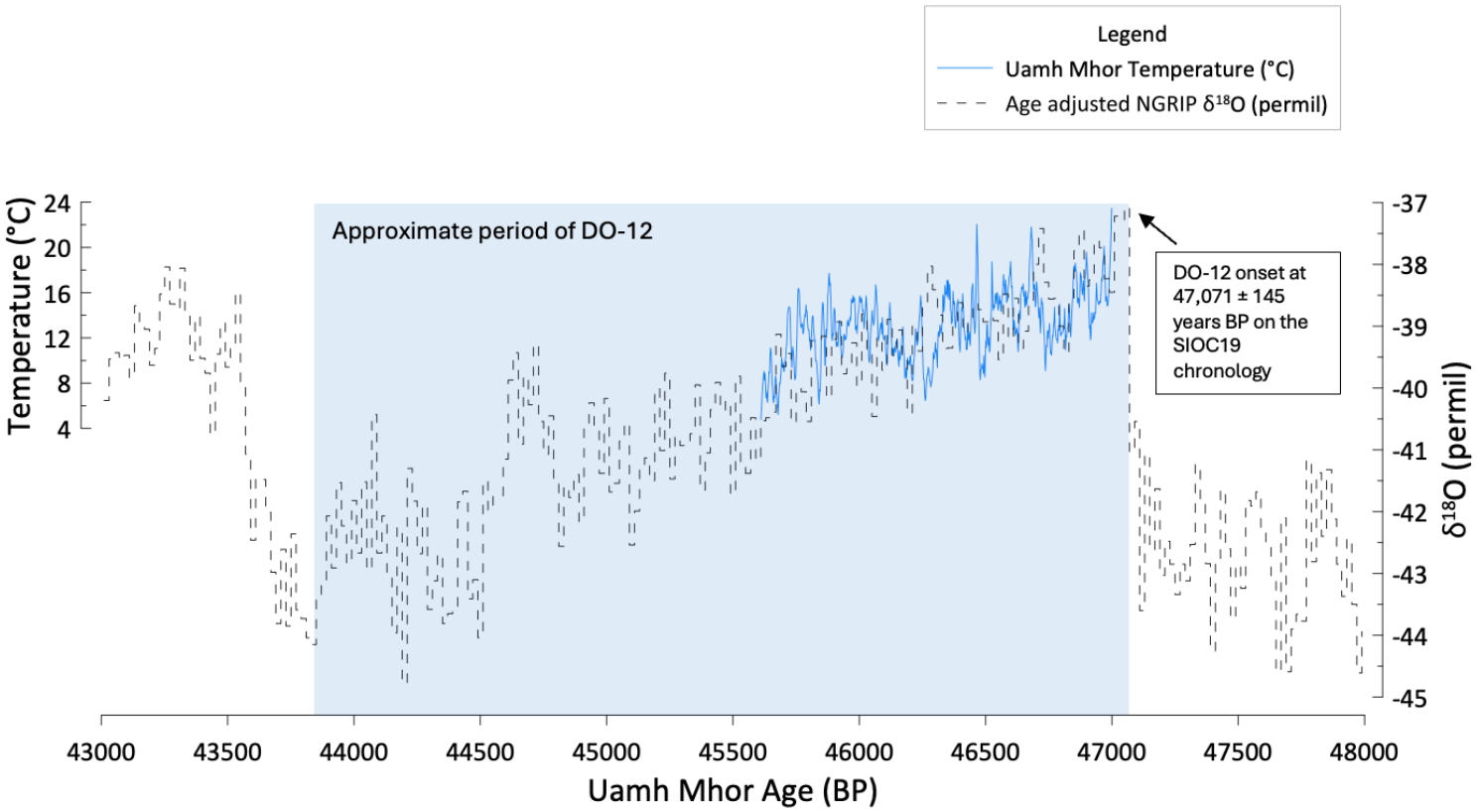

Figure 23. Temperature (°C) reconstruction from Uamh Mhor cross-compared with adjusted NGRIP $\delta^{18}O$ to the SIOC19 chronology, over the period 48,000-43,000 BP.

records suggests there is a correlation between the $\delta^{18}O$ of NGRIP and the temperature reconstruction from Uamh Mhor. Despite the lack of significant correlation between the $\delta^{18}O$ data from Uamh Mhor and reconstructed temperature, this may be explained from alternative environmental controls on $\delta^{18}O$. This is further supported by the significant correlation between Uamh Mhor $\delta^{18}O$ and the dryness index. Overall, there is a strong suggestion that the original NGRIP chronology is too young for the period, with SIOC19 offering a better

chronological estimate of DO-12 and its onset. Furthermore, the adjusted NGRIP $\delta^{18}O$ chronology shows a strong correlation with reconstructed temperature.

While these comparisons help refine the temporal placement of the Uamh Mhor record within the wider context of DO-12, full interpretation of climatic conditions needs to integrate geochemical, chronological, and external palaeoclimate evidence. The next section therefore synthesises the existing climate reconstruction approximations for DO-12 within the wider European context.

5.5.2 Comparison with European Speleothem Records

Bunker Cave, Germany, records speleothem growth initiating at ~47,267 BP, approximately 267 years earlier than the initial growth observed at Uamh Mhor (~47,000 BP). However, despite an earlier initiation than suggested in SIOC19, Bunker is still consistent with Uamh Mhor and SIOC19 based on chronological uncertainties of ±720 yrs (Fig. 14). Furthermore, lower latitude sites are expected to record speleothem growth earlier due to more rapid expression of warming closer to the equator relative to higher latitude sites such as Scotland. Speleothem growth continues at Bunker Cave until ~42,884 BP, matching Villars Cave, France, which also suggests DO-12 terminated ~41-42 ka BP. However, the onset of DO-12 at Villars cave matches with the NGRIP and GICC05 chronology suggested onset at ~46-47 ka BP. This may be a result of large chronological uncertainties with an average of ±960 yrs over the period 45.6-47 ka BP with a maximum uncertainty of ±2206 yrs (Genty *et al.,* 2010).

The discrepancy of speleothem growth termination between Bunker and Villers caves with Uamh Mhor may be attributed to i) larger dating uncertainties within existing records (Uamh Mhor = ±153 yrs, Villars = ±960 yrs, Bunker = ±720 yrs), ii) a more rapid deterioration back to stadial conditions at higher latitudes or iii) a result of site-specific growth termination due to local hydrological controls. Overall, the U-Th dating from Uamh Mhor is consistent with the SIOC19 chronology for the last glacial period in comparison to the previously dominant GICC05 chronology. Although further research of European speleothem during the period, with ideally lower dating uncertainties, would be required to determine a tightened chronology for the region during this period.

5.6 DO-12 Climate Reconstruction

5.6.1 Climate Variability During DO-12

Utilising the results of temperature and dryness index reconstructions from Uamh Mhor, alongside an analysis of NAO signal strength throughout the period (2.3-2.7 and 7.7 year NAO bands identified in the Uamh Mhor sample, Fig. 15 and 16), a coherent pattern of climatic amelioration and degradation emerges across DO-12 (Fig. 24). Overall, three distinct climate states can be recognised through the Uamh Mhor record, expressed in the temperature, dryness and NAO strength data, which closely align with the trends of $\delta^{13}C$ and $\delta^{18}O$ (green, orange and blue ovals in Fig. 21). However, there appears to be a lag in the dryness response, whilst temperature is at its peak at the start of growth (Bin 1, Fig. 24), dryness also remains elevated. This delayed moisture availability is most plausibly attributed to lags in the initial phase of climate development. In addition, an intriguing pattern of NAO weakening is observed during the middle of DO-12, the potential drivers behind this will be explored further.

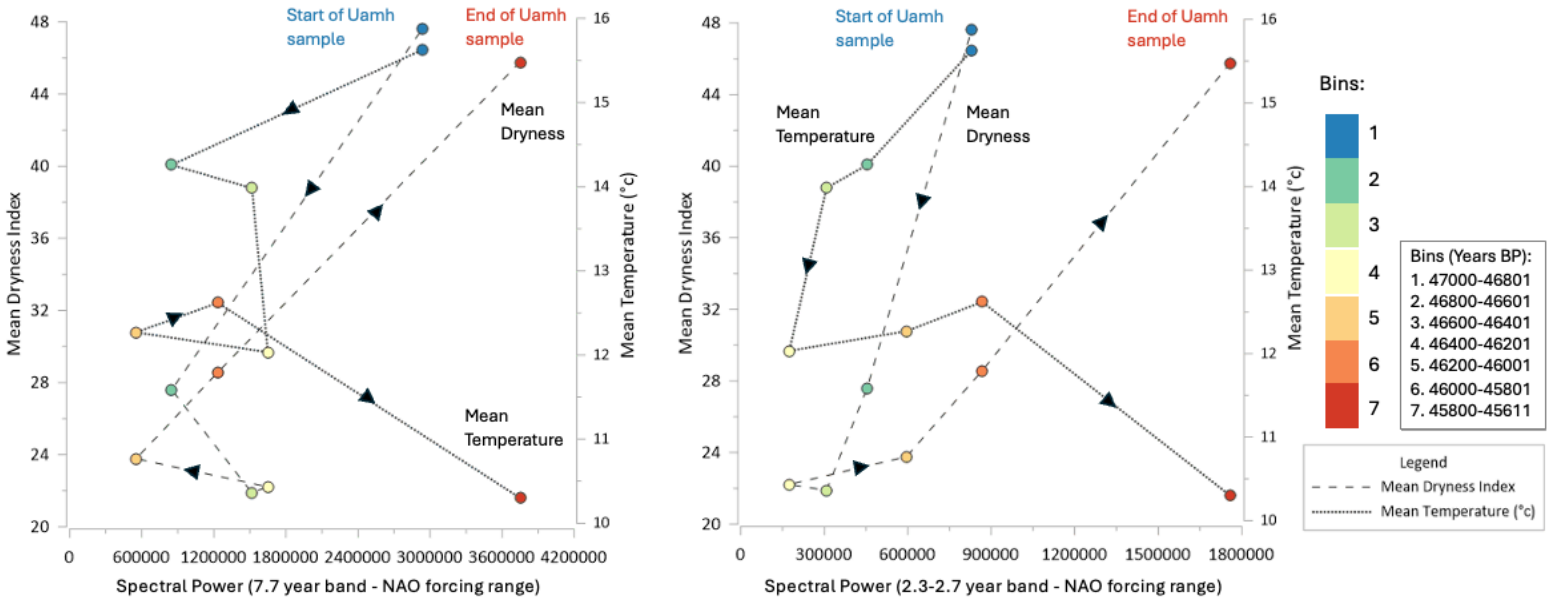

Figure 24. Graph of Scottish regional climate evolution through DO-12 within 7 binned time intervals. Spectral power of 7.7 year cycle and between 2.3-2.7 year cycles, as representative NAO forcing range for the entire dataset (see fig.16). The 7 individual bins are composed of ~200 year intervals through DO-12, representing the strength of NAO signal/cycle length within DO-12. Analysed against reconstructed

mean dryness (dashed line) and mean temperature (dotted line) values for each bin, showing the evolution of climate proxies through DO-12.

5.6.2 Shifts in NAO Band Strength

The strongest NAO signal across the study interval is observed at the termination of DO-12 (Bin 7, Fig. 24) and to a lesser extent, at its onset (Bin 1, Fig. 24). In contrast, the mid-phase of DO-12 is characterised by a pronounced weakening of NAO strength between 46,800-45,801 BP (Bins 2-6, Fig. 24). A likely explanation for this pattern is a dampened meridional temperature gradient resulting from ice-sheet retreat and the expansion of open-water areas during the interstadial. In stadial phases, steeper temperature gradients act to enhance NAO strength, consistent with the observed stronger NAO band signals at both the beginning and the end of DO-12.

A potential alternate explanation for the mid-interstadial weakening is a reorganisation of NAO node positioning. Substantial changes in the AMOC are known to occur during peak DO event warming, particularly following Heinrich stadials, which may have driven large scale shifts in the latitudinal positioning of both the ITCZ and associated NAO pressure centres (Icelandic low and Azores high) in the North Atlantic. Perturbations in AMOC are known to exert strong control over ITCZ position (Baldini *et al.,* 2015a). For example, a southwards shift of the ITCZ during North Atlantic stadials during the last glacial period has been documented by Chiang *et al.* (2014), matching with Deplazes *et al.* ‘s (2013) noting a northwards displacement of the ITCZ during interstadials. Together, these dynamics support the idea of a possible northwards shift in NAO nodes during interstadial periods such as DO-12. This mechanism will be further evaluated through comparison with modern NAO behaviour in the following section.

Further high-resolution research from alternative latitudinal settings within the North Atlantic would be required to more confidently identify the mechanisms underlying the weakening of NAO signal strength during DO-12. Despite these uncertainties, the Uamh Mhor record highlights a significant behavioural shift in NAO variability within DO-12.

5.7 Comparison of NAO Signal during DO-12 and Contemporary NAO Signals

5.7.1 Spatial Comparisons with Contemporary Signals

To place these reconstructed climate dynamics within a broader spatial framework, it is necessary to examine how the Uamh Mhor record compares with contemporary North Atlantic climate dynamics and potential forcing mechanisms. This section expands the focus from local processes to possible hemispheric-scale drivers. A comparison of Uamh Mhor NAO signals to contemporary NAO signals across the North Atlantic region was conducted to produce a more holistic interpretation of NAO variability during DO-12 (Fig. 25).

Four sites were analysed for NAO-like signals, these sites were chosen based on their proximity to the Atlantic and to represent NAO signals at different latitudes. The Uamh Mhor palaeodata appears to align more closely with Aberporth (Wales) and Bordeaux (France) than with the sites from Northern Scotland (Wick, Kinlochewe) (Figs. 16 & 25). Present-day Scotland exhibits somewhat similar, but not matching, NAO signals to Uamh Mhor (3.6, 3.1 and 2.1 years), whereas the palaeodata records generally shorter signal lengths (2.3 and 2.7 years). It is important to emphasise, however, that NAO signals are inherently noisy and can overlap with other modes of variability such as the AMO and AMOC, introducing a level of uncertainty into observed cycle lengths (Seip *et al.,* 2019).

As previously proposed in the last section, palaeo-NAO nodes may have been spatially displaced relative to their contemporary positioning. Modelling by Pausata *et al.* (2010) demonstrates that atmospheric pressure changes associated with ice retreat can alter NAO dynamics, with sea-ice reduction causing changes in intensity and extent of the Icelandic low, producing a NAO spatially shifted relative to its contemporary position. Nonetheless, the magnitude and nature of such spatial changes would depend on the specifics of each warming event, including the extent of sea-ice loss and the intensity of associated pressure anomalies, factors that are difficult to constrain and reconstruct with certainty.

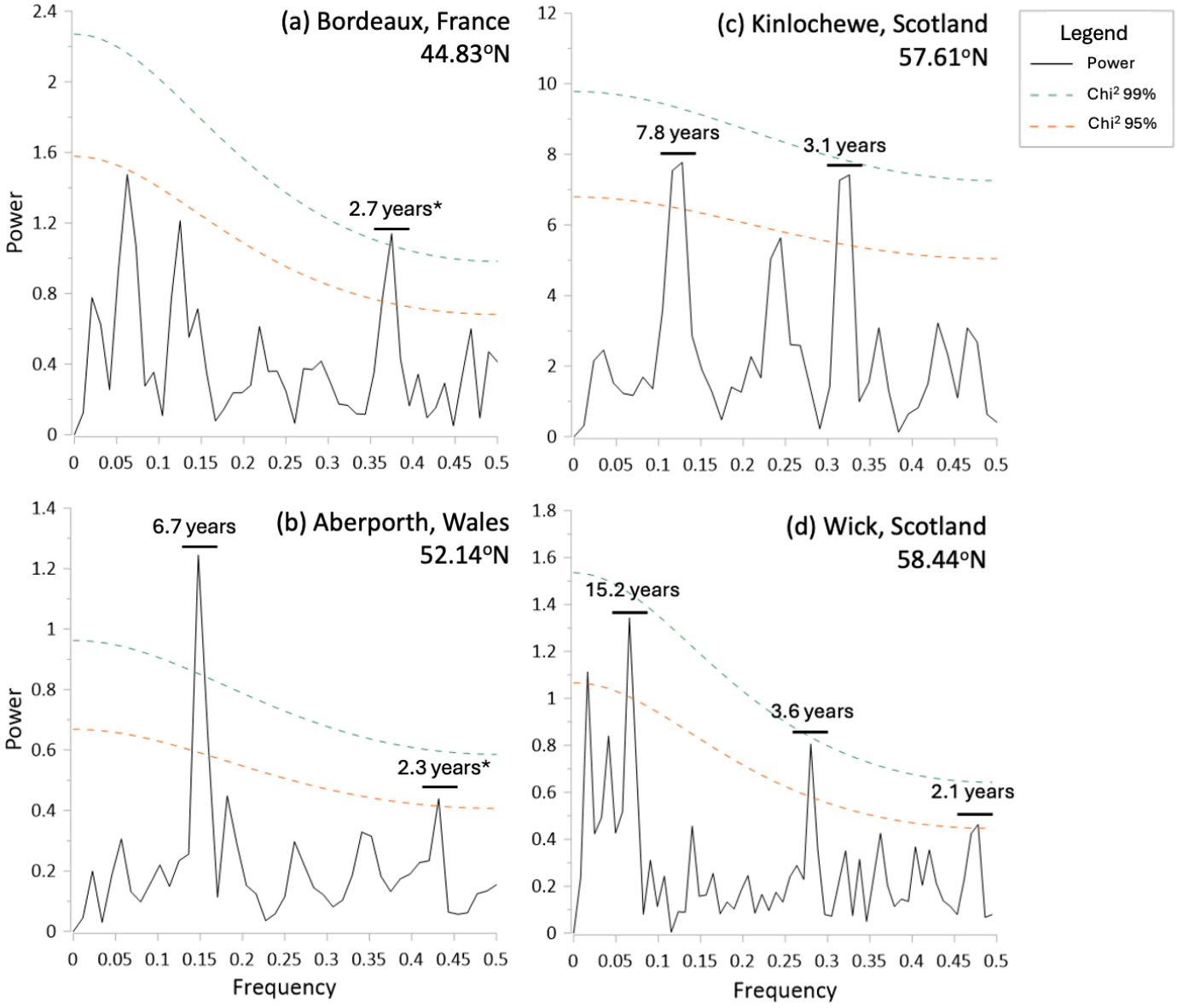

Figure 25. Modern precipitation data from Bordeaux, France (a), Aberporth, Wales (b), Kinlochewe, Scotland (c) and Wick, Scotland (d) (Menne *et al.,* 2012). Analysed through REDFIT spectral analysis to identify modern NAO cycle lengths recorded at different latitudes across the North Atlantic region. Years noted with an asterisk indicate the same cycle length as identified within palaeoclimate data from Uamh Mhor (see Fig 14 & 15 for Uamh Mhor spectral analysis results).

5.7.2 Latitudinal Forcing Mechanisms

Alternatively, contemporary Aberporth and Bordeaux may provide a closer analogue to the shorter NAO cycle lengths observed in the Uamh Mhor record due to shared forcing mechanisms. Northern Scotland is strongly influenced by precipitation variability linked to the NAO and ocean circulation, primarily through the North Atlantic Drift component of the AMOC (Fuller *et al.,* 2008). Research by Menviel *et al.* (2020) and Dima & Lohmann (2018) indicate that abrupt warming phases, such as DO warm events, can intensify AMOC triggering shifts in atmospheric circulation. Strengthening of the AMOC at the onset of a DO warm event is associated with ITCZ and storm tracks being pulled further northwards globally (Corrick *et al.*, 2020; Rasmussen *et al*., 2016). Consequently, the shorter cycle lengths in the palaeo-NAO record may reflect similarities with contemporary Southern European latitudes due to both being subject to stronger tropical influences. With large AMOC-driven changes in temperature gradients likely causing northwards shifts in key climate mechanisms, including the Jet Stream, storm tracks and the ITCZ (Nagashima *et al.,* 2011), this introduces a stronger relative influence of subtropical forcing on the NAO, particularly from the ITCZ (Deplazes *et al.,* 2013).

Current research suggests that NAO cycle length during DO-12 was more likely governed by faster tropical forcing than by major changes in NAO position relative to present-day. This alternate forcing was likely facilitated by AMOC, reduced sea-ice cover and possible alterations to Jet Stream and ITCZ pathways. However, this remains too broad a scope to be fully addressed within this thesis. Further palaeoclimate research is required to determine the extent of NAO variability and node positioning during DO events of the last glacial period in relation to contemporary NAO cycle dynamics. Nonetheless, the contribution of an NAO-like signal from Uamh Mhor introduces the first potential reconstruction of NAO and its respective behaviour within DO-12, creating a novel insight into North Atlantic climate mechanism dynamics during this period.

5.8 Limitations and Further Research

5.8.1 Limitations

Although this study provides important new insights into DO-12 climate dynamics, several uncertainties and methodological constraints remain. Firstly within laboratory analysis, the

dataset of stable isotopes ($\delta^{18}O$ and $\delta^{13}C$) was incomplete due to analytical errors that caused substantial delays in sample processing. This restricted the extent to which isotopic evidence could be incorporated alongside trace elements. Secondly within data analysis, a notable gap in the literature was encountered regarding flowstone and subaqueous partition equations (D_{Mg} and D_{Sr}). The absence of established data prevented robust cross-comparisons between the Uamh Mhor record and additional subaqueous speleothem analogues. Consequently, this limited the ability to fully evaluate the effective use of flowstones and subaqueous speleothem for Mg palaeothermometry.

5.8.2 Further Research

Further laboratory and field-based research is needed into the partitioning of Mg and Sr within non-drip-fed speleothems, such as subaqueous speleothems and flowstones. These depositional environments remain underrepresented in the literature yet show considerable potential as analogues for Mg based palaeothermometry. Expanding this area of research could allow for the expansion of regions able to facilitate palaeotemperature reconstructions. Additional high-resolution studies are needed to investigate NAO variability and node positioning both within and between DO events during the last glacial period. An improved understanding would allow for a more confident reconstruction of climate mechanism behaviour triggered by rapid warming events. Furthermore, their influence on European and global climate through teleconnections.

6. Conclusions

The flowstone record from Uamh Mhor provides valuable new insights into past climate conditions and cycles during DO-12 and overall within the last glacial period. Owing to its location, the record enables the reconstruction of North Atlantic climate whilst extending the known latitudinal reach of warming and moisture availability during DO-12. The record displays age dates consistent with the SIOC19 chronology, a more robust alternative to the previously dominant GICC05 chronology. The record demonstrates the potential of Mg and Sr as proxies for reconstructing palaeotemperature and hydrological variability through subaqueous and flowstone analogues, supported by cross-validation with stable isotope data. The reconstructed temperature range for Uamh Mhor is notably large, with three proposed

explanations: (i) a seasonal bias in deposition, (ii) strength of the DO event, or (iii) a different climate regime more closely aligned with subarctic conditions than present day Scotland.

Reconstruction of NAO band strength reveals a weakening of the NAO signal during the middle of DO-12. This weakening is most plausibly attributed to a dampened meridional temperature gradient resulting from ice-sheet retreat. Furthermore, the Uamh Mhor record indicates shorter NAO cycle lengths than those observed in contemporary Scotland. Current literature suggests this may reflect stronger subtropical forcing during DO-12, a feature consistent with shorter NAO cycles observed in lower-latitude contemporary sites. Such forcing is supported by evidence of northwards shifts in major climate mechanisms during interstadials, including storm tracks and the ITCZ, associated with changes in AMOC organisation.

Overall, the findings of this thesis contribute a new method for reconstructing temperature from speleothem, enhanced spatial and temporal information on North Atlantic climate during DO-12, the past behaviour of NAO under abrupt warming and the role of shifting climate mechanisms in shaping European climate. The expansion of knowledge on climate cycles and mechanisms under conditions of abrupt forcing is essential moving forwards for a better understanding of thresholds and controls within the holistic climate system. This in turn enhances the capacity to predict contemporary and future climate responses to ongoing forcing changes.

7. References

Allen, M., Deliege, A., Verheyden, S., Nicolay, S., Quinif, Y. and Fagel, N. (2018) ‘Evidence for solar influence in a Holocene speleothem record (Pere Noël cave, SE Belgium)’, *Quaternary Science Reviews*, 192, pp. 249-262.

Ampel, L., Bigler, C., Wohlfarth, B., Risberg, J., Lotter, A.F. and Veres, D. (2010) ‘Modest summer temperature variability during DO cycles in western Europe’, *Quaternary Science Reviews*, 29(11-12), pp. 1322-1327.

Arienzo, M.M., Swart, P.K., Broad, K., Clement, A.C., Pourmand, A. and Kakuk, B. (2017) ‘Multi-proxy evidence of millennial climate variability from multiple Bahamian speleothems’, *Quaternary Science Reviews,* 161, pp. 18-29.

Atkinson, T. and Lawson, T. (1995) *‘Karst Morphology’ in The Quaternary of Assynt and Coigach: field guide.* Cambridge: Quaternary Research Association. pp.61-86.

Auler, A.S. and Smart, P.L. (2001) ‘Late Quaternary Paleoclimate in Semiarid Northeastern Brazil from U-Series Dating of Travertine and Water-Table Speleothems’, *Quaternary Research*, 55, pp. 159-167.

Baez, J.C., Gimeno, L. and Real, R. (2021) 'North Atlantic Oscillation and fisheries management during global climate change', *Reviews in Fish Biology and Fisheries*, 31(2).

Baker, A., Ito, E., Smart, P.L. and McEwan, R.F. (1997) ‘Elevated and variable values of 13C in speleothems in a British cave system’, *Chemical Geology*, 136(3-4), pp. 263-270.

Baker, A., Wilson, R., Fairchild, I.J., Franke, J., Spötl, C., Mattey, D., Trouet, V. and Fuller, L. (2011) ‘High resolution δ18O and δ13C records from an annually laminated Scottish stalagmite and relationship with last millennium climate’, *Global and Planetary Change,* 79(3-4), pp. 303-311.

Baker, A., Hellstrom, J.C., Kelly, B.F.J., Mariethoz, G. and Trouet, V. (2015) ‘A composite annual-resolution stalagmite record of North Atlantic climate over the last three millennia’, *Nature,* 5(10307).

Baker, A., Mariethoz, G., Comas-Bru, L., Hartmann, A., Frisia, S., Borsato, A., Treble, P.C. and Asrat, A. (2021) 'The Properties of Annually Laminated Stalagmites- A Global Synthesis', *Reviews of Geophysics*, 59(2).

Baldini, J.U.L., McDermott, F. and Fairchild, I.J. (2002) 'Structure of the 8200-Year Cold Event Revealed by a Speleothem Trace Element Record', *Science*, 296(5576), pp. 2203-2206.

Baldini, J.U.L., McDermott, F., Baker, A., Baldini, L.M., Mattey, D.P. and Railsback, L.B. (2005) 'Biomass effects on stalagmite growth and isotope ratios: A 20th century analogue from Wiltshire, England', *Earth and Planetary Science Letters*, 240(2), pp. 486-494.

Baldini, L.M., McDermott, F., Baldini, J.U.L., Arias, P., Cueto, M., Fairchild, I.J., Hoffmann, D.L., Mattey, D.P., Müller, W., Nita, D.C., Ontañon, R., Garcia-Monco, C. and Richards, D.A. (2015a) 'Regional temperature, atmospheric circulation, and sea-ice variability within the Younger Dryas Event constrained using a speleothem from northern Iberia', *Earth and Planetary Science Letters*, 419, pp. 101-110.

Baldini, J.U.L., Brown, R.J. and McElwaine, J.N. (2015b) 'Was millennial scale climate change during the Last Glacial triggered by explosive volcanism?', *Scientific Reports,* 5(17442).

Baldini, J.U.L., Lechleitner, F.A., Breitenbach, S.F.M., van Hunen, J., Baldini, L.M., Wynn, P.M., Jamieson, R.A., Ridley, H.E., Baker, A.J., Walczak, I.W. and Fohlmeister, J. (2021) 'Detecting and quantifying palaeoseasonality in stalagmites using geochemical and modelling approaches', *Quaternary Science Reviews*, 254 (106784).

Banner, J.L. (1995) 'Application of the trace element and isotope geochemistry of strontium to studies of carbonate diagenesis', *Sedimentology*, 42(5), pp. 805-824.

Banner, J.L., Guilfoyle, A., James, E.W., Stern, L.A. and Musgrove, M-L. (2007) 'Seasonal Variations in Modern Speleothem Calcite Growth in Central Texas, U.S.A.', *Journal of Sedimentary Research*, 77(8), pp. 615-622.

Bar-Matthews, M., Ayalon, A. and Kaufman, A. (1997) 'Late Quaternary Paleoclimate in the Eastern Mediterranean Region from Stable Isotope Analysis of Speleothems at Soreq Cave, Israel', *Quaternary Research*, 47(2), pp. 155-168.

Bar-Matthews, M., Ayalon, A., Kaufman, A., Wasserburg, G.J. (1999) 'The Eastern Mediterranean paleoclimate as a reflection of regional events: Soreq cave, Israel', *Earth and Planetary Science Letters*, 166(1-2), pp. 85-95.

Barker, S., Cacho, I., Benway, H. and Tachikawa, K. (2005) 'Planktonic foraminifera Mg/Ca as a proxy for past oceanic temperatures: a methodological overview and data compilation for the Last Glacial Maximum', *Quaternary Science Reviews*, 24(7-9), pp. 821-834.

Belli, R., Borsato, A., Frisia, S., Drysdale, R., Maas, R. and Greig, A. (2017) 'Investigating the hydrological significance of stalagmite geochemistry (Mg, Sr) using Sr isotope and particulate element records across the Last Glacial-to-Holocene transition', *Geochimica et Cosmochimica Acta*, 199, pp. 247-263.

Birks, J., Battarbee, R., Mackay, A. and Oldfield, F. (2014) 'Reconstructing Holocene Climate Records from Speleothems', in *Global Change in the Holocene*, London: Routledge, pp. 242-264.

Boers, N., Ghil, M. and Rousseau, D.D. (2018) 'Ocean circulation, ice shelf, and sea ice interactions explain Dansgaard-Oeschger cycles', *Earth, Atmosphere, and Planetary Science,* 115(47), pp. E11005-E11014.

Böhm, E., Lippold, J., Gutjahr, M., Frank, M., Blaser, P., Antz, B., Fohlmeister, J., Frank, N., Andersen, M.B., Deininger, M. (2015) 'Strong and deep Atlantic meridional overturning circulation during the last glacial cycle', *Nature*, 517, pp. 73-76.

Börget, F., Frauen, C., Neumann, T. and Meier, H.E.M. (2020) 'The Atlantic Multidecadal Oscillation controls the impact of the North Atlantic Oscillation on the North European climate', *Environmental Research Letters*, 15(104025).

Born, A. and Stocker, T.F. (2014) 'Two Stable Equilibria of the Atlantic Subpolar Gyre', *Journal of Physical Oceanography,* 44(1), pp. 246-264.

Borsato, A., Frisia, S., Fairchild, I.J., Somogyi, A. and Susini, J. (2007) 'Trace element distribution in annual stalagmite laminae mapped by micrometer-resolution X-ray fluorescence: Implications for incorporation of environmentally significant species', *Geochimica et Cosomchimica Acta*, 71(6), pp. 1494-1512.

Bradwell, T. and Ballantyne, C.K. (2021) ‘The Far Northwest: Sutherland, Assynt and Coigach’ in *Landscapes and Landforms of Scotland*. London: Springer. pp. 233-250.

Braun, H., Christl, M., Rahmstorf, S., Ganopolski, A., Mangini, A., Kubatzki, C., Roth, K. and Kromer, B. (2005) ‘Possible solar origin of the 1,470-year glacial climate cycle demonstrated in a coupled model’, *Nature*, 438, pp. 208-211.

Breitenbach, S.F.M., Rehfeld, K., Goswami, B., Baldini, J.U.L., Ridley, H.E., Kennett, D.J., Prufer, K.M., Aquino, V.V., Asmerom, Y., Polyak, V.J., Cheng, H., Kurths, J. and Marwan, N. (2012) ‘Constructing Proxy Records from Age models (COPRA)’, *Climate of the Past*, 8(5), pp. 1765-1779.

Breitenbach, S. F. M., Homann, J., Couper, H., Fox, B. R. S., Kwiecien, O., Lawson, T. J., Hoffmann, T., Henderson, G. M., and Atkinson, T. C.: Resurrecting lost forests – speleothems inform on environmental changes in northern Scotland during MIS 5e, EGU General Assembly 2023, Vienna, Austria, 24–28 Apr 2023, EGU23-9362, https://doi.org/10.5194/egusphere-egu23-9362, 2023.

Breitenbach, S.F.M., Lawson, T.J., Atkinson, T.C., Fox, B.R.S., Kwiecien, O. and Henderson, G.M. (2024) ‘New high-precision U-Th dates for speleothems from the Assynt caves and their significance for past environmental change’, *Cave and Karst Science*, 51(3), pp. 123-128.

Broecker, W.S., Peteet, D.M. and Rind, D. (1985) ‘Does the ocean-atmosphere system have more than one stable mode of operation?’, *Nature*, 315, pp. 21-26.

British Geological Survey (1956) The Limestones of Scotland: Chemical analyses and petrography. Memoir of the Geological Survey of Great Britain, Sheet 36 (Scotland). London: HMSO.

British Geological Survey (1979) The geology of the Durness area: Memoir for 1:50,000. Sheet 114 (Scotland). London: HMSO.

Buizert, C., Cuffey, K.M., Severinghaus, J.P., Baggenstos, D., Fudge, T.J., Steig, E.J., Markle, B.R., Winstrup, M., Rhodes, R.H., Brook, E.J., Sowers, T.A., Clow, G.D., Cheng, H., Edwards, R.L., Sigl, M., McConnell, J.R. and Taylor, K.C. (2015) ‘The WAIS Divide deep

ice core WD2014 chronology – Part 1: Methane synchronization (68-31 ka BP) and the gas are-ice age difference', *Climate of the Past*, 11(2), pp. 153-173.

Burton, E.A. and Walter, L.M. (1991) 'The effects of PCO2 and temperature on magnesium incorporation in calcite in seawater and MgCl2-CaCl2 solutions', *Geochimica et Cosmochimica Acta*, 55(3), pp. 777-785.

Cheng, H., Edwards, R.L., Sinha, A., Spötl, C., Yi, L., Chen, S., Kelly, M., Kathayat, G., Wang, X., Li, X., Kong, X., Wong, Y., Ning, Y. and Zhang, H. (2016) 'The Asian monsoon over the past 640,000 years and ice age terminations', *Nature*, 534, pp. 640-646.

Chiang, J.C.H., Lee, S-Y., Putnam, A.E. and Wang, X. (2014) 'South Pacific Split Jet, ITCZ shifts, and atmospheric North-South linkages during abrupt climate changes of the last glacial period', *Earth and Planetary Science Letters,* 406, pp. 233-246.

Clement, A.C. and Peterson, L.C. (2008) 'Mechanisms of abrupt climate change of the last glacial period', *Reviews of Geophysics*, 46(4).

Clement, A., Bellomo, K., Murphy, L.N., Cane, M.A., Mauritsen, T., Rädel, G. and Stevens, B. (2015) 'The Atlantic Multidecadal Oscillation without a role for ocean circulation', *Science*, 350(6258), pp. 320-324.

Constantin, S. (2015) 'Speleothems as archives of the past - a beginner's guide' in Toulkeridis, T., Constantin, S. and Addison, A. (eds.) 3rd Simposio Internacional de Espeleología en el Ecuador, Boletín Científico, pp.74-87.

Corrick, E.C., Drysdale, R.N., Hellstrom, J.C., Capron, E., Rasmussen, S.O., Zhang, X., Fleitmann, D., Couchoud, I. and Wolff, E. (2020) 'Synchronous timing of abrupt climate changes during the last glacial period', *Science*, 369(6506), pp. 963-969.

Corrick, E., Drysdale, R.N., Hellstrom, J.C., Couchoud, I., Wong, H.K.Y., Didier, C., Hai, C., Jaillet, S. and Tocino, S. (2022) 'Characterising the expression of sub-millenial scale climate events in western Europe during the early last glacial period using multi-proxy speleothem records.' Paper presented to AQUA 2022 Conference, 6-8th December 2022, Adelaide. (pp. 36-37). Retrieved from: http://aqua.org.au/wp-content/uploads/2022/11/AQUA-2022-conference-program-and-abstract-booklet.pdf

Couchoud, I., Genty, D., Hoffmann, D., Drysdale, R. and Blamart, D. (2009) 'Millennial-scale climate variability during the Last Interglacial recorded in a speleothem from south-western France', *Quaternary Science Reviews*, 28(27-28), pp. 3263-3274.

Cruz, F.W., Burns, S.J., Jercinovic, M., Karmann, I., Sharp, W.D. and Vuille, M. (2007) 'Evidence of rainfall variations in Southern Brazil from trace element ratios (Mg/Ca and Sr/Ca) in a Late Pleistocene stalagmite', *Geochimica et Cosmochimica Acta*, 71(9), pp. 2250-2263.

Dabkowski, J., Limondin-Lozouet, N., Andrews, J., Marca-Bell, A. and Antoine, P. (2016) 'Climatic and environmental variations during the last interglacial recorded in a Northern France tufa (Caours, Somme basin). Comparisons with regional records.', International *Journal of the French Quaternary Association*, 27(3). pp. 249-261.

Dansgaard, W., Johnsen, S.J., Clausen, H.B., Dahl-Jensen, D., Gundestrup, N.S., Hammer, C.U. and Oeschger, H. (1984) 'North Atlantic Climate Oscillations Revealed by Deep Greenland Ice Cores', *Climate Processes and Climate Sensitivity*, 29.

Dansgaard, W., Johnsen, S.J., Clausen, H.B., Dahl-Jensen, D., Gundestrup, N.S., Hammer, C.U., Hvidberg, C.S., Steffensen, J.P., Sveinbjörnsdottir, A.E., Jouzel, J. and Bond, G. (1993) 'Evidence for general instability of past climate from a 250-kyr ice-core record', *Nature*, 364, pp.218-220.

Day, C.C. and Henderson, G.M. (2013) 'Controls on trace-element partitioning in cave-analogue calcite', *Geochimica et Cosmochimica Acta*, 120, pp. 612-627.

Delworth, T.L., Zeng, F., Zhang, L., Zhang, R., Vecchi, G.A. and Yang, X. (2017) 'The Central Role of Ocean Dynamics in Connecting the North Atlantic Oscillation to the Extratropical Component of the Atlantic Multidecadal Oscillation', *Journal of Climate*, 30(10), pp. 3789-3805.

Demeny, A., Nemeth, P., Czuppon, G., Lorincz-O., Szabo, M., Nemeth, T. and Jhasz, K. (2016) 'Formation of amorphous calcium carbonate in caves and its implications for speleothem research', *Scientific Reports*, 6(39602).

Demeny, A., Berentes, A., Rinyu, L., Kovacs, I., Suranyi, G. and Virag, M. (2024) 'Subaqueous carbonate speleothems as paleotemperature archives - clumped isotope

thermometry and stable isotope compositions of inclusion-hosted water', *International Journal of Speleology,* 53(1), pp. 25-37.

Deplazes, G., Lückage, A., Peterson, L.C., Timmermann, A., Hamann, Y., Hughen, K.A., Röhl, U., Laj, C., Cane, M.A., Sigman, D.M. and Haug, G.H. (2013) 'Links between tropical rainfall and North Atlantic climate during the last glacial period', *Nature Geoscience*, 6, pp. 213-217.

Dhungana, R. (2010) A High-Resolution Hydroclimate Record of the Last Three Millenia from a Cored Stalagmite at Desoto Caverns (Alabama, USA). Masters thesis, University of Alabama.

Dima, M. and Lohmann, G. (2007) 'A Hemispheric Mechanism for the Atlantic Multidecadal Oscillation', *Journal of Climate*, 20(11), pp. 2706-2719.

Ditlevsen, P.D., Anderson, K.K. and Svensson, A. (2007) 'The DO-climate events are probably noise induced: statistical investigation of the claimed 1470 year cycle', *Climate of the Past*, 3, pp. 129-134.

Dokken, T.M., Nisancioglu, K.H., Li, C., Battisti, D.S. and Kissel, C. (2013) 'Dansgaard-Oeschger cycles: Interactions between ocean and sea ice intrinsic to the Nordic seas', *Paleoceanography and Paleoclimatology*, 28(3), pp. 491-502.

Dong, J., Shen, C.C., Kong, X., Wang, Y. and Duan, F. (2018) 'Asian monsoon dynamics at Dansgaard/Oeschger events 14-8 and Heinrich events 5-4 in northern China', *Quaternary Geochronology*, 47, pp. 72-80.

Dorale, J.A., Gonzalez, L.A., Reagan, M.K., Picket, D.A., Murrell, M.T. and Baker, R.G. (1992) 'A High-Resolution Record of Holocene Climate Change in Speleothem Calcite from Cold Water Cave, Northeast Iowa', *Science*, 258(5088), pp. 1626-1630.

Drinkwater, K.F., Miles, M., Medhaug, I., Ottera, O.H., Kristiansen, T., Sundby, S. and Gao, Y. (2014) 'The Atlantic Multidecadal Oscillation: Its manifestations and impacts with special emphasis on the Atlantic region of 60N', *Journal of Marine Systems*, 133, pp. 117-130.

Drysdale, R.N., Paul, B.T., Hellstrom, J.C., Couchoud, I., Greig, A., Bajo, P., Zanchetta, G., Isola, I., Spötl, C., Baneschi, I., Regattieri, E. and Woodhead, J.D. (2012) 'Precise

microsampling of poorly laminated speleothems for U-series dating', *Quaternary Geochronology*, 14, pp.38-47.

Drysdale, R.N, Zanchetta, G., Baneschi, I., Guidi, M., Isola, I., Couchoud, I., Piccini, L., Greig, A., Wong, H., Woodhead, J.D., Regattieri, E., Corrick, E., Paul, B., Spötl, C., Denson, E., Gordon, J., Jaillet, S., Dux, F. and Hellstrom, J.C. (2019) 'Partitioning of Mg, Sr, Ba and U into a subaqueous calcite speleothem', *Geochimica et Cosmochimica Acta*, 264, pp. 67-91.

Drysdale, R., Couchoud, I., Zanchetta, G., Isola, I., Regattieri, E., Hellstrom, J., Govin, A., Tzedakis, P.C., Ireland, T., Corrick, E., Greig, A., Wong, H., Piccini, L., Holden, P. and Woodhead, J. (2020) 'Magnesium in subaqueous speleothems as a potential palaeotemperature proxy', *Nature Communications,* 11(5027).

Dulinski, M. and Rozanski, K. (1990) 'Formation of 13C/12C Isotope Ratios in Speleothems: A Semi-Dynamic Model', *Radiocarbon*, 32(1), pp. 7-16.

Duplessy, J.C., Labeyrie, J., Lalou, C. and Nguyen, H.V. (1970) 'Continental Climatic Variations between 130,000 and 90,000 Years BP', *Nature*, 226, pp. 631-633.

Egleton, R., Baldini, J., Breitenbach, S. (2025) *Geochemistry of Uamh Mhor flowstone during DO-12* [dataset]. Durham University. DRO-DATA. Available at: https://doi.org/10.15128/2kw52j813x [Accessed 19 September 2025].

Erhardt, T., Capron, E., Rasmussen, S.O., Schu4pbach, S., Bigler, M., Adolphi, F. and Fischer, H. (2019) 'Decadal-scale progression of the onset of Dansgaard-Oeschger warming events', *Climate of the past*, 15(2), pp. 811-825.

Fairchild, I.J., Borsato, A., Tooth, A.F., Frisia, S., Hawkesworth, C.J., Huang, Y., McDermott, F. and Spiro, B. (2000) 'Controls on trace element (Sr-Mg) compositions of carbonate cave waters: implications for speleothem climatic records', *Chemical Geology*, 166(3-4), pp. 255-269.

Fairchild, I.F., Baker, A., Borsato, A., Frisia, S., Hinton, R.W., McDermott, F. and Tooth, A.F. (2001) 'Annual to sub-annual resolution of multiple trace-element trends in speleothems', *Journal of the Geological Society*, 158(5), pp. 831-841.

Fairchild, I.J., Tuckwell, G.W., Baker, A. and Tooth, A.F. (2006) 'Modelling of dripwater hydrology and hydrogeochemistry in a weakly karstified aquifer (Bath, UK): Implications for climate change studies', *Journal of Hydrology*, 321(1-4), pp. 213-231.

Fairchild, I.J. and Treble, P.C. (2009) 'Trace elements in speleothems as recorders of environmental change', *Quaternary Science Reviews*, 28(5-6), pp. 449-468.

Fairchild, I.J., Spötl, C., Frisia, S., Borsato, A., Susini, J., Wynn, P.M. and Cauzid, J. (2010) 'Petrology and geochemistry of annually laminated stalagmites from an Alpine cave (Obir, Austria): seasonal cave physiology', *Geological Society Special Publication*, 336, pp. 295-321.

Fankhauser, A., McDermott, F. and Fleitmann, D. (2016) 'Episodic speleothem deposition tracks the terrestrial impact of millennial-scale last glacial climate variability in SW Ireland', *Quaternary Science Reviews*, 152, pp. 104-117.

Fleitmann, D., Burns, S.J., Neff, U., Mudelsee, M., Mangini, A. and Matter, A. (2004) 'Palaeoclimatic interpretation of high-resolution oxygen isotope profiles derived from annually laminated speleothems from Southern Oman', *Quaternary Science Reviews*, 23(7-8), pp. 935-945.

Fleitmann, D., Cheng, H., Baddertscher, S., Edwards, R.L., Mudelsee, M., Göktürk, O.M., Fankhauser, A., Pickering, R., Raible, C.C., Matter, A., Kramers, J. and Tüysüz, O. (2009) 'Timing and climatic impact of Greenland interstadials recorded in stalagmites from northern Turkey', *Geophysical Research Letters*, 36(19).

Fohlmeister, J. Schröder-Ritzrau, A., Scholz, D., Spötl, C., Riechelmann, D.F.C., Mudelsee, M., Wackerbarth, A., Gerdes, A., Riechelmann, S., Immenhauser, A., Richter, D.K. and Mangini, A. (2012) 'Bunker Cave stalagmites: an archive for central European Holocene climate variability', *Climate of the Past*, 8(5), pp. 1751-1764.

Fohlmeister, J., Sekhon, N., Columbu, A., Vettoretti, G., Weitzel, N., Rehfeld, K., Veiga-Pires, C., Ben-Yami, M., Marwan, N. and Boers, N. (2023) 'Global reorganization of atmospheric circulation during Dansgaard-Oeschger cycles', *PNAS,* 120(36), e2302283120.

Forman, E.C.G. (2024) Northward Gulf Stream Migration During the Little Ice Age Revealed using Monthly-Scale Geochemistry of a Bermudan Stalagmite. (Master's thesis). Durham University.

Forman, E.C.G., Baldini, J.U.L., Jamieson, R.A., Lechleitner, F.A., Walczak, I.W., Nita, D.C., Smith, S.R., Richards, D.A., Baldini, L.M., McIntyre, C., Müller, W. and Peters, A.J. (2025) 'The Gulf Stream moved northward at the end of the Little Ice Age', *Nature*, 6(552).

Frappier, A., Sahagian, D., Gonzalez, L.A. and Carpenter, S.J. (2002) 'El Niño Events Recorded by Stalagmite Carbon Isotopes', *Science,* 298(5593), p.565.

Fuller, L., Baker, A., Fairchild, I.J., Spötl, C., Marca-Bell, A., Rowe, P. and Dennis, P.F. (2008) 'Isotope hydrology of dripwaters in a Scottish cave and implications for stalagmite palaeoclimate research', *Hydrology and Earth System Sciences*, 12, pp. 1065-1074.

Gabitov, R.I., Sadekov, A. and Leinweber, A. (2014) 'Crystal growth rate effect on Mg/Ca and Sr/Ca partitioning between calcite and fluid: An in situ approach', *Chemical Geology,* 367, pp. 70-82.

Gascoyne, M., Schwarcz, H.P. and Ford, D.C. (1980) 'A palaeotemperature record for the mid-Wisconsin in Vancouver Island', *Nature*, 285, pp. 474-476.

Gascoyne, M. (1983) 'Trace-element partition coefficients in the calcite-water system and their paleoclimatic significance in cave studies', *Journal of Hydrology*, 61(1-3), pp. 213-222.

Gascoyne, M. (1992) 'Palaeoclimate determination from cave calcite deposits', *Quaternary Science Reviews*, 11(6), pp. 609-632.

Genty, D., Balmart, D., Ouahdi, R., Gilmour, M., Baker, A., Jouzel, J. and Van-Exter, S. (2003) 'Precise dating of Dansgaard-Oeschger climate oscillations in western Europe from stalagmite data', *Nature*, 421, pp.833-837.

Genty, D., Blamart, D., Ghaleb, B., Plagnes, V., Causse, C., Bakalowicz, M., Zouari, K., Chkir, N., Hellstrom, J., Wainer, K. and Bourges, F. (2006) 'Timing and dynamics of the last deglaciation from European and North African d13C stalagmite profiles – comparison with Chinese and South Hemisphere stalagmites', *Quaternary Science Reviews*, 25(17-18), pp. 2118-2142.

Genty, D., Combourieu-Nebout, N., Peyron, O., Blamart, D., Wainer, K., Mansuri, F., Ghaleb, B., Isabello, L., Dormoy, I., von Grafenstein, U., Bonelli, S., Landais, A. and Brauer, A. (2010) 'Isotopic characterization of rapid climatic events during OIS3 and OIS4 in Villars Cave stalagmites (SW-France) and correlation with Atlantic and Mediterranean pollen records', *Quaternary Science Reviews*, 29(19-20), pp. 2799-2820.

Goede, A. and Vogel, J.C. (1991) 'Trace element variations and dating of a Late Pleistocene Tasmanian speleothem', *Palaeogeography, Palaeoclimatology, Palaeoecology*, 88(1-2), pp. 121-131.

Goede, A. (1994) 'Continuous early last glacial palaeoenvironmental record from a tasmanian speleothem based on stable isotope and minor element variations', *Quaternary Science Reviews*, 13(3), pp. 283-291.

Greenland Ice-core Project (GRIP) Members (1993) 'Climate instability during the last interglacial period recorded in the GRIP ice core', *Nature*, 364, pp. 203-207.

Groots, P.M., Stuiver, M., White, J.W.C., Johnsen, S. and Jouzel, J. (1993) 'Comparison of oxygen isotope records from the GISP2 and GRIP Greenland ice cores', *Nature,* 366, pp. 552-554.

Guiot, J., de Beaulieu, J.L., Cheddadi, R., David, F., Ponel, P. and Reille, M. (1993) 'The climate in Western Europe during the last Glacial/Interglacial cycle derived from pollen and insect remains', *Palaeogeography, Palaeoclimatology, Palaeoecology,* 103(1-2), pp. 73-93.

Harrison, S.P. and Goñi, M.F.S. (2010) 'Global patterns of vegetation response to millenial-scale variability and rapid climate change during the last glacial period', *Quaternary Science Reviews,* 29(21-22), pp. 2957-2980.

Hartland, A., Fairchild, I.J., Lead, J.R., Borsato, A., Baker, A., Frisia, S. and Baalousha, M. (2012) 'From soil to cave: Transport of trace metals by natural organic matter in karst dripwaters', *Chemical Geology,* 304-305, pp. 68-82.

Hartley, G. and Mucci, A. (1996) 'The influence of PCO2 on the partitioning of magnesium in calcite overgrowths precipitated from artificial seawater at 25° and 1 atm total pressure', *Geochimica et Cosmochimica Acta*, 60(2), pp. 315-324.

Heinrich, H. (1988) ‘Origin and Consequences of Cyclic Ice Rafting in the Northeast Atlantic Ocean During the Past 130,000 Years’, *Quaternary Research*, 29(2), pp. 142-152.

Hellstrom, J.C. and McCulloch, M.T. (2000) ‘Multi-proxy constraints on the climatic significance of trace element records from a New Zealand speleothem’, *Earth and Planetary Science Letters,* 179(2), pp. 287-297.

Held, F., Cheng, H., Edwards, R.L., Tüysüz, O., Koç, K. and Fleitmann, D. (2024) ‘Dansgaard-Oeschger cycles of the penultimate and last glacial period recorded in stalagmites from Türkiye’, *Nature Communications*, 15(1183).

Hendy, C.H. & Wilson, A.T. (1968) ‘Palaeoclimatic Data from Speleothems’, *Nature*, 219, pp. 48-51.

Henry, L.G., McManus, J.F., Curry, W.B., Roberts, N.L., Piotrowski, A.M. and Keigwin, L.D. (2016) ‘North Atlantic ocean circulation and abrupt climate change during the last glaciation’, *Science,* 353(6298), pp. 470-474.

Hercman, H., Blaszczyk, M., Mulczyk, A. and Bella, P. (2020) ‘Uranium isotopic ratios and their implication for uranium-uranium dating and groundwater circulation studies: A case study from speleothems of Demänova caves, Nizke Tatry Mts., Slovakia’, *Geologica Carpathica*, 71(1), pp. 61-72.

Hill, C.A. (1992) ‘Subaqueous flowstone – a new speleothem subtype, Blanchard springs cavern, Arkansas’, *Bulletin of the National Speleological Society*, 54, pp. 11-13.

Hoffman, D.L., Spötl, C. and Mangini, A. (2009) ‘Micromill and in situ laser ablation sampling techniques for high spatial resolution MC-ICPMS U-Th dating of carbonates’, *Chemical Geology,* 259, pp. 253-261.

Howson, M.R., Pethybridge, A.D. and House, W.A. (1987) ‘Synthesis and distribution coefficient of low-magnesium calcites’, *Chemical Geology*, 64(1-2), pp. 79-87.

Hu, C., Huang, J., Fang, N., Xie, S., Henderson, G.M. and Cai, Y. ‘Absorbed silica in stalagmite carbonate and its relationship to past rainfall’, *Geochimica et Cosmochimica Acta*, 69(9), pp. 2285-2292.

Huang, Y., Fairchild, I.J., Borsato, A., Frisia, S., Cassidy, N.J., McDermott, F. and Hakesworth, C.J. (2001) 'Seasonal variations in Sr, Mg and P in modern speleothems (Grotta di Ernesto, Italy)', *Chemical Geology*, 175(3-4), pp. 429-448.

Huang, Y. and Fairchild, I.J. (2001) 'Partitioning of Sr2+ and Mg2+ into calcite under karst-analogue experimental conditions', *Geochimica et Cosmochimica Acta*, 65(1), pp. 47-62.

Huber, C., Leuenberger, M., Spahni, R., Flückiger, J., Schwander, J., Stocker, T.F., Johnsen, S., Landais, A. and Jouzel, J. (2006) 'Isotope calibrated Greenland temperature record over Marine Isotope Stage 3 and its relation to CH4', *Earth and Planetary Science Letters*, 243(3-4), pp. 504-519.

Isola, I., Ribolini, A., Zanchetta, G., Bini, M., Regattieri, E., Drysdale, R.N., Hellstrom, J.C., Bajo, P., Montagna, P. and Pons-Branchu, E. (2019) 'Speleothem U/Th age constraints for the Last Glacial conditions in the Apuan Alps northwestern Italy', *Palaeogeography, Palaeoclimatology, Palaeoecology,* 518, pp. 62-71.

Jakic, J., Labor, M. and Martinac, V. (2016) 'Charaterization of Dolomitic Lime as the Base Reagent for Precipitation of Mg(OH)_2 from Seawater', *Chemical and Biochemical Engineering Quarterly*, 30(3), pp. 373-379.

Jamieson, R.A., Baldini, J.U.L., Brett, M.J., Taylor, J., Ridley, H.E., Ottley, C.J., Prufer, K.M., Wassenburg, J.A., Scholz, D. and Breitenbach, S.F.M. (2016) 'Intro- and inter-annual uranium concentration variability in a Belizean stalagmite controlled by prior aragonite precipitation: A new tool for reconstructing hydro-climate using aragonitic speleothems', *Geochimica et Cosmochimica Acta,* 190, pp. 332-346.

Johnsen, S.J., Clausen, H.B., Dansgaard, W., Fuhrer, K., Gundestrup, N., Hammer, C.U., Iversen, P., Jouzel., J., Stauffer, B. and Steffensen, J.P. (1992) 'Irregular glacial interstadials recorded in a new Greenland ice core', *Nature,* 359, pp. 311-313.

Karmann, I., Cruz, F.W., Viana, O. and Burns, S.J. (2007) 'Climate influence on geochemistry parameters of waters from Santana-Perolas cave system, Brazil', *Chemical Geology*, 244(1-2), pp. 232-247.

Kathayat, G., Cheng, H., Sinha, Ashish, Spötl, C., Edwards, R.L., Zhang, H., Li, X., Yi, L., Ning, Y., Cai, Y., Lui, W.L. and Breitenbach, S.F.M. (2016) 'Indian monsoon variability on millennial-orbital timescales', *Scientific Reports*, 6(24374).

Kern, O.A., Koutsodendris, A., Allstädt, F.J., Mächtle, B., Peteet, D.M., Kalaitzidis, S., Christanis, K. and Pross, J. (2022) 'A near-continuous record of climate and ecosystem variability in Central Europe during the past 130 kyrs (Marine Isotope Stages 5-1) from Füramoos, southern Germany', *Quaternary Science Reviews*, 284(107505).

Kindler, P., Guillevic, M., Baumgartner, Schwander, J., Landais, A. and Leuenberger, M. (2014) 'Temperature reconstruction from 10 to 120 kyr b2k from the NGRIP ice core', *Climate of the Past,* 10(2) pp. 887-902.

Klose, J., Weber, M. and Scholz, D. (2024) 'Central European warm phases recorded by episodic speleothem growth during MIS 3', *Communications Earth and Environment*, 5(719).

Knudsen, M.F., Seidenkrantz, M-S., Jacobsen, B.H. and Kuijpers, A. (2011) 'Tracking the Atlantic Multidecadal Oscillation through the last 8,000 years', *Nature Communications,* 2(178).

Lachniet, M.S. (2009) 'Climatic and environmental controls on speleothem oxygen-isotope values', *Quaternary Science Reviews*, 28(5-6), pp. 412-432.

Landais, A., Chappellaz, J., Delmotte, M., Jouzel, J., Blunier, T., Bourg, C., Caillon, N., Cherrier, S., Malaize, B., Masson-Delmotte, V., Raynaud, D., Schwander, J. and Steffensen, J.P. (2003) 'A tentative reconstruction of the last interglacial and glacial inception in Greenland based on new gas measurements in the Greenland Ice Core Project (GRIP) ice core', *Journal of Geophysical Research Atmospheres*, 108(D18).

Landais, A., Sanchez Goñi, M.F., Toucanne, S., Rodrigues, T. and Naughton, F. (2021) Abrupt climatic variability: Dansgaard-Oeschger events. In: Palacios, D., Hughes, P.D., Garcia-Ruiz, J.M. and Andres, N. (eds), *European Glacial Landscapes*. Oxford: Elsevier pp. 175-180.

Lawson, T. (1981) 'First Scottish date from the Last Interglacial', *Scottish Journal of Geology*, 17(4), pp. 301-303.

Lawson, T.J. (1983) Quaternary geomorphology of the Assynt area, N.W. Scotland, PhD Thesis, Edinburgh University.

Lawson, T.J. (1993) 'Creag nan uamh' in Geological Conservation Review, Volume 6: Quaternary of Scotland, Chapter 6: North-West Highlands. JNCC. Available at: http://www.jncc.gov.uk/page-2731 (Accessed: 16th Nov 2024).

Lee, J., Sangheon, Y. and Lim, J. (2024) 'A modern pollen-climate dataset from South Korea and its application for pollen-based quantitative climate reconstruction during the Holocene', *CATENA*, 241(108032).

Liang, Y., Wang, Y., Wang, Q., Wu, J., Shao, Q., Zhang, Z., Yang, S., Kong, X. and Edwards, R.L. (2019) 'East Asian summer monsoon climates and cave hydrological cycles over Dansgaard-Oeschger events 14 to 11 revealed by a new stalagmite record from Hulu Cave', *Quaternary Research*, 92(3).

Liu, D., Wang, Y., Cheng, H., Edwards, R.L., Kong, W. and Li, T.Y. (2016) 'Strong coupling of centennial-scale changes of Asian monsoon and soil processes derived from stalagmite d18O and d13C records, southern China', *Quaternary Research*, 85(3), pp. 333-346.

Liu, D., Mi, X., Liu, S. and Wang, Y. (2023) 'Multi-phased Asian hydroclimate variability during Heinrich Stadial 5', *Climate Dynamics*, 60, pp. 4003-4016.

Lohmann, J., Lin, J., Vinther, B.M., Rasmussen, S.O. and Svensoon, A. (2024) 'State-dependent impact of major volcanic eruptions observed in ice-core records of the last glacial period', *Climate of the Past*, 20, pp. 313-333.

Lora, J.M., Mitchell, J.L., Risi, C. and Tripati, A.E. (2017) 'North Pacific atmospheric rivers and their influence on western North America at the Last Glacial Maximum', *Geophysical Research Letters,* 22(2), pp. 1051-1059.

Luterbacher, J., Xoplaki, E., Dietrich, D., Jones, P.D., Davies, T.D., Portis, D., Gonzalez-Rouco, J.F., von Storch, H., Gyalistras, D., Casty, C. and Wanner, H. (2004) 'Extending North Atlantic oscillation reconstructions back to 1500', *Atmospheric Science Letters*, 2(1-4), pp. 114-124.

Mangini, A., Spötl, C. and Verdes, P. (2005) ‘Reconstruction of temperature in the Central Alps during the past 2000 yr from a d18O stalagmite record’, *Earth and Planetary Science Letters,* 235(3-4), pp. 741-751.

Mann, L.E., Robel, A.A. and Meyer, C.R. (2021) ‘Synchronization of Heinrich and Dansgaard-Oeschger Events Through Ice-Ocean Interactions’, *Paleoceanography and Paleoclimatology,* 36(11).

Mattey, D., Lowry, D., Duffet, J., Fisher, R., Hodge, E. and Frisia, S. (2008) ‘A 53year seasonally resolved oxygen and carbon isotope record from a modern Gibraltar speleothem: Reconstructed drip water and relationship to local precipitation’, Earth and Planetary Science Letters, 269(1-2), pp. 80-95.

Mattey, D.P., Fairchild, I.J., Atkinson, T.C., Latin, J-P., Ainsworth, M. and Durell, R. (2010) ‘Seasonal microclimate control of calcite fabrics, stable isotopes and trace elements in modern speleothem from St Michaels Cave, Gibraltar’*, Geological Society*, 336, pp. 323-344.

Mattey, D., Lowry, D., Duffet, J., Fisher, R., Hodge, E. and Frisia, S. (2008) ‘A 53 year seasonally resolved oxygen and carbon isotope record from a modern Gibraltar speleothem: Reconstructed drip water and relationship to local precipitation’, *Earth and Planetary Science Letters,* 269(1-2), pp. 80-95.

McCarthy, G.D., Smeed, D.A., Cunningham, S.A. and Roberts, C.D. (2017) ‘Atlantic Meridional Overturning Circulation’, *MCCIP Science Review*, pp. 15-21.

McDermott, F., Frisia, S., Huang, Y., Longinelli, A., Spiro, B., Heaton, T.H.E., Hawkesworth, C.J., Borsato, A., Keppens, E., Fairchild, I.J., van der Borg, K., Verheyden, S. and Selmo, E. (1999) ‘Holocene climate variability in Europe: Evidence from d18O, textural and extension-rate variations in three speleothems’, *Quaternary Science Reviews*, 18, pp. 1021-1038.

McDermott, F. (2004) ‘Palaeo-climate reconstruction from stable isotope variations in speleothems: a review’, *Quaternary Science Reviews*, 23(7-8), pp.901-918.

McDonald, J., Drysdale, R. and Hill, D. (2004) ‘The 2002-2003 El Niño recorded in Australian cave drip waters: Implications for reconstructing rainfall histories using stalagmites’, *Geophysical Research Letters*, 31(22).

Menne, M.J., Durre, I., Vose, R.S., Gleason, B.E., and Houston, T.G. (2012) 'An Overview of the Global Historical Climatology Network-Daily Database', *Journal of Atmospheric Oceanic Technology,* 29, pp. 897-910. doi:10.1175/JTECH-D-11-00103.1.

Menviel, L., Timmermann, A., Friedrich, T. and England, M.H. (2014) 'Hindcasting the continuum of Dansgaard-Oeschger variability: mechanisms, patterns and timing', *Climate of the Past,* 10(1), pp. 63-77.

Menviel, L.C., Skinner, L.C., Tarasov, L. and Tzedakis, P.C. (2020) 'An ice-climate oscillatory framework for Dansgaard-Oeschger cycles', *Nature Reviews Earth and Environment*, 1, pp. 677-693.

Modeley, G.E., Spötl, C., Svensson, A., Cheng, H., Brandstätter, S. and Edwards, R.L. (2014) 'Multi-speleothem record reveals tightly coupled climate between central Europe and Greenland during Marine Isotope Stage 3', *Geology,* 42(12), pp. 1043-1046.

Mook, W. G. Environmental Isotopes in the Hydrological Cycle, Volume II (Atmospheric Water) UNESCO, Paris/IAEA, Vienna, 2000.

Mucci, A. (1987) 'Influence of temperature on the composition of magnesian calcite overgrowths precipitated from seawater', *Geochimica et Cosmochimica Acta*, 51(7), pp. 1977-1984.

Mucci, A. and Morse, J.W. (1983) 'The incorporation of Mg2+ and Sr2+ into calcite overgrowths: influences of growth rate and solution composition', *Geochimica et Cosmochimica Acta*, 47(2), pp. 217-233.

Nagashima, K., Tada, R., Tani, A., Sun, Y., Isozaki, Y., Toyoda, S. and Hasegawa, H. (2011) 'Millenial-scale oscillations of the westerly jet path during the last glacial period', *Journal of Asian Earth Sciences,* 40(6), pp. 1214-1220.

Olafsdottir, K.B., Geirsdottir, A., Miller, G.H. and Larson, D.J. (2013) 'Evolution of NAO and AMO strength and cyclicity derived from a 3-ka varve-thickness record from Iceland', *Quaternary Science Reviews*, 69, pp. 142-154.

Olsen, J., Anderson, N.J. and Knudsen, M.F. (2012) 'Variability of the North Atlantic Oscillation over the past 5,200 years', *Nature Geoscience*, 5, pp. 808-812.

Oomori, T., Kaneshima, H., Maezato, Y. and Kitano, Y. (1987) ‘Distribution coefficient of Mg2+ ions between calcite and solution at 10-50C’, *Marine Chemistry,* 20(4), pp. 327-336.

Oster, J.L., Weisman, I.E. and Sharp, W.D. (2020) ‘Multi-proxy stalagmite records from northern California reveal dynamic patterns of regional hydroclimate over the last glacial cycle’, *Quaternary Science Reviews*, 241(106411).

Past Interglacials Working Group of PAGES (2015) ‘Interglacials of the last 800,000 years’, *Reviews of Geophysics*, 54(1), pp. 162-219.

Pausata, F.S.R., Li, C., Wettstein, J.J., Kageyama, M. and Nisancioglu, K.H. (2011) ‘The key role of topography in altering North Atlantic atmospheric circulation during the last glacial period’, *Climate of the Past*, 7, pp. 1089-1101.

Pawlak, J., Hercman, H., Sierpien, P., Pruner, P., Gasiorowski, M., Mihevc, A., Hajna, N.Z., Bosak, P., Błaszczyk, M. and Wach, B. (2019) ‘Estimation of the durations of breaks in deposition - Speleothem Case Study’*, Geochronometria*, 47, pp. 154-170.

Pederzani, S., Britton, K., Aldeias, V., Bourgon, N., Fewlass, H., Lauer, T., McPherron, S.P., Rezek, Z., Sirakov, N. Smith, G.M., Spasov, R., Tran, N-H., Tasanova, T. and Hublin, J-J. (2021) ‘Subarctic climate for the earliest Homo sapiens in Europe’, *Science Advances*, 7(39).

Pederzani, S., Britton, K., Trost, M., Fewlass, H., Bourgon, N., McCormack, J., Jaouen, K., Dietl, H., Döhle, H-J., Kirchner, A., Lauer, T., Le Corre, M., McPherron, S.P., Meller, H., Mylopotamitaki, D., Orschiedt, J., Rougier, H., Ruebens, K., Schüler, Sinet-Mathiot, V., Smith, G.M., Talamo, S., Tütken, T., Welker, F., Zavala, E.I., Weiss, M. and Hublin, J-J. (2024) ‘Stable isotopes show Homo Sapiens dispersed into cold steppes ~45,000 years ago at Ilsenhöhle in Ranis Germany’, *Nature Ecology & Evolution*, 8, pp.578-588.

Pedro, J.B., Andersson, C., Vettoretti, G., Voelker, A.H.L., Waelbroeck, C., Dokken, T.M., Jensen, M.F., Rasmussen, S.O., Sessford, E.G., Jochum, M. and Nisancioglu, K.H. (2022) ‘Dansgaard-Oeschger and Heinrich event temperature anomalies in the North Atlantic set by sea ice, frontal position and thermocline structure’, *Quaternary Science Reviews*, 289(107599).

Peral, M., Marchegiano, M., Verheyden, S., Goderis, S., Van Helden, T., Vanhaecke, F., Van Acker, T., Jia, X., Cheng, H., Fiebig, J., Fourcade, T., Snoeck, C. and Claeys, P. (2024) ‘A

new insight of the MIS 3 Dansgaard-Oeschger climate oscillations in western Europe from the study of a Belgium isotopically equilibrated speleothem', *Quaternary Science Reviews,* 329(108564).

Proctor, C.J., Baker, A., Barnes, W.L. and Gilmour, M.A. (2000) 'A thousand year speleothem proxy record of North Atlantic climate from Scotland', *Climate Dynamics*, 16, pp. 815-820.

Proctor, C.J., Baker, A. and Barnes, W.L. (2002) 'A three thousand year record of North Atlantic climate', *Climate Dynamics*, 19, pp. 449-454.

Putnis, C.V., Ruiz-Agudo, E. and Hövelmann, J. (2014) 'Coupled fluctuations in element release during dolomite dissolution', *Mineralogical Magazine*, 78(6), pp. 1355-1362.

Ramirez, V.M., Cruz, F.W., Vuille, M., Novello, V.F., Strikis, N.M., Cheng, H., Zhang, H.W., Bernal, J.P., Du, W.J., Ampuero, A., Deiniger, M., Chiessi, C.M., Tejedor, E., Campos, J.L., Brahim, Y.A. and Edwards, R.L. (2023) 'Summer insolation controlled movements of Intertropical Convergence Zone during last glacial cycle in northern South America', *Communications Earth & Environment*, 4(495).

Rasmussen, S.O., Bigler, M., Blockley, S.P., Blunier, T., Buchardt, S.L., Clausen, H.B., Cvijanovic, I., Dahl-Jensen, D., Johnsen, S.J., Fischer, H., Gkinis, V., Cuillevic, M., Hoek, W.Z., Lowe, J.J., Pedro, J.B., Popp, T., Seierstad, I.K., Steffensen, J.P., Svensson, A.M., Vallelonga, P. and Winstrup, M. (2014) 'A stratigraphic framework for abrupt climatic changes during the Last Glacial period based on three synchronized Greenland ice-core records: refining and extending the INTIMATE event stratigraphy', Quaternary Science Reviews, 106, pp. 14-28.

Rasmussen, T.L., Thomsen, E. and Moros, M. (2016) 'North Atlantic warming during Dansgaard-Oeschger events synchronous with Antarctic warming and out-of-phase with Greenland climate', *Scientific Reports*, 6.

Riechelmann, D.F.C., Riechelmann, S., Wassenburg, J.A., Fohlmeister, J., Schöne, B.R., Jochum, K.P., Richter, D.K. and Scholz, D. (2020) 'High-Resolution Proxy Records From Two Simultaneously Grown Stalagmites From Zoolithencave (Southeastern Germany) and

their Potential for Palaeoclimate Reconstruction', *Geochemistry, Geophysics, Geosystems*, 21(6).

Ridley, W.I., Pribil, M.J., Koenig, A.E. and Slack, J.F. (2015) 'Measurement of in Situ Sulfur Isotopes by Laser Ablation Multi-Collector ICPMS: Opening Pandora's Box', *Procedia Earth and Planetary Science,* 13, pp. 116-119.

Roberts, M.S., Smart, P.L. and Baker, A. (1998) 'Annual trace element variations in a Holocene speleothem', *Earth and Planetary Science Letters*, 154(1-4), pp. 237-246.

Rossi, A., Massei, N. and Laignel, B. (2011) 'A synthesis of the time-scale variability of commonly used climate indices using continuous wavelet transform', *Global and Planetary Change*, 78(1-2), pp. 1-13.

Sanchez Goñi, M.F., Landais, A., Fletcher, W.J., Naughton, F., Desprat, S. and Duprat, J. (2008) 'Contrasting impacts of Dansgaard-Oeschger events over a western European latitudinal transect modulated by orbital parameters', *Quaternary Science Reviews*, 27(11-12), pp. 1136-1151.

Sanchez-Moreno, E.M., Font, E., Pavón-Carrasco, F.J., Dimuccio, L.A., Hillaire-Marcel, C., Ghaleb, B. and Cunha, L. (2022) 'Paleomagnetic techniques can date speleothems with high concentrations of detrital material', *Scientific Reports*, 12(17936).

Scholz, D., Hoffmann, D.L. (2008) '230^{Th}/U-dating of fossil reef corals and speleothems', *Quaternary Science Journal,* 57(1-2), pp. 52-77.

Scholz, D., Tolzmann, J., Hoffman, D.L., Jochum, K.P., Spötl, C. and Riechelmann, D.F.C. (2014) 'Diagenesis of speleothems and its effect on the accuracy of ^230Th/U-ages', *Chemical Geology*, 387, pp. 74-86.

Schulz, M. (2002) 'On the 1470-year pacing of Dansgaard-Oeschger warm events', *Paleoceanography and Paleoclimatology*, 17(2), pp. 4-9.

Seip, K.L., Grøn, Ø. and Wang, H. (2019) 'The North Atlantic Oscillations: Cycle Times for the NAO, the AMO and the AMOC', *Climate*, 7(3).

Sinclair, D.J. (2011) ‘Two mathematical models of Mg and Sr partitioning into solution during incongruent calcite dissolution: Implications for dripwater and speleothem studies’, *Chemical Geology*, 283(3-4), pp. 119-133.

Sinclair, D.J., Banner, J.L., Taylor, F.W., Partin, J., Jenson, J., Mylroie, J., Goddard, E., Quinn, T., Jocson, J. and Miklavic, B. (2012) ‘Magnesium and strontium systematics in tropical speleothems from the Western Pacific’, *Chemical Geology*, 294-295, pp. 1-17.

Spötl, C. and Mattey, D. (2006) ‘Stable isotope microsampling of speleothems for palaeoenvironmental studies: A comparison of microdrill, micromill and laser ablation techniques’, *Chemical Geology*, 235, pp. 48-58.

Spötl, C. and Boch, R. (2019) ‘Uranium series dating of speleothems’ in White, W.B., Culver, D.C. and Pipan, T. (eds.) *Encyclopaedia of Caves*. London: Elsevier, pp.1096-1102.

Stoll, H. M., Müller, W. and Prieto, M. (2012) ‘I-STAL, a model for interpretation of Mg/Ca, Sr/Ca and Ba/Ca variations in speleothems and its forward and inverse application on seasonal to millennial scales’, *Geochemistry, Geophysics, Geosystems*, 13(9).

Strikis, N.M., Cruz, F.W., Barreto, E.A.S., Naughton, F., Vuille, M., Cheng, H., Voelker, A.H.L., Zhang, H., Karmann, I., Edwards, R.L., Auler, A.S., Santos, R.V. and Sales, H.R. (2018) ‘South American monsoon response to iceberg discharge in the North Atlantic’, *Earth, Atmosphere, and Planetary Science,* 115(15), pp. 3788-3793.

Sun, C., Li, J. and Jin, F-F. (2015) ‘A delayed oscillator model for the quasi-periodic multidecadal variability of the NAO’, *Climate Dynamics*, 45, pp. 2083-2099.

Svensson, A., Andersen, K.K., Bigler, M., Clausen, H.B., Dahl-Jensen, D., Davies, S.M., Johnsen, S.J., Muscheler, R., Rasmussen, S.O., Röthlisberger, R., Seierstad, I., Steffensen, J.P. and Vinther, B.M. (2008) ‘A 60 000 year Greenland stratigraphic ice core chronology’, *Climate of the Past*, 4(1), pp. 47-57.

Thompson, G.M., Lumsden, D.N., Walker, R.L. and Carter, J.A. (1975) ‘Uranium series dating of stalagmites from Blanchard Springs Caverns, U.S.A.’, *Geochimica et Cosmochimica Acta,* 39(9), pp.1211-1218.

Tolzmann, J. (2013) The reconstruction of paleoclimate variability in Northern Germany, during Marine Isotope Stage 5 (Doctoral thesis). Johannes Gutenberg Universität Mainz, Germany.

Treble, P., Shelley, J.M.G. and Chappell, J. (2003) 'Comparison of high resolution sub-annual records of trace elements in a modern (1911-1992) speleothem with instrumental climate data from southweat Australia', *Earth and Planetary Science Letters*, 216(1-2), pp. 141-153.

Tremaine, D.M., Froelich, P.N. and Wang, Y. (2011) 'Speleothem calcite farmed in situ: Modern calibration of d18O and d13C paleoclimate proxies in a continuously-monitored natural cave system', *Geochimica et Cosmochimica Acta*, 75(17), pp. 4929-4950.

Tremaine, D.M. and Froelich, P.N. (2013) 'Speleothem trace element signatures: A hydrologic geochemical study of modern cave dripwaters and farmed calcite', *Geochimica et Cosmochimica Acta*, 121, pp. 522-545.

Ulusoy, Ü., Anbar, G., Bayari, S. and Uysal, T. (2014) 'ESR and ^230Th/^234U dating of speleothems from Aladağlar Mountain Range (AMR) in Turkey', *Quaternary Research*, 81, pp. 367-380.

Vaks, A. Woodhead, J., Bar-Matthews, M., Ayalon, A., Cliff, R.A., Zilberman, T., Matthews, A. and Frumkin, A. (2013) 'Pliocene-Pleistocene climate of the northern margin of Saharan-Arabian Desert recorded in speleothems from the Negev Desert, Israel', *Earth and Planetary Science Letters*, 368, pp. 88-100.

Van Beynen, P.E., Soto, L. and Polk, J. (2008) 'Variable calcite deposition rates as proxy for paleo-precipitation determination as derived from speleothems in central Florida, U.S.A.', *Journal of Cave and Karst Studies*, 70(1), pp. 25-34.

Vansteenberge, S., de Winter, N.J., Sinnesael, M., Verheyden, S., Goderis, S., Van Malderson, S.J.M., Vanhaecke, F. and Claeys, P. (2020) 'Reconstructing seasonality through stable-isotope and trace-element analyses of the Proserpine stalagmite, Han-sur-Lesse cave, Belgium: indications for climate-driven changes during the last 400 years', *Climate of the Past*, 16(1), pp. 141-160.

Vettoretti, G., Ditlevsen, P., Jochum, M. and Rasmussen, S.O. (2022) ‘Atmospheric CO2 control of spontaneous millennial-scale ice age climate oscillations’, *Nature Geoscience*, 15, pp.300-306.

WAIS Divide Project Members (2015) ‘Precise interpolar phasing of abrupt climate change during the last ice age’, *Nature*, 520, pp. 661-665.

Wang, Y., Li, S. and Luo, D. (2009) ‘Seasonal response of Asian monsoonal climate to the Atlantic Multidecadal Oscillation’, *Journal of Geophysical Research Atmospheres*, 114(D2).

Wang, Y.-H., Magnusdottir, G., Stern, H., Tian, X. and Yu, Y. (2012) ‘Decadal variability of the NAO: Introducing an augmented NAO Index’, *Geophysical Research Letters*, 39.

Warken, S.F., Fohlmeister, J., Schröder-Ritzrau, A., Constantin, S., Spötl, C., Gerdes, A., Esper, J., Frank, N., Arps, J., Terente, M., Riechelmann, D.F.C., Mangini, A. and Scholz, D. (2018) ‘Reconstruction of the late Holocene autumn/winter precipitation variability in SW Romania from a high-resolution speleothem trace element record’, *Earth and Planetary Science Letters,* 499, pp. 122-133.

Wassenburg, J.A., Richelmann, S., Schröder-Ritzrau, A., Riechelmann, D.F.C., Richter, D.K., Immenhauser, A., Terente, M., Constantin, S., Hachenberg, A., Hansen, M. and Scholz, D. (2020) ‘Calcite Mg and Sr partition coefficients in cave environments: Implications for interpreting prior calcite precipitation in speleothems’, *Geochimica et Cosmochimica Acta*, 269, pp. 581-596.

Weber, M., Scholz, D., Schröder-Ritzrau, A., Deininger, M., Spötl, C., Lugli, F., Mertz-Kraus, R., Jochum, K.P., Fohlmeister, J., Stumpf, C.F. and Riechelmann, D.F.C. (2018) ‘Evidence of warm and humid interstadials in central Europe during early MIS 3 revealed by a multi-proxy speleothem record’, *Quaternary Science Reviews*, 200, pp. 276-286.

Wendt, K.A., Li, X. and Edwards, R.L. (2021) ‘Uranium-Thorium Dating of Speleothems’, *Elements*, 17(2), pp. 87-92.

White, W. (1956) ‘Birmingham Crawlway cave’, Netherworld News, 4, p.53.

Williams, P.W. and Fowler, A. (2002) ‘Relationship between oxygen isotopes in rainfall, cave percolation waters and speleothem calcite at Waitomo, New Zealand’*, Journal of Hydrology,* 41(1), pp. 53-70.

Woillez, M.N., Kageyama, M., Combourieu-Nebout, N. and Krinner, G. (2013) ‘Simulating the vegetation response in western Europe to abrupt climate changes under glacial background conditions’, *Biogeosciences,* 10(3), pp. 1561-1582.

Wong, C.I. and Breecker, D.O. (2015) ‘Advancements in the use of speleothems as climate archives’, *Quaternary Science Reviews*, 127, pp.1-18.

Wroblewski, W., Gradzinski, M., Motyka, J. and Stankovic, J. (2017) ‘Recently growing subaqueous flowstones: Occurrence, petrography, and growth conditions’, *Quaternary International*, 437(A), pp. 84-97.

Wu, Y., Li, T-Y., Yu, T-L., Shen, C-C., Chen, C-J., Zhang, J., Li, J-Y., Wang, T., Huang, R. and Xiao, S-Y. (2020) ‘Variation of the Asian summer monsoon since the last glacial-interglacial recorded in a stalagmite from southwest China’, *Quaternary Science Reviews*, 234.

Wu, C-C., Shen, C-C., Günther, D. and Hattendorf, B. (2024) ‘LA-ICPMA for In Situ U-Th Dating of Holocene Stalagmite’, *Analytical Chemistry*, 96(31), pp. 12640-12648.

Zhang, X., Knorr, G., Lohmann, G. and Barker, S. (2017) ‘Abrupt North Atlantic circulation changes in response to gradual CO2 forcing in a glacial climate state’, *Nature Geoscience*, 10, pp. 518-523.

Zhou, J., Lundstrom, C.C., Fouke, B., Panno, S., Hackley, K., and Curry, B. (2005) ‘Geochemistry of speleothem records from southern Illinois: Development of (234U/238U) as a proxy for paleoprecipitation’, *Chemical Geology*, 221(3-4), pp. 279-304.

8. Supplementary Materials

Data Access Statement

The raw data supporting this thesis are openly available from the Durham University DRO-DATA repository at: [DOI: 10.15128/r2kw52j813x].

The dataset, *Geochemistry of Uamh Mhor flowstone during DO-12* [dataset], contains trace element data (Mg, Al, Si, P, Ca, Cu, Sr, Ba, Pb, Th, and U) and stable isotope data (δ18O and δ13C).

Citation of dataset:

Egleton, R., Baldini, J., Breitenbach, S. (2025) *Geochemistry of Uamh Mhor flowstone during DO-12* [dataset]. Durham University. DRO-DATA. Available at: https://doi.org/10.15128/r2kw52j813x [Accessed 19 September 2025].